Differential Impact of a Telomeropathy-causing Mutation in Shelterin Protein TPP1 on Mouse Hematopoiesis and Germline

by

Jacqueline Graniel

A dissertation submitted in partial fulfillment
of the requirements for the degree of
Doctor of Philosophy
(Cellular and Developmental Biology)
in the University of Michigan
2024

Doctoral Committee:

Associate Professor Benjamin Allen, Chair
Professor Catherine E. Keegan
Assistant Professor Scott Leiser
Associate Professor Jayakrishnan Nandakumar
Associate Professor Sunny Wong

Jacqueline V. Graniel

jgraniel@umich.edu

ORCID iD: 0000-0002-0405-4159

Dedication

To my father, Fabricio R Graniel, for all the sacrifices he has made to get me to this moment. Everything I do will always be because of you and for you ((&& the munchkins)).

I am very proud to be the first person in my immediate family to graduate high school let alone now be defending my PhD.

¡Si se puede!

¡Te quiero mucho, Papa! Gracias por tu amor, tu esfuerzo y por levantar a todos nosotros.

Olivessss!!

Acknowledgements

First and foremost, I must thank my mentor, Jayakrishnan Nandakumar. Thank you JK for your patience and unwavering support while we embarked on a beast of a project together. I am so grateful to have had the opportunity to train under you. I can't imagine going through the PhD I've had without you as a mentor. You have helped challenge the way I think about science and have helped me develop into the scientist I strive to be. You have encouraged me to think outside the box while learning the rules of the game all while being a great human. You have accepted all of me and always been someone I could talk to when science and/or life got hard or got in the way. From bringing me food when I was on bed rest to SLACKing months straight trying to get my paper out, you have really been a light during some storms in this journey.

I would also like to thank Ivan Maillard and Katy Keegan, who were in their own way co-mentors to me during my PhD. Being the bridge between the various branches of this project would have been impossible without the guidance of you both. Ivan, even from that one rotation during my first year of grad school, I still find myself thinking back to scientific conversations we had and applying that critical thinking each time I was faced with a new hematopoietic finding (or lack thereof) during my PhD. I'll also never be able to thank you for being an amazing person and doctor and caring enough about me to drive me home after being discharged from the hospital. Katy, thank you for opening up your lab to me and taking the time to teach me things I only know because of your mentoring. Despite your busy schedule, you always tried to

make time to chat about how the project was going and I am thankful for that. My PhD experience would not be the same if it weren't for your mentorship. Thank you for the opportunity to become independent and gain confidence as I grew during my PhD.

I would also like to thank Sue Hammoud for her guidance as I tackled a new field as my project took a turn. Thank you for sharing Adrienne with me and for being a great teammate as we crossed the finish line.

Along with Katy, I would like to thank the rest of my thesis committee: Ben Allen, Scott Leiser and Sunny Wong for their wonderful suggestions, feedback and more. Ben…asking you to be my chair was one of the best decisions I ever made. I don't have the words to properly express what your support has meant to me over all these years. You knew me as PREP student and have seen me grow and I only hope that I have shown you that you were right to advocate for me those many years ago. Thank you for pushing me to be a better version of myself just by example. Scott. Hopefully I've gone from nice Colin to nice Jackie lol. I am so thankful for your great advice and your willingness to work with me when I naively thought I could balance a worm and mouse project at the same time. It was amazing to have been accepted into your lab and have had the opportunity to be mentored by you. Sunny. You were on my prelim committee and now on my thesis committee and I'm still so grateful to have had you on both because each meeting with you I always came out feeling inspired and challenged. Thank you for sharing your wisdom with me.

I would like to thank the Nandakumar lab, past and present for all their support: Kamlesh, Sheri, Eric, Devon, Alam, Valerie, Ritvija, Shilpa, Cassie, Kirsten, and Jonathan. Kamlesh was my first mentor in the lab and he was brilliant. I am so thankful for that time because I realize now what a treasure that was. Thanks for your brilliance, Kamlesh! Sheri, you were the only one who went to the "shelterin meetings" with me and so it was always so great to have you there as a sounding board and learn from you. I'll also be thankful for your kindness during a rough time in my life where you, Eric and Valerie got me through. Valerie and Shilpa, thank you for taking the time to teach me how to measure telomeres the OG way! While my project typically kept me on the periphery of the other projects in the lab, I really want to thank all of you for sticking in there while I talked on about mouse hematopoiesis and germline and for being good friends. Ritvija, thank you for checking in when mouse work kept me in MSRB3 or writing had me pulling my hair out. Devon, your work ethic while looking fabulous is something that always impressed me, #goals! Valerie, thank you for the amazing dinners you hosted and your infectious laughter. Shilpa, thank you for being my PokemonGo friend and your appalled expression at the way I eat string cheese. Cassie, thank you for our grocery hauls and the dunes that we did not climb. Kirsten, thank you for our emo playlist and being s'mores queen. Finally, Jonathan, thank you for being an awesome fellow MSTP and not hating me for crushing you in a game of Scrabble.

I would also like to thank the CDB staff for their support throughout the years. From general amazement at the amount of work they do for the CDB community to actual hiccups I've had that they've helped resolve. I'm so thankful to each and every one of you. A special thank you to Karen, Lori, and Kristen for helping me as lead host, 801 coordinator, or just a fumbling graduate student. Likewise, I have to thank the MSTP office for their support as well. Not only

the current office: Kathy, Justine, Gretchen, and Liz, but also Ron, Ellen, Laurie and Hilkka. Ron, I'll always be thankful for your faith in me.

I would like to thank the Biology of Aging Training Grant for assembling amazing seminars even before I was a trainee and of course for taking me in and playing a part in my growth as a scientist. I would also like to thank Rackham and CDB for their support throughout the years. I have been a part of many organizations throughout my time here and I'd like to briefly thank those who have helped enrich my PhD experience. Roberta Fuller, thank you for leading the SACNAS Chapter even before we truly existed. Your dedication to increasing DEI allowed us to succeed in such amazing ways. I am so proud of our chapter and the amazing people I have met by being a part of it. Mara Duncan, thank you for all that you do to advocate for URMs in and outside of CDB. As advisor of the CDB DEI committee I've grown so much and feel empowered as we continue to advocate for change. Our DEI committee is an awesome group of advocates and I know it'll continue to do wonderful things. Ben Allen, Scott Barolo, and Laura Buttitta, thank you for being amazing faculty advisors for Developing Future Biologists. I also have to thank the amazing instructors I had the chance to work with during my time there: Kaylee, Sam, Angela, Anna, Tyler, **Becky**, Jessica, **Krista**, Matt, Millie, Kelsey, Sarah, Fatima, Eli, Isha, and Pilar. We did amazing things despite a pandemic and that experience has reinvigorated my efforts at wanting to help shape the way we tackle DEI efforts across campus.

I also have many friends to thank. The sASS crew: Breane, Seth, Kristin, Ashley, Jeff, and Steve. My rocks: Rosie, Ginette, and Jun. The Eurodance crew: Andreia and Marjana. && the MVPs: Mike, Pam, Carla, Colin, Rishi, Brenda, Rosa, Jessie, Patrick, and Jairus. My acknowledgements

would be longer than my actual thesis if I detail how each one of you has impacted my life. Briefly, sASS: you managed to make every hard part of this experience manageable and there was never a dull moment. Thank you for your unconditional love and support. I literally couldn't have done it without you. Having had even the smallest time with you OGs (Kristin, Seth and Breane) has been incredible. Ashley. Girl…no tengo las palabras. Not only have you been an incredible colleague and mentor to me throughout my PhD, but you are an amazing human being and I am so lucky to have you as one of my best friends. Jeff. You're cray but you somehow made it lol. You fit so well in our bubble and you have been a wonderful friend. I cannot wait to see the amazing things you are capable of. Steve…since UCLA you've been my soul friend and that's only truer now. We don't need to see each other every day to know that. Te quiero, niño. My rocks: what can I say that your name doesn't already say? Our text thread kept me connected on days I felt the most alone. You all are my lifeline in this long program. Eurodance: we're the coolest. That's all there is to say <3. MVPs: you're each on here for different reasons but I'm a better person for having known and learned from each one of you. Colin. You were my first mentor ever here in Michigan. Thank you for your craziness. My work ethic has grown because of the unbelievable scientist you are. Carla, you're my sister from another mister. True sunshine amidst the clouds and the fiercest Latina scientist I hope to be one day.

Finally, I have to thank my family. From a young age I've seen my dad do amazing things to support his family and I like to think that my work ethic comes from seeing him do it all. Thank you for your unbelievable strength, love, and wisdom. I learned at an early age what life is really about and from that have forged an incredible bond with my two siblings, Gigie and Bito. Gigie. You are one of the most amazing people I have ever met and the fact that we're related and

you're stuck with me is one of my happiest treasures. You're an amazing young woman and I know you will do the most amazing things because you're so smart and your heart is so big. Bito, your life has changed and so I hope you take this as an opportunity to observe the choices we've all made and make a choice that benefits your new baby. While you may not follow in my path, dream big, because I would not be where I am if I didn't want to be someone you could all look up to and respect. Ma, regardless of everything, I am who I am because of you. You've reminded me of the frailty of life, and it's kept me grounded.

Table of Contents

List of Figures

Abstract

Chromosome ends face two problems: the end-protection (end-to-end fusions) and the end-replication (progressive telomere shortening) problems. The protein complex shelterin binds to the telomeric DNA repeats at chromosome ends to protect them from illicit end joining and other unwanted recombination or resection events. The ribonucleoprotein complex telomerase extends chromosome ends in somatic and germline stem cells to overcome the end-replication problem and ensure continued proliferation. Mutations in genes important for telomerase and/or shelterin function often result in diseases termed telomeropathies, the most prominent example of which being dyskeratosis congenita (DC). Severe shortening of telomeres in patients with DC results in depletion of stem cells and bone marrow (BM) failure, the primary cause of death.

TPP1 is the only shelterin component known to both protect chromosome ends and recruit telomerase to telomeres. We have previously defined regions of TPP1 that are critical for recruiting telomerase and characterized the consequences of a patient-derived DC mutation in TPP1 (K170Δ) resulting in decreased telomerase activity, impaired recruitment, and short telomeres in cultured human cells. While these studies provide a direct cause-effect relationship, they do not provide insights into stem cell dysfunction *in vivo*.

A DC mutation in TPP1 (K170Δ) that specifically compromises telomerase recruitment to telomeres is a valuable tool to evaluate telomerase-dependent telomere length maintenance in

mice. In this dissertation, I first present work on how we used CRISPR-Cas9 to generate a mouse knocked in for the equivalent of the TPP1 K170Δ mutation (TPP1 K82Δ) and investigated both its hematopoietic (Chapter 2) and germline (Chapter 3) compartments in unprecedented detail. TPP1 K82Δ caused progressive telomere erosion with increasing generation number but did not induce steady-state hematopoietic defects. Strikingly, K82Δ caused mouse infertility, consistent with gross morphological defects in the testis and sperm, the appearance of dysfunctional seminiferous tubules, and a decrease in germ cells. Intriguingly, both TPP1 K82Δ mice and previously characterized telomerase knockout mice show no spontaneous BM failure but rather succumb to infertility at steady-state. Our work suggests a species-specific sensitivity in the germline rather than the soma in mice, which is reversed in human patients with this disease. We speculate that the species-specific differences in the response to severe telomere shortening arises from the distinct proliferation burdens on the mouse and human, soma and germline. Small and short-lived species like mice may boost germline proliferation to increase gamete production and maximize the number of offspring produced in a lifetime, while large and long-lived species like humans prioritize somatic development to survive to the age of reproduction (and nurturing) to produce fewer, but healthy, offspring.

Chapter 1 : Introduction

1.1 Telomeres

In all eukaryotes, nucleoprotein complexes called telomeres are responsible for maintaining the ends of linear chromosomes. In mammals, telomeres consist of multiple, tandem DNA repeats (of GGTTAG sequence) that are largely double stranded (ds) (10-15 kb in humans) and end in short single-stranded (ss) G-rich overhangs (50-500 nucleotides in humans) (Palm & de Lange, 2008). While telomeres are conserved across eukaryotes, the repeated sequence (e.g., *C. elegans*: TTAGGC, etc.) and length (e.g., laboratory mouse telomeres = ~50 kb) can vary across species (Kipling & Cooke, 1990). The concept of telomeres was developed in the 1930s separately by two scientists: Hermann Muller and Barbara McClintock. Muller demonstrated through his work on x-ray irradiation of *Drosophila melanogaster* that while breaks and fusions occurred in chromosomes, the terminal ends were "special" in that they did not participate in such events. He coined the term telomeres (*telos*:end; *meros*:part) to describe chromosome ends (Muller, 1938). Furthermore, McClintock's observations of maize chromosomes under the microscope revealed the ends of chromosomes – telomeres - as essential elements, and introduced the concept of chromosome end protection (McClintock, 1941) that I will expand on in the following section. Since then, the telomere field has uncovered not only the sequence and nature of telomeric DNA but also key proteins necessary for the maintenance of chromosomes ends. In the introductory chapter, I will share our current understanding of how telomeres protect our genome and how they help prevent senescence of proliferating cells like germline and somatic stem cells.

1.2 End protection: shelterin

Genomic stability is critical for life. While many factors work in tandem to maintain chromosome integrity, a key component in this is the DNA damage response machinery (DDR) that recognizes and repairs double stranded breaks (DSBs) (Palm et al., 2009). Due to the linear nature of mammalian chromosomes, their natural ends can be perceived as DSBs by DDRs, which can lead to end-to-end fusions and genomic instability. This is the end-protection problem. Telomeric DNA can form two high order structures that have been hypothesized to help protect telomeres to help solve the end-protection problem: t-loops and G-quadruplexes. In t-loops, the 3' overhang of the telomere folds back to invade an internal telomeric duplex region. By sequestering the 3' end of the overhang within a duplex, the t-loop structure is thought to protect telomeres from being recognized as broken DNA (Stansel et al., 2001). Intra-strand G-quadruplexes can form due to the G-rich nature of telomeric repeats, providing a second DNA-structure mediated avenue for protecting the natural 3' end of chromosomes (Sen & Gilbert, 1988). While telomeres can organize themselves into these structures, much is still unknown about how, when, and why these structures are employed to protect ends. What is more appreciated is how a multimeric protein complex known as shelterin physically binds along the entire length of the telomere to provide chromosome end protection (Palm & de Lange, 2008). Shelterin consists of six proteins: TRF1, TRF2, Rap1, TIN2, POT1 and TPP1. Chromosome end-protection by shelterin is essential, as individual knockout (KO) of five of the six shelterin proteins in mice (Rap1 being the outlier) results in embryonic lethality.

1.2.1 TRF1

TRF1 (telomere repeat-binding factor 1), encoded by *TERF1*, was the first mammalian shelterin component identified (Zhong et al., 1992). TRF1 has three domains: an acidic N-terminus, a central TRF homology (TRFH) domain and a C-terminal DNA-binding domain (Chong et al., 1995). TRF1's C-terminal SANT/Myb domain binds specifically to ds telomeric DNA (Boyer et al., 2004; Broccoli, Chong, et al., 1997; Broccoli, Smogorzewska, et al., 1997) while its TRFH domain is responsible for its homodimerization (Bianchi et al., 1997). The TRFH domain also binds shelterin component TIN2, and to a meiosis-specific telomere protein called TERB1 (telomere repeats binding bouquet formation protein 1) (Smith et al., 2020). TERB1 along with two other meiosis-specific proteins TERB2 and MAJIN form a complex that connects telomeres to the inner nuclear membrane that allows for telomeres to be tethered to cytoskeletal motors, a step that is crucial for chromosomal movements important to facilitate homologous recombination during meiosis (Pendlebury et al., 2017). The acidic N-terminus of TRF1 has been associated with recruitment of specific shelterin accessory proteins such as Tankyrase 1 and Tankyrase 2, which can sequester TRF1 from telomeres and positively regulate telomere length (Sbodio & Chi, 2002; Sbodio et al., 2002; Smith et al., 1998). Functionally, TRF1 has also been implicated in maintaining telomere length. In experimental studies in a telomerase-positive context, over-expression of TRF1 results in telomere shortening and reduction of TRF1 results in telomere elongation (Smogorzewska et al., 2000; van Steensel & de Lange, 1997). In mice, knock out of TRF1 is lethal and conditional KO of TRF1 results in major developmental defects, severe telomeric defects such as "fragile" telomeres, which constitute broken telomere fluorescence *in situ* hybridization (FISH) signals seen at the ends of metaphase chromosomes (Karlseder et al., 2003; Sfeir et al., 2009). Through TRF1's multiple domains, it has roles in

stabilizing shelterin for genome protection, regulating telomerase-mediated telomere lengthening, as well as tethering telomeres to the inner nuclear membrane during meiosis.

1.2.2 TRF2

TRF2 (telomere repeat factor 2), encoded by *TERF2*, has a similar domain layout as TRF1. While both proteins share a central TRFH domain and C-terminal SANT/Myb domain, TRF2 has a basic N-terminus rather than an acidic one like TRF1 (Bilaud et al., 1997; Broccoli, Smogorzewska, et al., 1997). The N-terminus of TRF2 is referred to as a GAR domain as it contains a Gly/Arg-rich region known to bind proteins such as WRN (Werner syndrome helicase) and ORC (Origin Recognition Complex) that are implicated in the formation and resolution of t-loops (Doksani et al., 2013). Just like TRF1, TRF2 binds specifically to ds telomeric DNA through its C-terminus. Between TRF2's TRFH and C-terminal Myb domains are individual regions required for binding to shelterin component Rap1 and TIN2 (Kim et al., 2009; Li et al., 2000). Similar to studies done in TRF1 KO mice, TRF2 KO mice are also embryonic lethal (Celli & de Lange, 2005). Further work also showed similarities to TRF1, including telomere shortening upon overexpression and telomere elongation upon knockdown (Karlseder et al., 1999; Smogorzewska et al., 2000; Takai et al., 2010). The TRFH domain of TRF2 is also responsible for binding key proteins like Apollo SNM1-type nuclease, Ku70 and other proteins involved in DNA repair or DNA damage signaling (Chen et al., 2008; Kim et al., 2009). While TRF2 is important for shelterin stabilization and is known to facilitate t-loop formation, one of TRF2's most important roles that distinguishes it from TRF1 is in repressing the ATM (ataxia telangiectasia mutated) pathway, a major pathway for responding to DSBs in the cell. Exposure of ds telomeric DNA due to TRF2 removal evokes a strong ATM response

due to activation of ATM kinase as a result of DSBs recognized by the MRE11/RAD50/NBS1 (MRN) complex, which is involved in the initial processing of DSBs (D'Amours & Jackson, 2002; Karlseder et al., 1999; Karlseder et al., 2004; Takai et al., 2003; van Steensel et al., 1998).

1.2.3 Rap1

Rap1 (repressor/activator protein 1) is encoded by *TERF2IP* (telomeric repeat-binding factor 2-interacting protein 1) (Li et al., 2000). It is one of 3 shelterin proteins that do not bind to telomeric DNA. Rap1 has three discernible domains: an N-terminal BRCT domain thought to phosphorylate a target protein, a Myb domain that can bind to other proteins and a C-terminal domain that serves to connect the protein in shelterin by binding to TRF2 (Li et al., 2000). Without TRF2, Rap1 cannot be recruited to telomeres and is the only shelterin component dispensable for end-protection (Celli & de Lange, 2005). Aside from binding TRF2 within shelterin, there is no isolated role of Rap1 at telomeres. Accordingly, Rap1 KO mice are viable, however, they exhibit shortened telomeres, skin hyperpigmentation, and an obesity phenotype in females that likely results from Rap1 binding to genomic sites outside of telomeres (Martínez & Blasco, 2011; Martinez et al., 2010).

1.2.4 TIN2

TRF1-interacting nuclear protein 2 (TIN2) is encoded by *TINF2* and bridges the proteins that bind ds telomeric DNA to those that bind ss telomeric DNA. The N-terminal domain of TIN2 allows for binding of shelterin proteins TPP1 and TRF2, and a central region of the TIN2 protein binds to the TRFH domain of TRF1 (Kim et al., 1999). TIN2 KO causes embryonic lethality and

loss of TIN2 in mouse embryonic fibroblasts (MEFs) results in a reduction in localization of all shelterin components to telomeres (Chiang et al., 2004; Takai et al., 2011). TIN2 is the first shelterin component shown to be mutated in patients with telomeropathies and *TINF2* is also one of the most frequently mutated genes in these diseases (see 1.4 for more information; (Savage et al., 2008; Walne et al., 2008)).

1.2.5 POT1

POT1 (protection of telomeres 1) is encoded by *POT1* and is the only shelterin component that binds ss telomeric DNA. It has two distinct domains: an N-terminal DNA-binding domain and a C-terminal domain that binds TPP1 (Baumann & Cech, 2001; Baumann et al., 2002). OB-folds (oligonucleotide/oligosaccharide-binding) are small domains used for binding ss nucleic acids and/or proteins. In case of POT1, two OB-folds of the N-terminal DNA-binding domain bind ss telomeric DNA in a sequence specific manner (Lei et al., 2004). POT1 forms an obligate heterodimer with the sixth shelterin protein TPP1 (see below) using a C-terminal domain that contains a Holliday junction resolvase-like domain (HJRL) inserted within a third OB domain in POT1 (Lei et al., 2004; Liu et al., 2004; Loayza et al., 2004). Similar to TRF2 in its role in shielding telomeres from DDR, exposure of the ss telomeric DNA evokes a strong ataxia telangiectasia and RAD3-related (ATR) response that POT1 normally suppresses (Loayza & De Lange, 2003). In mice, POT1 has two paralogs, Pot1a and Pot1b (Hockemeyer et al., 2006). While they both bind ss telomeric DNA like human POT1, they each have separate functions (Hockemeyer et al., 2006). KO of Pot1a results in embryonic lethality whereas Pot1b KO mice are viable (He et al., 2006; Hockemeyer et al., 2005; Wu et al., 2006). Pot1a not Pot1b is important for repressing the ATR response, while Pot1b is important for Tpp1-mediated

telomerase recruitment to telomeres (see next section; (He et al., 2009)). Furthermore, Pot1b helps to maintain the proper 3' G-overhang length by regulating the resection of the complementary C-rich strand by nucleases (Gu et al., 2021).

1.2.6 TPP1

The protein TPP1 (adrenocortical dysplasia homolog/TINT1-PTOP-PIP1, hereafter mentioned as TPP1) encoded by *ACD* was the last shelterin component identified independently by three different groups (Houghtaling et al., 2004; Liu et al., 2004; Ye et al., 2004). Human TPP1 is 544 amino acids (aa) long but can exist as two main isoforms TPP1 short (TPP1S), the most abundant isoform starting at aa Met87, and TPP1 long (TPP1L) that exists primarily in testes (Grill et al., 2019; Liu et al., 2004). Mouse TPP1 exists as a single isoform containing 458 aa and is equivalent to the TPP1S isoform of humans. TPP1S contains three distinct domains, an N-terminal OB domain, a central POT1 binding domain, and a C-terminus TIN2 domain. The N-terminal OB domain of TPP1 is important for recruiting telomerase to telomeres (see section 1.3 for more detail). Although TPP1 is not known to directly bind DNA, it increases affinity of POT1 for telomeric ss DNA (Wang et al., 2007; Xin et al., 2007). Work in a mouse model harboring a spontaneous autosomal recessive splice site mutation in the *Acd* gene has shed some light on the importance of TPP1 *in vivo*. This model of TPP1 results in 2% of WT *Acd* mRNA and is therefore referred to as a hypomorphic allele of TPP1 rather than a null allele (Keegan et al., 2005). *acd/acd* mice often die after birth (depending on genetic background) and those that survive suffer from many developmental defects including urogenital and neuronal defects. MEFs derived from these mice exhibit mild telomere defects resulting from chromosome de-protection. The mild nature of the phenotype can be attributed to the persistence of WT TPP1,

which when eliminated through small hairpin RNAs (shRNAs), results in a robust end de-protection phenotype (Hockemeyer et al., 2007).

Although there is more to elucidate about shelterin assembly at telomeres, our current understanding is that TRF1 and TRF2/Rap1 are independently recruited to telomeres followed by TIN2, TPP1 and finally POT1. In summary, shelterin caps the ends of our chromosomes to block DDR from attempting to fuse natural chromosome ends to each other (Fig. 1.1).

1.3 End-replication: telomerase

An additional task of telomeres is to solve the end-replication problem in dividing cells. As cells divide, telomeres shorten. This is because DNA polymerases require an RNA primer that provides a 3′ hydroxyl group for DNA synthesis at the 5′ end of the lagging strand. However, once the primer has been removed, a gap is left that cannot be filled by DNA polymerases, resulting in shorter telomeres with every cell division (Palm & de Lange, 2008). This is the end-replication problem. While progressive telomere shortening is warranted in our somatic cells, as it can help prevent unregulated cell division associated with cancer, the end replication problem must be countered in long-lived proliferating cells such as germline and somatic stem cells (Shay & Wright, 2010). Telomerase is instrumental to the solution of the end replication problem. Discovered in 1985 by Greider and Blackburn, telomerase was found to be a unique ribonucleoprotein that contains a reverse transcriptase component (TERT) and an internal RNA component (TR) (Greider & Blackburn, 1985, 1989). Originally discovered in the ciliate *Tetrahymena thermophila*, it was shown that telomerase solves the end-replication problem by

synthesizing new telomeric DNA repeats at the ends of chromosomes using its internal RNA template (Greider & Blackburn, 1989; Lingner et al., 1997; Meyerson et al., 1997).

TERT consists of four domains: the TERT RNA binding domain (TRBD), the thumb domain also called the C-terminal extension (CTE), the reverse transcriptase domain (RT), and the telomerase essential N-terminal domain (TEN) (Podlevsky & Chen, 2012).

The TRBD domain is required for proper function of telomerase. It is responsible for binding the RNA subunit TR, resulting in the formation of the core telomerase ribonucleoprotein (RNP) complex. The catalytic RT domain is composed of seven conserved RT motifs (1, 2 and A, B, C, D, and E), common to all reverse transcriptases (Bryan et al., 2000b). Motifs 1 and 2 are organized in a "fingers" domain important for interacting with nucleic acids. Motifs A-E organize in a "palm" domain known to contain the catalytic active site with motif E connecting the fingers and palm domain with a "primer grip" region interacting with telomeric DNA (Bryan et al., 2000a). TERT distinguishes itself from other conventional reverse transcriptases (e.g., HIV reverse transcriptase) by presence of two major TERT-specific insertions, motif 3 (Xie et al., 2010) and insertion in fingers domain (IFD) (Lingner et al., 1997; Lue et al., 2003). The CTE domain contains the thumb domain, which works together with the finger and palm domains in the RT domain essential for telomerase activity. The TEN domain is the least evolutionarily conserved sequence of TERT but its structural core is conserved (Jacobs et al., 2006; Petrova et al., 2018). The TEN domain functions to bind ss telomeric DNA repeats but has also been implicated in telomerase activity, telomere maintenance, and recruitment of telomerase to the telomere (Armbruster et al., 2003; Armbruster et al., 2004; Zhong et al., 2012).

However, telomerase doesn't act alone. Many other proteins work with telomerase either for its biogenesis or activity. For example, Dyskerin is important for TR stability, TCAB1 is important for telomerase localization in Cajal bodies (before it is recruited to telomeres), and most notably for my thesis, TPP1 is required for telomerase recruitment to telomeres (Abreu et al., 2010; Collins, 2008; Egan & Collins, 2010). Since telomerase and POT1 bind the same G-rich sequences at chromosome ends, POT1 is thought to be an inhibitor of telomerase. However interestingly enough, the POT1-TPP1 complex stimulates telomerase processivity compared to POT1 or TPP1 alone (Latrick & Cech, 2010; Wang et al., 2007).

TPP1's N-terminal OB domain was first shown to bind TERT through pull down experiments (Xin et al., 2007) . It was later demonstrated through immunofluorescence and fluorescence *in situ* hybridization (IF-FISH) and chromatin immunoprecipitation (ChIP) assays that TPP1 is necessary for the recruitment of telomerase to telomeres (Abreu et al., 2010). Furthermore, loss of the OB-fold of TPP1 resulted in the disruption of telomerase recruitment to telomeres. TPP1 OB was also found to not only be necessary but also sufficient to recruit telomerase to telomerase via a LacO/LacI-tethering system that recruited telomerase to a non-telomeric locus in the genome (Zhong et al., 2012). Mutagenesis studies revealed a surface of the OB domain of TPP1 including seven essential amino acids (E168, E169, E171, R180, L183, L212 and E215), called the TEL patch (TPP1 glutamate (E) and leucine (L)-rich patch), that is responsible for the interaction between TPP1 and telomerase (Nandakumar et al., 2012; Sexton et al., 2012; Zhong et al., 2012). In addition to data from *in vitro* pull-down and telomerase activity assays showing the importance of the TEL patch for telomerase function, it was also shown that the TEL patch

mutations decrease the extent of telomere elongation by telomerase in cultured human cells (Nandakumar et al., 2012). In 2018, a new region in the very N-terminus of the OB domain termed NOB was shown to also be important for recruiting telomerase to telomeres as well (Grill et al., 2018). Thus, TPP1 uses both the TEL patch and NOB regions to bind TERT.

Previous work has also shed light on the residues on TERT that are required for telomerase binding to TPP1. Functional data suggests that the TEN domain is essential for telomerase recruitment to telomeres through a direct ionic interaction between K78 of the TEN domain and E215 of the TEL patch of TPP1 (Schmidt et al., 2014; Zaug et al., 2010). We have also learned a lot about the structure of mammalian telomerase from recent cryo-EM studies (Ghanim et al., 2021; He et al., 2021; Jiang et al., 2018; Nguyen et al., 2018). The TEN domain and IFD have been shown to interact through a surface named IFD TRAP. Through a mutagenesis screen, key mutations in the TEN domain and IFD TRAP were found to be required for telomerase recruitment to telomeres, highlighting the importance of these domains of TERT in telomerase recruitment to telomeres (Tesmer et al., 2019). This is in agreement with previous studies implicating the IFD in telomere maintenance and telomeropathies (Chu, D'Souza, et al., 2016; Chu, MacNeil, et al., 2016). Modeling the structure of the human telomerase-TPP1 complex based on currently available structural data suggests that two distinct patches on the TEN and IFD domains of TERT are oriented toward the TEL patch and NOB regions of TPP1, forming the structural basis for telomerase recruitment to telomeres (Chu, D'Souza, et al., 2016; Chu, MacNeil, et al., 2016; Tesmer et al., 2019).

1.4 Telomerase knockout mice and human telomeropathies

Telomerase is expressed in germline and somatic stem cells. Germ stem cells form gametes to generate offspring, while somatic stem cells bear the burden of tissue regeneration and repair throughout life. Stem cells can be pluripotent or multipotent with the ability to self-renew and/or differentiate. Telomerase is active in somatic stem cells but over time telomerase activity declines and telomeres shorten, providing the basis for the strong correlation between telomere length and age of an individual (Shay & Wright, 2010). In contrast, germ cells maintain telomere length throughout life, consistent with the evolutionary pressure to avoid penalizing an offspring with shorter starting telomere length in their cells as a result of being born later in the parent's life (de Lange et al., 1990). Studies looking at telomerase KO (either TR or TERT) in mice have demonstrated the importance of proper functioning telomerase at the organism level. It was found that such mice exhibit infertility and reduced regeneration in highly proliferative organs following injury such as in the skin, GI, and hematopoietic system (Blasco et al., 1997; Herrera et al., 1999; Lee et al., 1998; Rudolph et al., 1999). These mice also had shorter lifespans (Herrera et al., 1999). It's important to note that most of these phenotypes did not emerge until later generations as laboratory mice have abnormally long telomeres and successive breeding of homozygous mutants is required to reveal a telomere shortening phenotype. In humans, much of what we have learned about telomerase deficiency is from diseases such as dyskeratosis congenita (DC) and other telomeropathies.

Germline mutations that compromise telomere length maintenance result in diseases termed telomeropathies or telomere biology disorders (TBD) (Ballew & Savage, 2013; Savage, 2014). TBDs are a heterogeneous group of diseases that result in a range of clinical conditions often

caused by severely short telomeres and mutations in proteins important for telomerase function or telomere maintenance. Some of the telomeropathies that plague patients with TBDs span a spectrum of symptoms that manifest with bone marrow (BM) failure, pulmonary fibrosis, increased cancer risk, or even premature greying. Although these diseases are mostly caused by mutations in a number of different genes, the cause of the disease is generally considered to be deficiency of telomerase and telomere shortening, leading to reduced function of stem cells. To date, mutations in 14 genes have been implicated in the etiology of TBDs: *DKC1*, *NOP10*, *NHP2*, *NAF1*, *PARN*, *ZCCHC8*, *WRAP53* (codes for TCAB1), *RTEL1*, *CTC1*, *STN1*, *TERT*, *TERC* (codes for TR), *TINF2* (codes for TIN2), and *ACD* (codes for TPP1) (Grill & Nandakumar, 2020). RTEL1, STN1, and CTC1 are proteins important for telomere replication. TCAB1/WRAP53, PARN, ZCCHC8, NOP10, NHP2, NAF1, DKC1, TERC and TR are important for telomerase maturation and assembly, while TIN2 and TPP1 are shelterin components as already described above. Mutations in one of the 14 genes can result in different diseases depending on where the mutation lies in the gene, the dosage, and other associated factors such as inheritance of short telomeres. Due to the various manifestations of disease strongly indicative of somatic stem-cell failure, TBDs are also referred to as stem-cell biology disorders.

Telomeropathies display an earlier onset and worse prognosis of the disease in later generations, a phenomenon known as genetic anticipation. Genetic anticipation in these diseases results from progressive shortening of telomeres caused by inheritance of both short telomeres and the causative mutation from the affected parent's gamete.

1.4.1 Dyskeratosis congenita

The most prominent of telomeropathies is dyskeratosis congenita (DC). DC is a rare inherited disorder that can present with a broad phenotypic spectrum, including a diagnostic triad of epithelial manifestations (dysplastic nails, abnormal skin pigmentation, and oral leukoplakia) (Dokal, 2011). Although rare, DC is the second most common type of inherited BM failure system. BM failure is usually the cause of mortality in patients with DC, accounting for 80% of deaths followed by pulmonary disease and cancer.

Patients with DC can present very differently and do not always require the presence of the triad as DC can present with variable expressivity. Patients with DC may also present with several other clinical features including pulmonary fibrosis, liver disease, immune deficiency, dental and bone defects, endocrine, urological, neurological deficiencies, and/or cancer (Niewisch & Savage, 2019).

DC can be inherited in an X-linked, autosomal dominant or autosomal recessive manner, the most common being the X-linked form caused by mutations in Dyskerin (DKC1). There are also cases of *de novo* germ line mutations causative of DC often arising in TIN2. However,30% of the genetic cause of DC is still unknown, suggesting there may be genes not yet discovered. Typically, DC presents in children but more mild forms of the disease can present later in life. More severe forms of DC are Revesz syndrome and Hoyeraal-Hreidarsson, which present during infancy and often result in BM failure early in life. Patients identified with this disease have been found to harbor mutations in *TERT, TERC, DKC1, NOP10, NHP2, PARN, WRAP53, ACD, TINF2, RTEL1,* and *CTC1* (Grill & Nandakumar, 2020; Tummala et al., 2018).

1.4.2 Revesz syndrome

Revesz syndrome presents in early childhood, and like DC, can present with the classical triad and BM failure. However, unlike DC, Revesz syndrome is also associated with cerebellar hypoplasia, cerebral calcifications, developmental delays, and exudative retinopathy (Savage, 2014; Savage & Bertuch, 2010). Patients identified with this disease have been found to harbor mutations in the shelterin gene *TINF2*.

1.4.3 Hoyeraal-Hreidarsson (HH)

HH is also a very severe form of telomeropathy. Patients with HH suffer developmental delays, intrauterine growth retardation, immunodeficiency, and ultimately die of BM failure at an early age. They can present with some of the symptoms of the diagnostic triad of DC, but due to their young age may not present all of them (Guo et al., 2014; Kocak et al., 2014; Savage, 2014). Patients identified with this disease have been found to harbor mutations in *DKC1, RTEL1, PARN, TINF2, WRAP53, TERT, TERC,* and *ACD*.

1.4.4 Aplastic anemia (AA)

AA is a common complication in patients with DC, however, it is now considered its own TBD. Patients with AA can present at any age, but this disease is typically associated with adults. AA presents with pancytopenia, which is the reduction in all cells in the peripheral blood due to defects in hematopoiesis. Patients with AA have been found to harbor mutations in *TERT, TERC, TINF2* and *ACD* (Guo et al., 2014; Mason & Bessler, 2011).

1.4.5 Idiopathic pulmonary fibrosis (IPF)

Similar to patients with AA, patients with IPF tend to also have mutations in telomerase. These patients suffer chronic and progressive lung disease that is caused by shortening of telomeres in alveolar cells of the lungs that cause them to senesce (Armanios, 2012). Patients with IPF tend to present later in life compared to other TBDs. Interestingly, studies comparing patients with IPF and BM failure were found to be predictive of germline mutations in telomerase with 100% accuracy (Parry et al., 2011). In addition to *TERT* and *TERC* mutations, *PARN, ZCCHC8, NAF1, DKC1* and *TINF2* mutations are also associated with IPF.

1.5 Modeling telomeropathies in mice

Fundamental differences between mouse and human telomere and telomerase biology complicate the use of mice to study human telomerase function. For example, laboratory mice have much longer telomeres than humans (~50 kb vs 10-15 kb) (Kipling & Cooke, 1990). Additionally, telomerase transcript is present in all adult tissues in mice compared to humans where expression is limited to somatic and germ stem cells (and reactivated in cancer cells) (Forsyth et al., 2002). Nevertheless, telomerase KO mouse models have provided insights into the differential manifestation of phenotypes in KO mice versus humans suffering from telomeropathies. Notably, when telomerase is knocked out in mice, they are viable (Blasco et al., 1997; Herrera et al., 1999; Lee et al., 1998). Complete KO of the mouse telomerase RNA subunit ($mTR^{-/-}$) resulted in a decrease in telomere length in successive generations, as expected from genetic anticipation. Surprisingly, the mice did not develop any overt BM failure even after six

generations. Unlike patients with DC, the *mTR*$^{-/-}$ mice showed no uniform hematopoietic failure through complete blood count (CBC) or altered cellular composition in the spleen and BM by flow cytometry under steady-state conditions (Lee et al., 1998; Rudolph et al., 1999). However, under conditions of stress, such as caused by serial BM transplantation and/or severely short starting telomere length, hematopoietic defects did appear in *mTR*$^{-/-}$ mice (Allsopp et al., 2003; Armanios et al., 2009; Choudhury et al., 2007; Rossi et al., 2007; Samper et al., 2002; Sekulovic et al., 2011). While some hair graying or alopecia occurred in later generation *mTR*$^{-/-}$ mice, the diagnostic triad of cutaneous DC symptoms was also absent (Rudolph et al., 1999). DC-like features appeared in genetic backgrounds combining telomerase KO with KO of the shelterin protein Pot1b (Hockemeyer et al., 2008) or in strains of laboratory-derived inbred mice with short telomeres (e.g., CAST/EiJ) (Armanios et al., 2009), but not in the wild-type laboratory strain. Despite a clear lack of spontaneous BM failure in *mTR*$^{-/-}$ mice under steady-state, a conspicuous infertility phenotype emerged in late-generation *mTR*$^{-/-}$ mice (Lee et al., 1998). Fertility diminished in both males and females, and deeper analysis revealed morphological defects in male and female reproductive organs and apoptotic clearance of germline cells in the early stages of sperm development (Hemann et al., 2001; Lee et al., 1998).

Telomerase deletion in mice does not recapitulate the somatic stem cell deficiency seen in DC patients and instead points to a selective disruption of germline stem cells in the absence of telomerase. However, it has not been established if the observed reproductive phenotypes are the result of complete KO of telomerase, which has been proposed to have non-telomeric roles in the cell (Akincilar et al., 2021), including regulation of wnt signaling (Park et al., 2009), NF-κB-dependent transcription (Ghosh et al., 2012) and RNAi pathways (Maida et al., 2009). While

these non-canonical functions have been the focus of much debate (Friedman, 2011; Listerman et al., 2014; Strong et al., 2011), they prevent us, at least in theory, from unequivocally and exclusively assigning all telomerase KO phenotypes to the loss of telomere length maintenance by telomerase. Moreover, a full telomerase KO is unlikely to propagate in the human population. DC mutations provide a physiologically relevant avenue to evaluate the importance of telomere length regulation in different tissues, including those of the soma and germline. DC mutations in the *TINF2* gene coding for shelterin protein TIN2 have been modeled in mice, but their underlying mechanism is complicated, with several proposed models relying both on telomerase-dependent and independent modes of action. With most pathogenic *TINF2* mutations being heterozygous and *de novo*, understanding their molecular mechanism has been challenging (Walne et al., 2008). TIN2 is an essential component of shelterin and mutations that disrupt end-protection would result in massive genome instability and inviability. In agreement with this, mutations in *TINF2* tend to cluster within a specific region known as a DC hotpot that is outside of all of TIN2's end-protection domains (Frescas & de Lange, 2014). Patients were found to harbor shorter telomeres but intact telomerase levels (Yang et al., 2011). Two studies have shown using human cancer cell lines *in vitro* that overexpression of TIN2 mutant variants resulted in telomere shortening, though one of these studies revealed no change in telomerase activity despite pulling down less TR and another showed a reduction in telomerase recruitment (Frank et al., 2015; Yang et al., 2011). This aligns with other studies that have implicated TIN2 pathogenesis to be independent of telomerase-mediated telomere length maintenance. One study found that TIN2 TBD mutant variants *in vitro* resulted in a cohesion defect at telomeres that could contribute to the telomere erosion we see (Canudas et al., 2011). Another group created a TIN2 TBD mutant mouse model, and surprisingly, these mice were not viable, indicating

homozygosity of TIN2 K280E (mTIN2 K267E) is lethal. Furthermore, heterozygous mTIN2 K267E mice in a *mTR*$^{-/-}$ background resulted in shorter telomeres than in *mTR*$^{-/-}$ mice, lending credence to the idea of a telomerase-independent mechanism for telomere length maintenance (Frescas & de Lange, 2014). Regardless of the precise mechanism(s) underlying *TINF2* mutations in telomeropathies, it is clear that these mutations are not ideal for assessing the physiological importance of telomerase-mediated telomere lengthening.

1.6 Hematopoiesis development

BM failure as the primary cause of mortality in telomeropathies suggests that proliferating hematopoietic cells succumb to the end-replication problem in these patients. Hematopoiesis is the process by which blood is formed. The key lymphoid organs are the BM, thymus, spleen, and lymph nodes with the primary source being the BM (Doulatov et al., 2012). All blood cells arise from a hematopoietic stem cell (HSC), a multipotent stem cell that can self-renew and differentiate (Fig. 1.2). Consequently, blood is one of the most highly regenerative tissues. A major distinction between comparing human and mice HSCs is that in mice, HSC can be separated into three categories: long-term HSCs (LT-HSCs), intermediate-term HSCs (IT-HSCs), and short-term HSCs depending on duration of repopulation (Doulatov et al., 2012). HSCs are indispensable for lifelong blood production. HSCs are responsible for the differentiation of all blood cells originally deriving from either a myeloid progenitor cell or lymphoid progenitor cell and therefore the hematopoietic system can be divided into two main branches, the myeloid and lymphoid branches. As these progenitor cells differentiate, these intermediates eventually become limited and assume the identity of a terminally differentiated blood cell (e.g., red blood cells and innate immune cells are derived from myeloid progenitor

cells and adaptive immunity cells are derived from lymphoid progenitors). Studying HSC and the hematopoietic system from human samples can be challenging but fortunately the pathways and cells that are critical for hematopoietic development are mostly conserved in mice. Much work has already been done to optimize mouse models, primary, and immortal cell lines to better elucidate the key signals that arise during blood development and what occurs in the context of disease. A powerful tool that has driven much of what we know of hematopoiesis is flow cytometry, which allows these cell types to be defined by cell surface markers.

1.7 Germline development

Proliferation of the germline is also expected to suffer from the disruption of telomerase-mediated telomere length maintenance, potentially providing an explanation for why telomerase KO mice ultimately fail to reproduce. Germline proliferation is part of a larger developmental program that is called spermatogenesis in males and oogenesis in females. The proliferative stages of these programs, which are likely to depend on telomerase-mediated telomere length maintenance, occurs in females while they are still in the womb. As the same steps occur in a sexually mature male testis, that is more amenable to investigation, much of our understanding of germline proliferation comes from studying the male germline. Spermatogenesis involves three major developmental phases: spermatogonial proliferation, spermatocyte differentiation, and spermiogenesis, all of which occur in the seminiferous tubules of the testis. These developmental phases occur asynchronously in a radially organized manner, initiating at the basement membrane and moving toward the lumen as spermatogenesis proceeds (Fig. 1.3) (Larose et al., 2019). The germline stem cells reside along the basement membrane and undergo a series of mitotic divisions before differentiating to form primary spermatocytes. Primary spermatocytes

enter meiosis I to produce secondary spermatocytes, which complete meiosis II to generate early spermatids. Spermatids then undergo spermiogenesis, which is a 16-step process defined by the development of the acrosome from early spermatid (no acrosome, step 1) to premature spermatozoa (hooked acrosomes, step 16) (Nakata et al., 2015). In addition to hosting germ cells, seminiferous tubules also contain Sertoli cells. Sertoli cells are somatic cells that are essential "nurse" cells critical for germ cell development and the progression of spermatogenesis. These cells not only contribute to the niche required to maintain spermatogonia but also provide growth factors and nutrients for the developing germ cells (França et al., 2016). As opposed to hematopoiesis, which is routinely investigated using flow cytometric methods, spermatogenic development is most readily studied using histological and IF-based methods due to the availability of germ cell type-specific markers.

1.8 The TPP1 K170Δ telomeropathy mutation

Using exome sequencing, a mutation was identified in TPP1 in a family affected by the most severe form of DC, HH (Kocak et al., 2014). The proband (NCI-275-1) was an identical twin whose brother died at 4 months. He presented with clinical features during the first year of his life and required regular platelet and red blood cell transfusions for BM failure at barely 20 months of age and ultimately required a BM transplant by age 3. He had inherited the mutation from his father who did not present with DC, however, he harbored very short telomeres, premature gray hair, and minor dental abnormalities. His three sisters did not inherit the mutation and presented as healthy, although they harbored telomeres at the first percentile or less. This marked the first-identified telomeropathy mutation in TPP1. The mutation was located amidst

the TEL patch on the surface of TPP1 and is the deletion of a single basic amino acid K170 (K170Δ) that is surrounded by the TEL patch residues E168, E169, and E171.

The same variant mutation (K170Δ) was identified in another family with a history of aplastic anemia, in which the proband had pancytopenia at age 8 with their mother presenting with thrombocytopenia in her 20s and her grandmother having mild macrocytic anemia and BM defects (Guo et al., 2014). In 2018, whole exome sequencing revealed the first instance of homozygous TPP1 OB-fold NOB variants in patients from two unrelated families with symptoms of DC including short telomeres, leukoplakia, BMF, and AA (Tummala et al., 2018). Together, these studies demonstrate the *in vivo* ramifications of mutations in TPP1 NOB and TEL patch in human disease.

Extensive work has been performed to reveal the mechanism by which TPP1 K170Δ affected telomere maintenance in human cells in culture. K170Δ abrogates telomerase recruitment to telomeres and reduces the ability of TPP1 to stimulate telomerase processivity *in vitro* (Kocak et al., 2014). However, consistent with this mutation being outside of TPP1's end protection domains, it does not impact binding to POT1 or the protection of telomeres *in vivo* (Bisht et al., 2016; Grill et al., 2021; Kocak et al., 2014). CRISPR-Cas9 mediated knock-in of one allele of K170Δ into HEK 293T cells retaining one wild-type (WT) allele resulted in a progressive shortening of telomeres with population doubling, suggesting that this one amino acid deletion in TPP1 protein is sufficient to shorten telomeres in human cells (Bisht et al., 2016). Structural analysis of TPP1 OB-containing K170Δ suggests that the K170 residue ensures proper orientation of the acidic residues in the TEL patch loop to facilitate TERT binding (Bisht et al.,

2016). Together, these studies provide a structural and biochemical basis for telomere shortening caused in the proband as a result of decreased telomerase recruitment in his stem cells. Thus, the wealth of data surrounding TPP1 K170Δ that directly link the disruption of protein structure and function caused by this mutation to telomere shortening makes it a valuable tool to investigate telomerase-mediated telomere length maintenance in the mouse soma and germline.

In the following chapters, I will show how we introduced the equivalent of human TPP1 mutation K170Δ in mice, TPP1 K82Δ, and performed a detailed investigation of hematopoietic (chapter 2) and germline development (chapter 3). This is the first mouse model to evaluate the importance of telomerase-mediated telomere lengthening without perturbing end-protection, or the telomerase holoenzyme. Our study also marks, to our knowledge, the most in-depth analysis of the stem cell compartments involved in both hematopoiesis and reproduction in a mouse model of a DC mutation. We observed that TPP1 K82Δ shortened telomeres with successive generations. However, K82Δ did not lead to BM failure or other defects in the hematopoietic hierarchy. In stark contrast, K82Δ mice showed reproductive defects that ultimately resulted in sterility in late generations, suggesting that telomere shortening induced by a single amino acid deletion in TPP1 is sufficient to elicit a mouse germline defect and infertility. Our studies support a model wherein the mouse germline, but not the mouse BM, is especially vulnerable towards defects in telomerase-dependent telomere length maintenance, having important implications for the differential sensitivities of mice and humans towards telomere shortening.

1.9 Figures

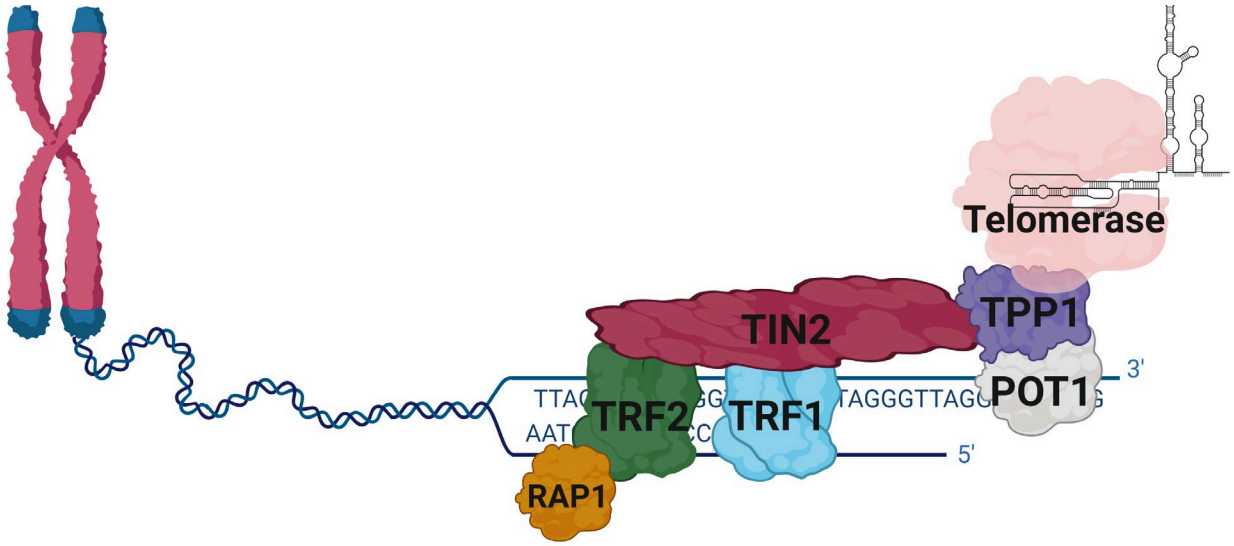

Figure 1.1 Schematic of shelterin and telomerase at telomeres.

Cartoon of a chromosome displaying how shelterin caps chromosome ends created on biorender.com. TRF1 and TRF2 bind double-stranded telomeric DNA. RAP1 binds TRF2. TIN2 bridges TRF2 and TRF1 with TPP1, which recruits the single-stranded telomeric DNA-binding protein POT1. Telomerase is recruited to the chromosome end by TPP1.

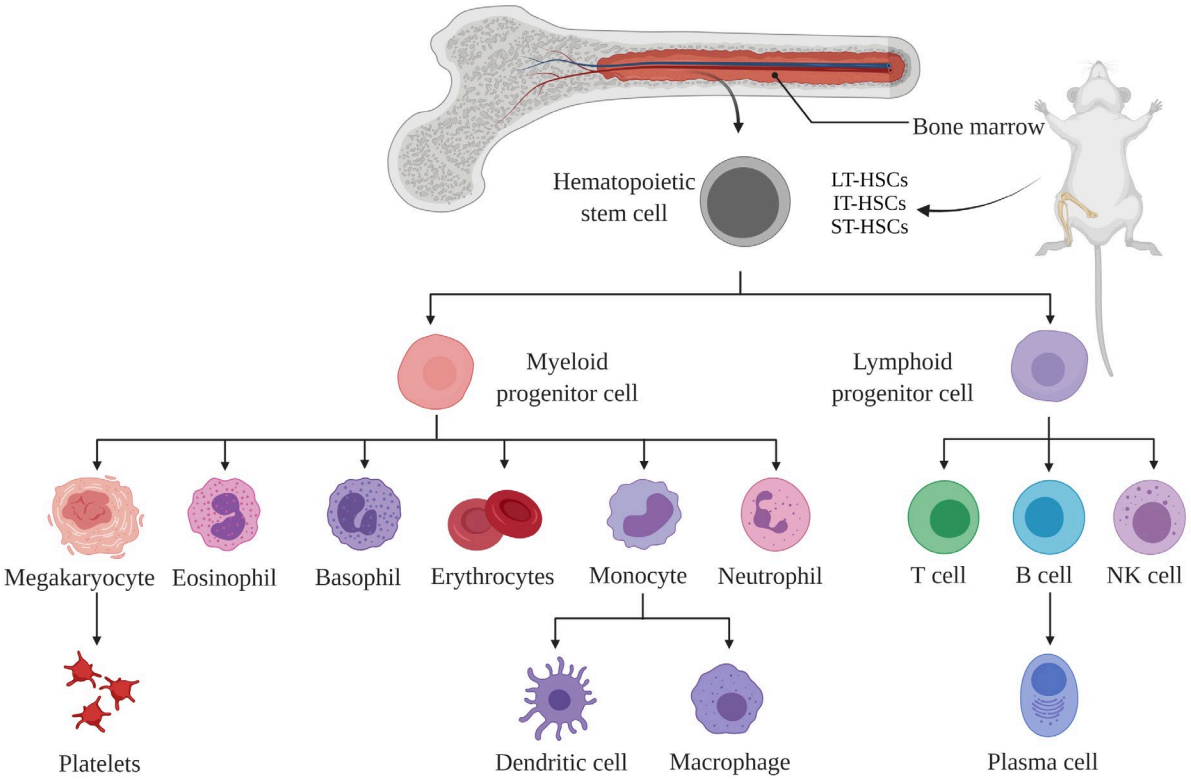

Figure 1.2 Hematopoietic lineage: stem cell differentiation from bone marrow.

Cartoon of the differentiation scheme of hematopoietic stem cells created and modified from biorender.com. HSCs from the BM can either self-renew or differentiate into myeloid or lymphoid progenitor cells. These intermediate progenitors then give rise to more differentiated cell types that comprise the peripheral blood system.

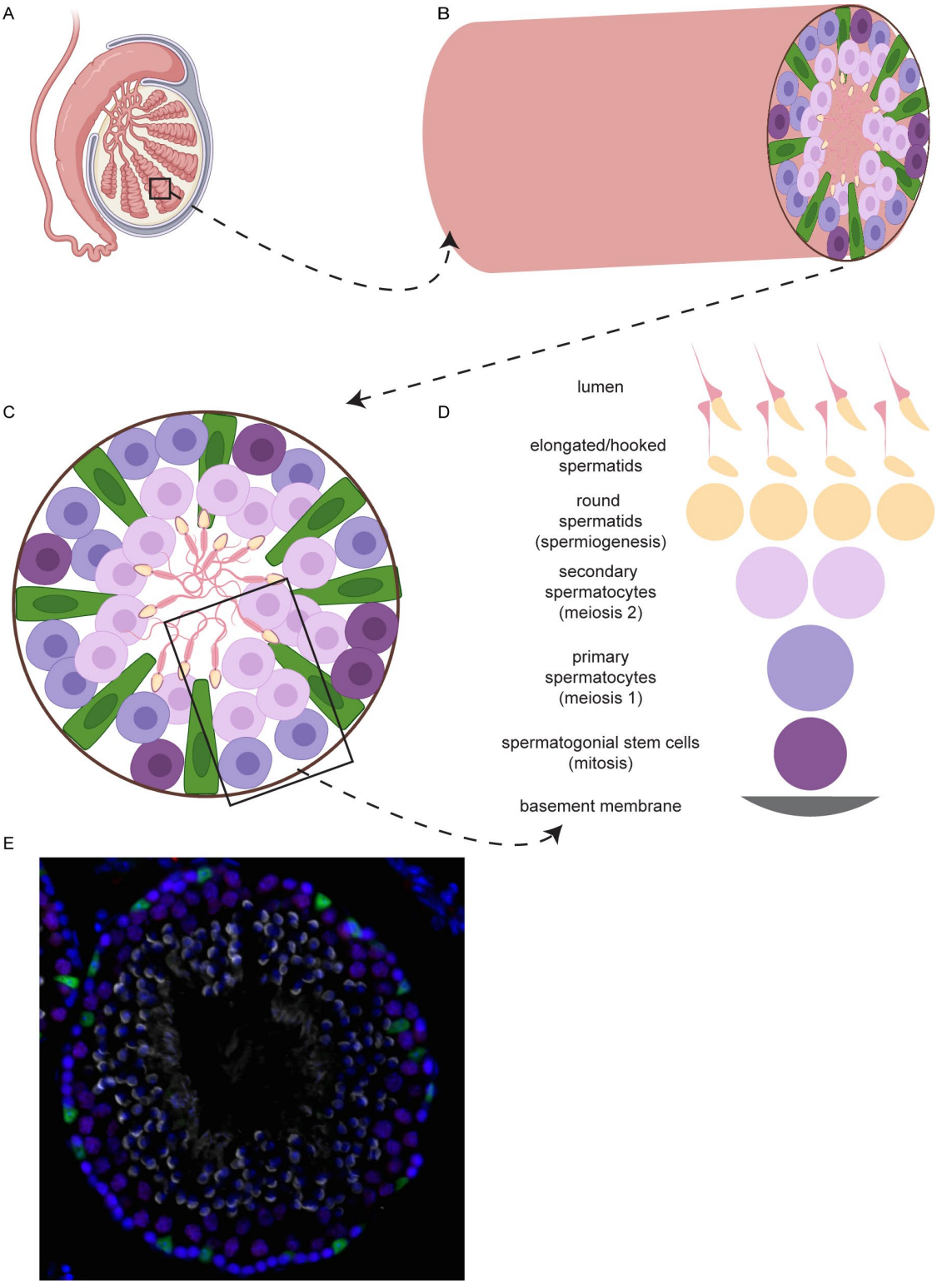

Figure 1.3 Schematic for seminiferous tubule organization and spermatogenesis

(A) Cartoon of testis created on biorender.com. (B) Magnified view of a seminiferous tubule with a cross-section of germ cells and somatic Sertoli cells. (C) Cartoon of a seminiferous tubule cross-section showing Sertoli cells (green), spermatogonia (dark purple), primary spermatocytes (light purple), secondary spermatocytes (pink), and spermatids/spermatozoa in the lumen. (D) Schematic to show the spatial orientation of germline cells within a tubule. (E) Representative image of a G5 WT testis cross-section. Sertoli cells (green), spermatocytes (red/purple), nuclei (blue), spermatids (grey).

Chapter 2 : Role of TPP1 K82Δ in the Hematopoietic System

Portions of this chapter have been adapted from the following publication:

Graniel JV, Bisht K, Friedman A, White J, Perkey E, Vanderbeck A, Moroz A, Carrington LJ, Brandstadter JD, Allen F, Shami AN, Thomas P, Crayton A, Manzor M, Mychalowych A, Chase J, Hammoud SS, Keegan CE, Maillard I, Nandakumar J. (2021). Differential impact of a dyskeratosis congenita mutation in TPP1 on mouse hematopoiesis and germline. Life Sci Alliance 5(1):e202101208.

AUTHOR CONTRIBUTIONS: J.V.G., K.B., J.N., I.M., and C.E.K. conceived the study. K.B. performed the CRISPR-editing experiments in conjunction with the Transgenic Animal Core of the University of Michigan. J.V.G. was involved in the design, execution, and analysis of all remaining experiments with assistance from others as indicated below. A. Moroz, P.T., A.C., M.M., A. Mychalowych, J.W., and J.V.G., performed mouse maintenance, including feeding, setting up breeding cages, genotyping, terminal harvests, and organ preservation/embedding. A.F., E.P., A.V., J.V.G., L.J.C, J.D.B, and F.A. performed hematopoiesis experiments. J.V.G adapted Flow-FISH for mouse BM telomere length determination following up on pilot experiments by J.C. All authors contributed to data analysis. J.V.G., I.M., and J.N. developed the first draft of the manuscript, followed by contributions from C.E.K, and S.S.H., and input from all authors

2.1 Introduction

Cells that have a higher replicative burden throughout the organisms' life (e.g., somatic stem cells and/or germ stem cells) are more vulnerable to the loss or defects in telomere length maintenance. Therefore, it is not surprising that patients with telomeropathies succumb to BM failure as the highly proliferative hematopoietic system requires proper telomerase function and telomere maintenance.

Severe shortening of telomeres in patients with DC results in hematopoietic failure eventually resulting in BM failure, which is the most common cause of death (Armanios & Blackburn, 2012; Dokal, 2011; Niewisch & Savage, 2019). Given the heterogeneity of the disease including differing levels of severity, there is a range of symptoms that result from DC including an 11-fold increased risk of cancer (e.g., leukemia, etc.) and hematological concerns like cytopenias, which can be found in 86% of patients in the dyskeratosis congenita registry (Savage & Alter, 2009).

Hematopoietic stem cells (HSCs) and hematopoietic progenitors derived from DC patients exhibit reduced self-renewal, providing a cellular basis for BM failure (Jones et al., 2016). Hematopoietic stem cells in *acd/acd* hypomorphic mice were found to be severely defective in transplantation assays and complete inactivation of *ACD* results in severe depletion of hematopoietic progenitors (Jones et al., 2014). Other models have looked at the role of shelterin components and its influence on hematopoiesis. The only mouse model to date to show phenotypes characteristic of human dyskeratosis congenita is a $POT1b^{-/-}$ $mTR^{+/-}$ mouse mutants (Hockemeyer et al., 2008). However, mouse models that show defects in hematopoiesis have

only done so in the context of end de-protection. In *mTR*$^{-/-}$ mice, under steady state conditions, there is no spontaneous BM failure. As I described in Chapter 1, the symptoms seen in patients with DC are not recapitulated in mouse models of telomeropathies. Given the robust data surrounding the human telomeropathy mutation TPP1 K170Δ, we have an ideal tool to study the importance of telomerase-mediated telomere length maintenance that in humans in the absence of chromosome end de-protection or telomerase deletion.

Here I report the generation of mice with the equivalent mutation of a single amino acid mutation in TPP1 K170Δ in a region that affects only end replication and keeps end protection intact. This chapter will focus on how homozygous deletion of this amino acid impacts the mouse hematopoietic system.

2.2 Materials/Methods

Oligonucleotides and Sanger DNA sequencing: All DNA oligonucleotides, including PCR primers, DNA coding for guide RNAs, and the ssODN repair templates were purchased from Integrated DNA Technologies. Sanger sequencing was performed in the Advanced Genomics Core at the University of Michigan.

Mice: A CRISPR-Cas9 mouse line carrying a specific mutation in the *TPP1* gene (K82Δ; equivalent to human mutation K170Δ) in a C57BL/6 (B6) background was generated at the Transgenic Animal Model Core at the University of Michigan under the supervision of Dr. Thomas Saunders. Purified DNA/RNA was microinjected into fertilized eggs obtained by mating (C57BL/6 X SJL)F1 or C57BL/6 female mice with (C57BL/6 X SJL)F1 male mice and

pronuclear microinjection was performed as described (Pease et al., 2011). A heterozygous founder was obtained using this approach and was genotyped using Sanger sequencing for the existence of the K82Δ mutation and the absence of any other unwanted changes in the flanking regions on the *Acd* locus. The founder mouse was crossed with WT B6 mouse to generate the line and backcrossed for 4 generations, thereby eliminating any off-target effects of genome editing. Once backcrossed, heterozygous mice were intercrossed to produce homozygous mice starting with generation 1 (G1). Homozygous mice were crossed together to breed successive generations (G2, G3, and so on). +/+ (WT) mice were also bred in parallel. All animals were housed in environmentally controlled conditions with 14 h light and 10 h dark cycles with food and water provided *ad libitum*. Mice were harvested at the indicated times for the generations tested in this study: G1: 23-25 months, G3: 16-16.5 months, G4: 14-21 months, and G5: 15.5-17 months. All protocols were approved by the Institutional Animal Care & Use Committee (IACUC) at the University of Michigan and the University of Pennsylvania and comply with policies, standards, and guidelines set by the States of Michigan and Pennsylvania and the United States Government.

Screening for CRISPR-Cas9 editing and mutagenesis efficiency: In preliminary experiments leading up to the generation of CRISPR-Cas9 edited mice, the efficiency of *Acd* gene editing was evaluated. For this, blastocysts were harvested after injection with guide RNAs and donor oligonucleotide template. PCR reactions were conducted using blastocyst genomic DNA as a template and primers flanking the edited *Acd* locus. KpnI digestion was conducted with the PCR products to screen for the successful editing of the *Acd* locus.

TRF analysis by Southern blot: Telomere length analysis was performed as described previously (Bisht et al., 2016) with a few modifications. Briefly, genomic DNA was isolated from harvested calf thymocytes using the GenElute kit (Sigma) after washing the cell pellets twice with PBS. Genomic DNA was similarly isolated from TPP1-S cells, which were used as a control (Grill et al., 2019). During DNA extraction, proteinase K treatment was conducted for 2.5 h at 55°C followed by incubation for 30 min at 70°C. 1 µg of genomic DNA was digested overnight with RsaI and HinfI at 37°C. DNA digests were run on a 0.7% agarose 1X TAE gel at 50V for 4.5 h. The gel was imaged using EtBr staining with a fluorescent phospho-ruler aligned to wells and gel. Next, the gel was placed in denaturation buffer for 20 min and then rinsed in water for 10 min. The gel was then placed on two sheets of Whatman 3MM filter paper for 1h at RT. Once dried, the gel was placed in neutralizing solution for 15 min. After a water rinse, the gel was pre-hybridized in prewarmed church buffer for 20 min at 55°C. After pre-hybridization, 5′ ^{32}P-labeled $(TTAGGG)_4$ oligonucleotide (labeled using [γ-^{32}P]ATP and T4 PNK; New England Biolabs) was added, and hybridization was continued overnight. After hybridization, the gel was washed thrice with 2x SSC followed by two more washes in 0.1X SSC/0.1%SDS at RT. The gel was transferred to filter paper, wrapped in plastic wrap, and exposed to a phosphorimager screen, analyzed using the Imagequant TL software, and visualized on ImageJ. The gel was calibrated (Imagequant TL software) using the known molecular weights of the radiolabeled DNA ladder run on the same gel.

Flow-FISH: This method uses fluorescence *in situ* hybridization (FISH) and flow cytometry to measure telomere length (Baerlocher et al., 2006). Single cell suspensions were prepared from BM followed by red blood cell lysis (Sigma R7757). After resuspending cells with DMEM and

4% FBS, cells were counted. Each sample was split into four different centrifuge tubes with 1 x 10^6 cells per tube. Of these tubes, two were mixed with calf thymocytes (1 x 10^6 cells) of known telomere length (determined using TRF Southern blot analysis; see below) as an internal control. One set of single and mixed samples was stained with a FITC PNA probe, and the other set was left unstained to correct for auto-fluorescence (Dako telomere kit). DNA was denatured for 10 min at 82°C and allowed to hybridize overnight. The excess probe was removed using wash solution (Dako telomere kit) and heat (40°C for 10 min). After two rounds of washing, DNA was counterstained with LDS 751 for 5 h at 4°C (protected from light using Al foil). Cells were analyzed using a BD LSRFortessa flow cytometer and data were analyzed with FlowJo (Treestar/BD). Relative telomere length was calculated as a ratio of the difference of PNA signal in mouse BM samples with and without PNA probe and the difference of PNA signal in calf thymocytes in the same tube with and without PNA probe. Relative telomere length was then multiplied by 16.521 kb, which is the TRF length of calf thymocytes determined by Southern blot analysis, to obtain absolute telomere length.

Flow cytometry: Single cell suspensions were prepared from spleen, BM, or thymus, followed by red blood cell lysis (for spleen and BM only) (Sigma R7757). The following antibodies were from BioLegend: anti-CD4 (clone GK1.5), anti-CD8 (clone 53-6.7), anti-CD11b (clone M1/70), anti-CD19 (clone 6D5), anti-CD48 (clone HM48-1), anti-CD150 (clone TC15-12F12.2), anti-Ly6C/G (Gr-1) (clone RB6-8C5), anti-B220 (clone RA3-6B2), anti-Ly6A/E (Sca-1) (clone D7), anti-Ter119 (clone TER-119), anti-CD41 (clone MWReg30), anti-CD105 (clone MJ7/18), anti-CD16/32 (clone 93), anti-CD43 (clone S11), anti-IgM (clone AF6-78), anti-CD93 (clone AA4.1), anti-CD44 (clone IM7), anti-cKit/CD117 (clone 2B8) and anti-Lineage, with an

antibody cocktail containing the following: anti-CD3e (clone 17A2), CD4 (clone GK1.5), CD8 (clone 53-6.7), TCRβ (clone H57-597), TCRγδ (clone GL3), NK1.1 (clone PK136), CD11b (clone M1/70), CD11c (clone N418), Ter119 (clone TER-119), Gr-1 (clone RB6-8C5), B220 (clone RA3-6B2), and CD19 (clone 6D5). Dead cells were excluded with Zombie Aqua Fixable Viability Dye (BioLegend). Cells were analyzed using a BD LSRFortessa flow cytometer (Becton Dickinson) and data were analyzed with FlowJo (TreeStar/BD).

Complete Blood Counts: Blood was obtained through submental or submandibular bleeding and transferred to EDTA-treated tubes. Complete blood counts were determined using the Advia 2120 (Siemens) and the Hemavet 950 veterinary analyzer (Drew Scientific).

Statistical analysis

Statistical tests were performed using Prism software (GraphPad version 8). Experiments were analyzed between WT and mutant mice only. Analysis between generations was not included as they were not conducted at the identical age or cohort size. Student's t-tests were used between WT and mutant mice for each experiment. Graphs were generated in Prism software and represented as mean with 95% confidence interval for hematopoietic data and mean with SEM for germline data. Adjusted p values for comparisons were reported as $*p < 0.05$, $**p < 0.01$, and $***p < 0.001$. M or F symbols were superscripted to denote significance in either males (M) or females (F). It should be noted that due to the many outcomes studied, there are some stochastic statistically significant results that are not consistent across genotype, generation, or sex. Independent confirmatory experiments would need to be conducted in a larger scale to follow up any of these isolated findings, especially those approaching $p = 0.05$.

2.3 Results

2.3.1 Generation of viable mice homozygous for the dyskeratosis congenita mutation TPP1 K82Δ/ K82Δ via CRISPR-Cas9 knock-in

Previous *in vitro* work in the lab demonstrated the importance of TPP1 K170 in the recruitment of telomerase (Bisht et al., 2016). It was found that this residue lies at the center of the TEL patch, allowing for the formation of a knuckle structure that directly interacts with telomerase and facilitates recruitment to the telomeres. Furthermore, deletion of K170 results in a structural change of that knuckle disrupting the interface between TPP1 and telomerase (Fig. 2.1A). Introducing the equivalent mutation in mice (Fig. 2.1B) using CRISPR-Cas9 technology in the presence of a ss oligo donor (ssODN) containing the K82Δ mutation as a template for homologous recombination, we successfully edited the mouse *Acd* genomic locus to generate a mouse heterozygous for TPP1 K82Δ (Fig. 2.1C-F). After five generations of backcrossing of this heterozygous founder to the C57BL/6 inbred background (N1 → N5), we intercrossed the resulting progeny to obtain generation 1 (G1) TPP1 K82Δ/K82Δ homozygous mice (referred to as K82Δ hereafter) and TPP1 +/+ age-matched mice (referred to as WT hereafter) as controls (Fig. 2.1G). While K170Δ is heterozygous in human DC, we studied the mutation in a homozygous context to accelerate phenotypic progression in mice. This was important as laboratory mice have significantly longer telomeres than humans (Kipling & Cooke, 1990), making it unlikely for phenotypes to appear in a heterozygous context or over a few generations. Accordingly, we intercrossed G1 K82Δ (and in parallel, G1 WT) mice to generate successive generations of mice (G2, G3, G4, and G5) using a breeding scheme closely resembling that used for the generation of *mTR*$^{-/-}$ mice (Fig. 2.1G) (Blasco et al., 1997; Herrera et al., 1999).

2.3.2 BM Flow-FISH reveals the TPP1 K82Δ mutation causes progressive telomere shortening with generation number

The gold standard in the field to measure telomeres is to perform a telomere restriction fragment (TRF) analysis by Southern blot. However, due to the extremely long telomeres of laboratory mice, this assay lacks the resolution to accurately measure the length of these telomeres without further modification. Instead, we adapted Flow-FISH, a highly quantitative approach used routinely in the clinical setting, to measure the length of telomeres in WT and K82Δ mouse BM cells (Baerlocher et al., 2006; Sekulovic et al., 2011). Flow cytometry coupled with Fluorescence *in situ* Hybridization (Flow-FISH) combines the power of high-speed single-cell analysis to evaluate distinct populations of cells with FISH to visualize telomeric DNA and measure telomere length in these cells. To optimize Flow-FISH for mouse cells and provide internal calibration controls, we used calf thymocytes, which are phenotypically distinct and contain much shorter telomeres than mouse BM cells. We hybridized a fluorescently labeled telomeric PNA probe to telomeres and used LDS-751 to stain DNA in the nucleus of mouse BM cells from mutant and WT mice (Fig. 2.2A-B). Quantitation of calf thymocyte telomere length using Southern blot analysis was used as a calibration step to calculate the length of mouse BM telomeres (Fig. 2.2C). Dot plot visualization of the fluorescence intensity in the PNA and LDS-751 channels in the presence and absence of fluorescent telomere PNA probe confirmed the distinct flow cytometric features and telomere length signals of mouse BM cells versus calf thymocytes (Fig. 2.2D-I and Fig. 2.3A-C). Histograms derived from the flow cytometry plots revealed that G1 WT BM had a mean telomere length of 38.1 kb while G1 K82Δ had significantly shorter telomeres (mean = 33.3 kb) (Fig. 2.2J and Fig. 2.3D-E). Telomeres in K82Δ BM cells shortened progressively with generation number, with G5 K82Δ BM exhibiting a mean

telomere length of 25.7 kb (Fig. 2.2J and Fig. 2.3F-G). These findings, which reveal a ~2 kb shortening of telomeres per generation in the K82Δ BM, are consistent with observations made with the equivalent human mutation, which is associated with severely shortened telomeres in affected individuals and causes telomere shortening in cultured cells (Kocak et al., 2014).

2.3.3 Analysis of complete blood counts in K82Δ mice does not reveal defects in hematopoiesis

Given that BM failure is the primary cause of morbidity in DC patients, including in the proband harboring TPP1 K170Δ, we evaluated the hematopoietic system of WT and K82Δ mice across successive generations. Complete blood counts (CBCs) were measured at multiple time points in G1 and G3 mice (Fig. 2.4). We did not observe any consistent differences between WT and mutant CBCs in either sex, within generations, or across generations, that would be reflective of BM failure in the mutant mice. Specifically for the white blood cell count (WBC), most time points did not reveal significant differences in female K82Δ mice except for a decreased WBC in G3 mice at seven months. In males, an apparent decreased WBC was observed in G1 16-month-old mice, but it was not sustained at two years of age. Male G3 K82Δ mice had a decreased WBC at seven months that was not recapitulated at 12 or 16 months of age (Fig. 2.4A). Both male and female K82Δ mice had no changes in platelets, red blood cells, or hemoglobin levels (Fig. 2.4B-D). Male but not female K82Δ mice had a mildly increased mean corpuscular volume compared to WT (Fig. 2.4E). The lack of gross changes in CBC with K82Δ is consistent with previous studies with *mTR*$^{-/-}$ mice (Lee et al., 1998).

2.3.4 Analysis of bone marrow mature and progenitor cells in K82Δ mice does not reveal defects in hematopoiesis

Peripheral blood measurements in steady-state conditions do not fully reflect hematopoietic stem and progenitor cell health in the BM. For a more comprehensive investigation of the hematopoietic system, we performed terminal harvests of G3, G4, and G5 mice, and probed stem, progenitor, and mature cell populations in the following hematopoietic and lymphoid organs: BM, spleen, and thymus. Even at the latest generations, G4 and G5 K82Δ mice showed preserved BM cellularity compared to WT mice (Fig. 2.5A-B). Flow cytometric analysis showed a preserved frequency of lineage negative (Lin^-) cells (Fig. 2.5C-E), $Lin^-Sca\text{-}1^+cKit$ (LSK) cells (Fig. 2.5F-H), and $CD150^+$ $CD48^-$ LSK cells, which are highly enriched for long-term hematopoietic stem cells (LT-HSCs), in G5 K82Δ mice compared to WT (Fig. 2.5I-K). When we quantified additional progenitor and mature cell subsets in the BM, there was no consistent change in K82Δ mice compared to WT, although selected sex-related differences were apparent (Fig. 2.6A-O).

2.3.5 Analysis of splenic cells in K82Δ mice does not reveal defects in hematopoiesis

The spleen has two major structures with different functions: the white pulp contains mainly lymphoid cells for immune responses and the red pulp which functions as a reservoir of macrophages and erythrocytes in an emergency (Coppin et al., 2018). During development, HSCs migrate into the spleen around embryonic day 14 and then migrate into the BM around embryonic day 17, resulting in HSCs residing in both hematopoietic organs. To examine K82Δ role in hematopoiesis in the spleen, we analyzed overall cellularity and downstream cell populations to gauge for hematopoietic defects in this organ. Spleen cellularity was mildly elevated in female G3 K82Δ mice but was not recapitulated in G4 or G5 and male G5 K82Δ mice showed an increase in cellularity compared to WT. However, both WT and K82Δ male mice showed a lower cellularity than G5 females and compared to G3 and G4 mice (Fig. 2.7A).

Splenic myeloid cells seemed to be generally elevated in G5 female mice compared to male mice and G5 male K82Δ mice specifically showed a mild elevation compared to WT (Fig. 2.7B). Observation of splenic B cells revealed a mild increase in female K82Δ mice at G3 that did not persist in later generations and the emergence of an increase in B cell at G5 in male K82Δ mice (Fig. 2.7C). CD8+ T cells in the spleen showed a reduction in G3 K82Δ mice compared to WT (Fig. 2.7D) and CD4+ T cells were elevated in male G5 K82Δ mice (Fig. 2.7E). There was no difference in K82Δ mice across generations in terms of TCRB+ T Cells (Fig. 2.7F), and Ter119+ erythroid cells were elevated in G3 and G5 K82Δ male mice but not in G4 or in female K82Δ mice (although levels of Ter199+ erythroid cells were elevated in female G5 mice compared to male G5 mice in both WT and K82Δ mice) (Fig. 2.7G). Considering the lack of a consistent phenotype between WT and mutant mice, we conclude that there is no discernible change in splenic cell populations that persisted over generations in K82Δ mice or were consistently shared between males and females.

2.3.6 Analysis of thymic cells in K82Δ mice does not reveal defects in hematopoiesis

The thymus is a bilobed organ that is large at birth and decreases in size with age in a process known as thymic involution (Famili et al., 2017). The thymus is the site of T cell development, furnishing cells necessary for adaptive immune function. Hematopoietic progenitor cells migrate from the BM to the thymus where they commit to the T cell lineage eventually maturing to terminally differentiated T cells. To see if loss of K82 resulted in defects in thymic hematopoiesis we analyzed early T lineage progenitors and successive downstream populations of developing thymocytes for any changes. Thymic cellularity was mildly decreased in female G4 K82Δ mice and although overall thymic cellularity was much lower for both WT and K82Δ G5 mice, there seemed to be a mild increase in K82Δ male mice compared to WT (Fig. 2.8A). In

double negative (DN) cells, we observed the greatest population in G4 mice compared to G3 or G5 WT and K82Δ mice. Furthermore, we observed a decrease in G4 female K82Δ mice compared to WT and an increase in G5 male K82Δ mice (Fig. 2.8B). G3 female K82Δ mice showed a modest increase in DN1, ETP, and DN2 populations (Fig. 2.8C-E). Male G5 K82Δ mice showed an increase in all compartments measured but this increase could be a result of the increase in cellularity observed compared to WT (Fig. 2.8A-G). Finally, terminally differentiated CD4 and CD8 double positive T cells showed a slight decrease in G4 female K82Δ mice but an increase in G5 male K82Δ mice (though all G5 mice showed decreased levels of this population compared to G3 and G4 (Fig. 2.8G). While the data seems to show a trend for an increase in thymic lineage populations in G5 male K82Δ mice, further work needs to be performed to determine if this is physiologically relevant. Considering there was no sign of overt BM failure in any of the hematopoietic compartments analyzed, we conclude that the presence of a TPP1 K82Δ mutation does not result in spontaneous BM failure in mice up to at least five generations. In agreement with our results in the BM, we did not observe skin aberrations, including fur loss or hyperpigmentation, indicating that K82Δ did not have clinically apparent effects on epidermal cell homeostasis up to G5 (data not shown). Our results, combined with the rich literature surrounding *mTR*$^{-/-}$ mice, strongly suggest a distinct resilience of the mouse BM and other somatic components to telomerase-dependent telomere shortening as compared to DC patients.

2.4 Discussion

We report the first mouse model for telomerase-dependent telomere shortening caused by a telomeropathy mutation that leaves end protection and the structure and composition of telomerase intact. Homozygosity for this mutation results in telomere shortening that is

discernible as early as in G1 and progresses with each successive generation. To our knowledge, our study also provides the most rigorous analysis of the HSC compartment in mice undergoing telomere shortening. We conducted a comprehensive analysis of the hematopoietic compartment spanning stem, progenitor, and mature cells of the BM, spleen, thymus, and blood. CBC analysis revealed age-related changes for both WT and K82Δ mice, but no consistent differences between the two genotypes were observed across time points in any of the hematopoietic compartments tested. Unlike in patients, but like telomerase KO mice, K82Δ mice do not develop spontaneous BM failure. Based on other mouse models of telomerase deficiency (Allsopp et al., 2003; Armanios et al., 2009; Choudhury et al., 2007; Herrera et al., 2000; Herrera et al., 1999; Hosokawa & Arai, 2018; Jones et al., 2016; Lee et al., 1998; Rossi et al., 2007; Rudolph et al., 1999; Samper et al., 2002; Sekulovic et al., 2011), we would predict that K82Δ hematopoiesis would become defective if exposed to severe stress caused by serial transplantations, or other types of hematopoietic stress including BM defects and possible contribution of extramedullary hematopoiesis from the spleen. However, at least in steady state, these mice are resilient to BM failure.

It should be noted that due to the many outcomes studied, there are some stochastic statistically significant results that are not consistent across genotype, generation, or sex. An even more extensive analysis at multiple time points in more mice in each generation would be needed to determine if these changes are indicative of disease. Since most of the changes were not recapitulated, their characterization was not pursued any further. The data that seems the most consistent is an increase in T lineage populations in male K82Δ mice at G5. It is possible that the thymus is more sensitive to telomere shortening in males and this could be the emergence of a

phenotype. However, compared to G3 and G4 mice, the cellularity is much lower in G5 mice and the increases in each compartment are quite modest. Though age-matched, these mice were also older than one year, and the thymus had already begun involution. A more detailed examination of this compartment could help explain some of these discrepancies.

In conclusion, a TPP1 mutation that decreases telomere length in both humans and mice causes BM failure in humans but no deleterious changes at any stage of mouse hematopoiesis for up to five successive generations of breeding.

2.5 Figures

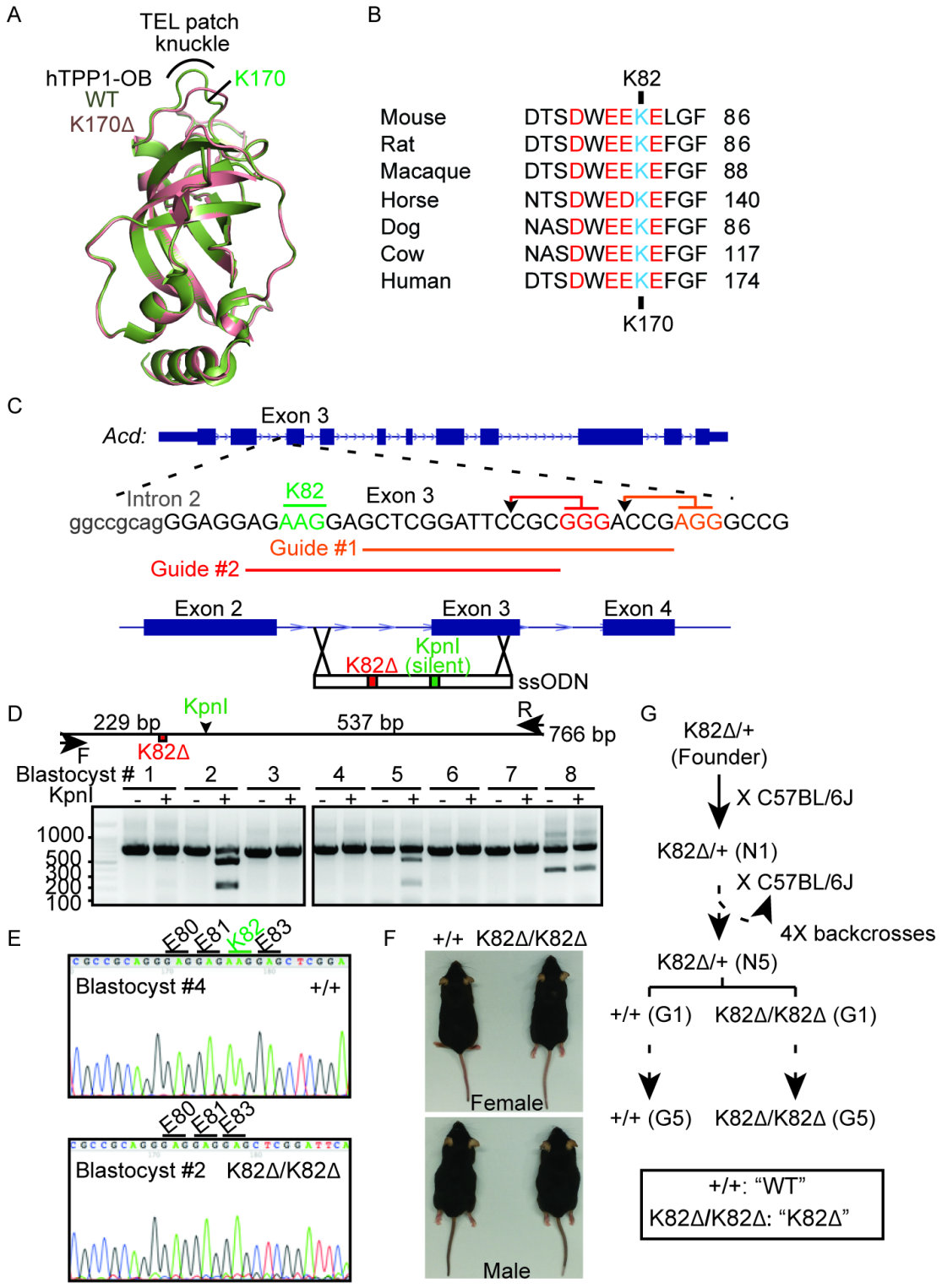

Figure 2.1 CRISPR-Cas9 generation of a mouse model of a dyskeratosis congenita mutation in TPP1.

(A) Overlay of the crystal structures of human TPP1 OB (hTPP1 OB) domains from WT and K170Δ proteins. The deletion of K170 distorts the acidic TEL patch knuckle. **(B)** Strict conservation of the TEL patch loop (acidic amino acids shown in red) that also harbors the human TPP1 K170 residue (shown in cyan) that is deleted in dyskeratosis congenita. The mouse equivalent of this residue is K82. **(C)** The PAM sites (GGG and AGG highlighted in red and orange, respectively) and Cas9 cleavage sites (arrowheads) for the two guide RNAs used to cleave the exon coding for mouse TPP1 K82Δ are shown. The schematic for the homologous recombination repair template shows not only the deletion of the K82 codon (red) but also a silent mutation that creates a KpnI site (green) for screening purposes. **(D)** PCR amplification and KpnI restriction digestion screening of 8 blastocysts after injection with guide RNAs and repair template for introducing the TPP1 K82Δ mutation. Expected sizes for PCR amplicon and its KpnI cleavage products used to screen the editing of the *Acd* locus of mouse blastocysts by CRISPR-Cas9 are shown above the gel. **(E)** Sanger sequencing of the PCR products of the indicated blastocysts (same as those analyzed in panel D) showing accurate editing of the *Acd* locus. **(F)** Images of G1 WT and K82Δ (homozygous), male and female mice. **(G)** Breeding scheme to backcross the CRISPR-edited K82Δ/+ founder mouse and generate WT and homozygous K82Δ mice that were bred for five generations (G1 → G5).

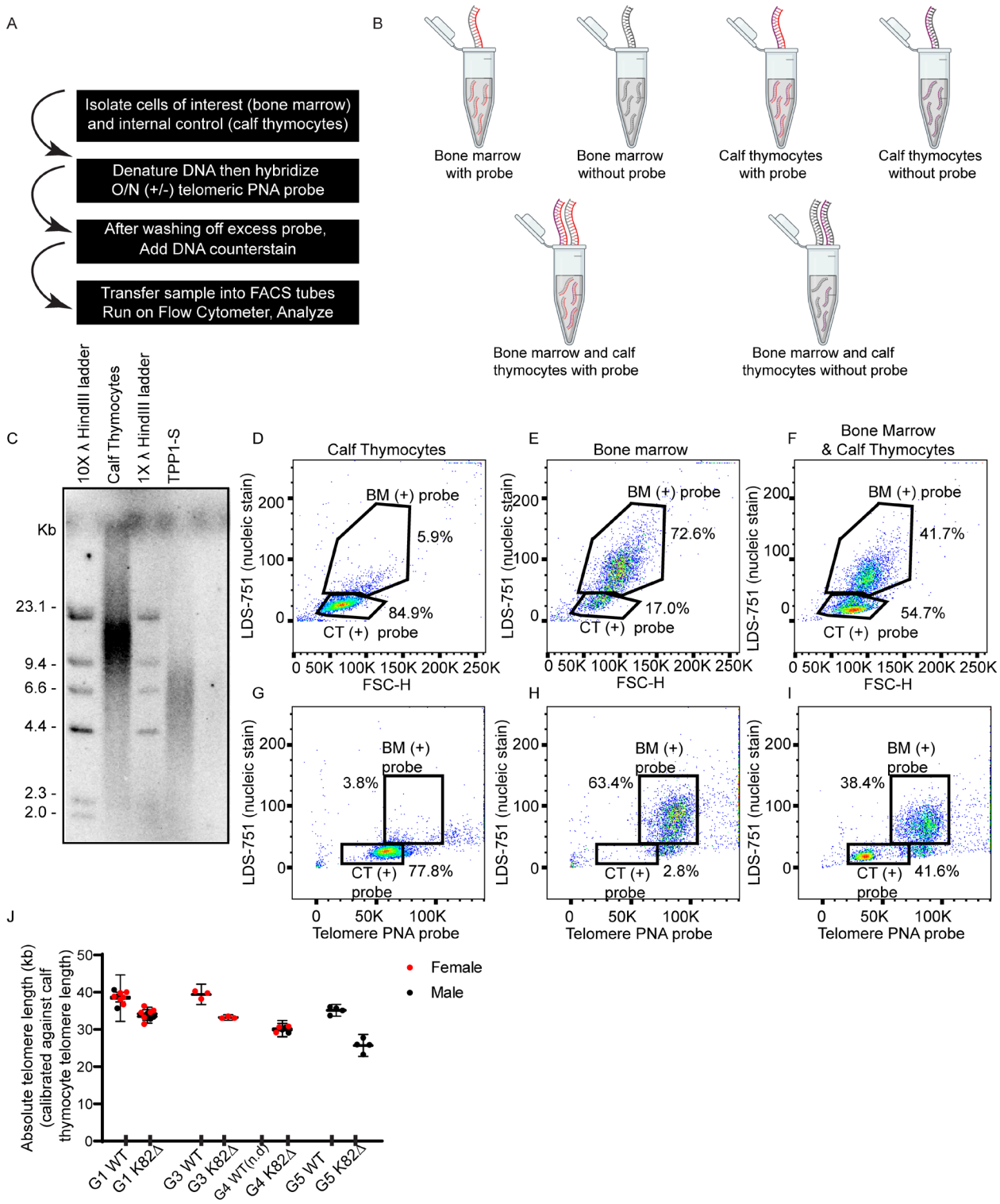

Figure 2.2 Establishment of Flow-FISH-based approach to determine BM telomere length of WT and K82Δ mice.

(A) Schematic of Flow-FISH procedure optimized for mouse BM. **(B)** Each mouse sample is run separately (visualized as grey DNA strand) and in combination with calf thymocytes (visualized as purple DNA strand; used as an internal control for telomere length and as a calibration control for determining the absolute length of mouse telomeres). Each mouse replicate includes a non-probe control to account for any autofluorescence. Red DNA strand indicates DNA with telomeric PNA probe. **(C)** Telomere restriction fragment Southern blot of genomic DNA from calf thymocytes and TPP1-S stable cell line (Grill et al., 2019) with two concentrations of λ HindIII digest DNA ladder. **(C-I)** Representative flow cytometry plots of single controls used **(D, G)** calf thymocytes-only, **(E, H)** BM-only, and **(F, I)** combined. **(D-F)** Gates were drawn based on nucleic stain signal on the y-axis and forward scatter on the x-axis and due to differences in size can be gated separately. **(G-I)** Better distinction between populations can be achieved when gated with nucleic stain signal on the y-axis and telomeric DNA probe on the x-axis instead of FSC-H. **(J)** Cumulative data for the quantitation of telomere lengths across generations showing decreased telomere length in each generation of K82Δ mice. G4 WT telomere length was not determined (n.d.). No sex differences were observed.

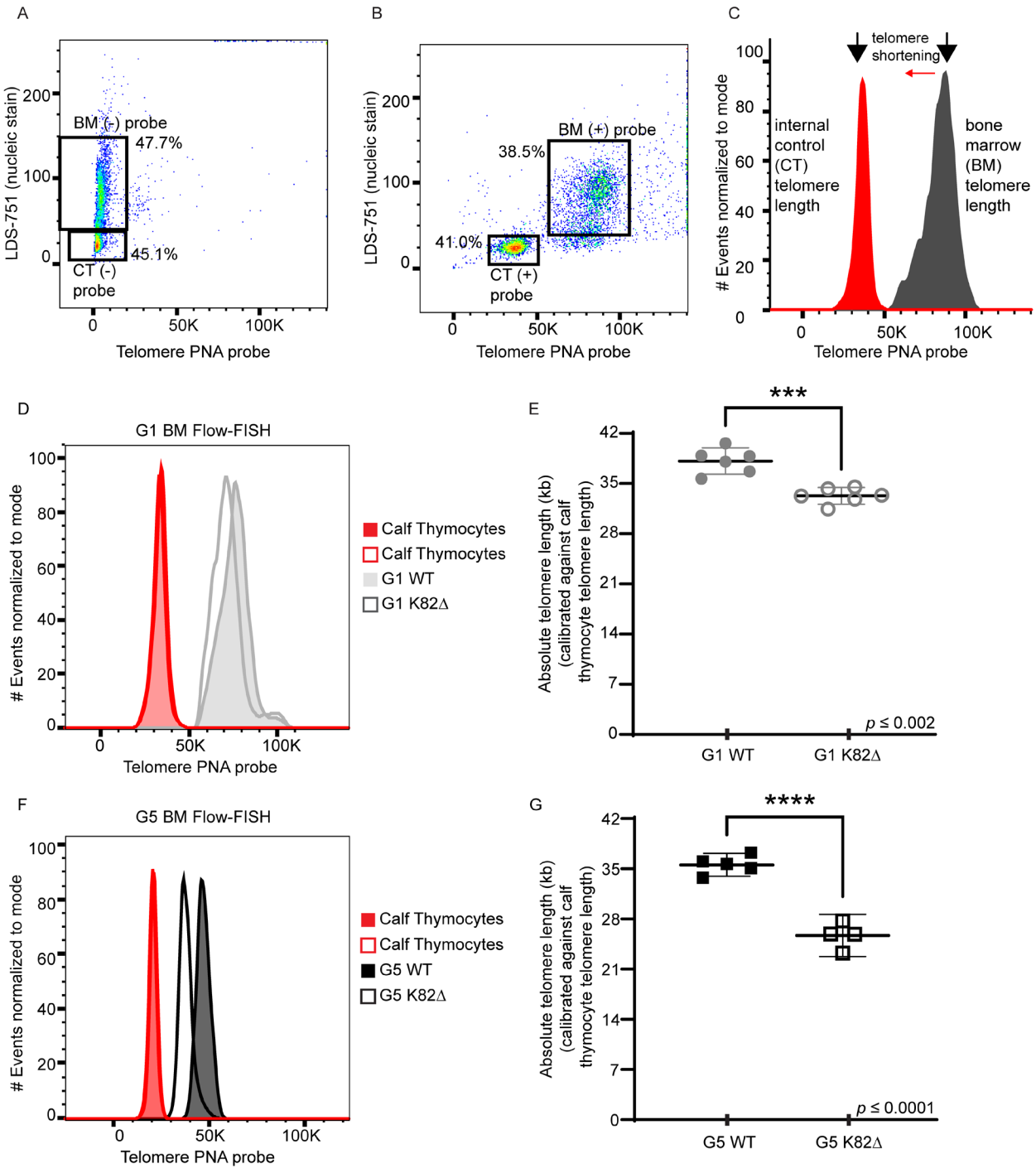

Figure 2.3 Flow-FISH to measure telomere length reveals progressive telomere shortening in K82Δ mutant mice.

(A-B) Representative flow cytometry plots of Flow-FISH of WT G1 mouse samples with **(A)** no probe and **(B)** PNA telomere probe. Gating includes calf thymocytes (+/- probe) and BM (+/- probe). **(C)** The histogram shows data with the probe. Red indicates calf thymocyte telomeric

probe signal. Grey indicates BM telomeric probe signal. **(D)** Histogram showing telomeric probe signal of G1 WT (grey filled peak) and K82Δ (grey open peak) alongside their internal calf thymocyte controls used in the same experiment. **(E)** Quantitation of absolute telomere length of G1 WT and K82Δ calibrated against calf thymocytes telomere length obtained by TRF analysis **(F)** Histogram showing telomeric probe signal of G5 WT (black filled peak) and K82Δ (black open peak) alongside their calf thymocyte controls used in the same experiment. **(G)** Quantitation of absolute telomere length of G5 WT and K82Δ calibrated against calf thymocytes telomere length obtained by TRF analysis. n = 4-6 mice per condition; mean with 95% CI; significance calculated with Prism software using Student's *t*-test for individual experiments; *** $p \leq 0.002$, **** $p \leq 0.0001$.

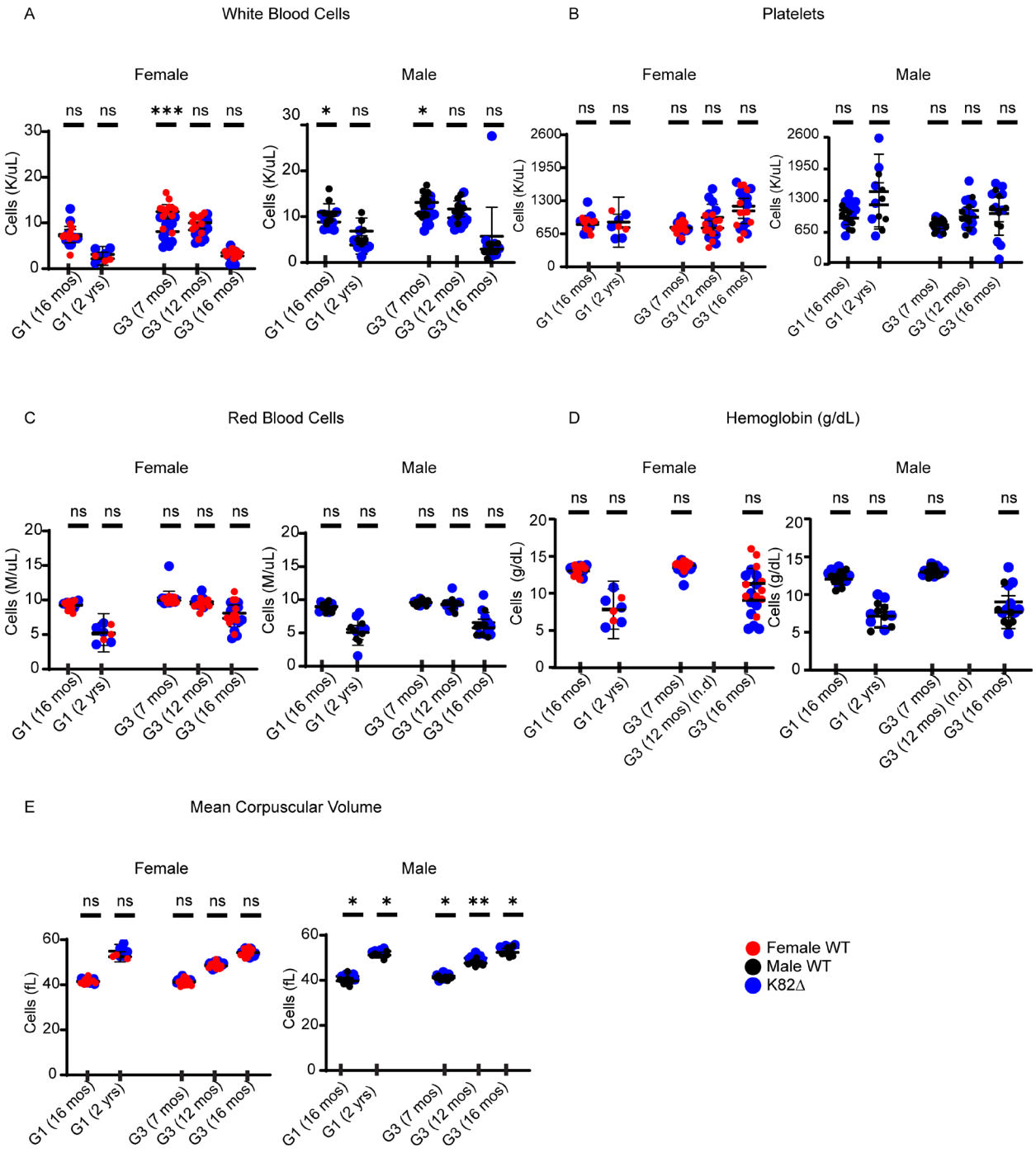

Figure 2.4 Analysis of complete blood counts in K82Δ mice does not reveal defects in steady-state hematopoiesis.

(A-E) Complete blood counts at a given generation and age indicated on the x-axis showing no consistent defect in hematopoiesis. Red circles indicate female WT mice, black circles indicate male WT mice, and corresponding blue circles indicate mutant K82Δ mice. Specific parameters

studied include **(A)** white blood cells, **(B)** platelets, **(C)** red blood cells, **(D)** hemoglobin, and **(E)** mean corpuscular volume. G1 (16 months) WT: n = 18 (9 males and 9 females); G1 (16 months) K82Δ: n = 19 (9 males and 10 females). G1 (2 years) WT: n = 9 (6 males and 3 females); K82Δ: n = 11 (6 males and 5 females). G3 (7 months) WT: n = 24 (12 males and 12 females); K82Δ: n = 24 (12 males and 12 females). G3 (12 months) WT: n = 19 (8 males and 11 females); K82Δ: n = 20 (10 males and 10 females). G3 (16 months) WT: n = 18 (7 males and 11 females); K82Δ: n = 20 (9 males and 11 females). Mean with 95% confidence interval. * <0.05, ** <0.01, *** <0.001 for p values determined by Student's *t*-test.

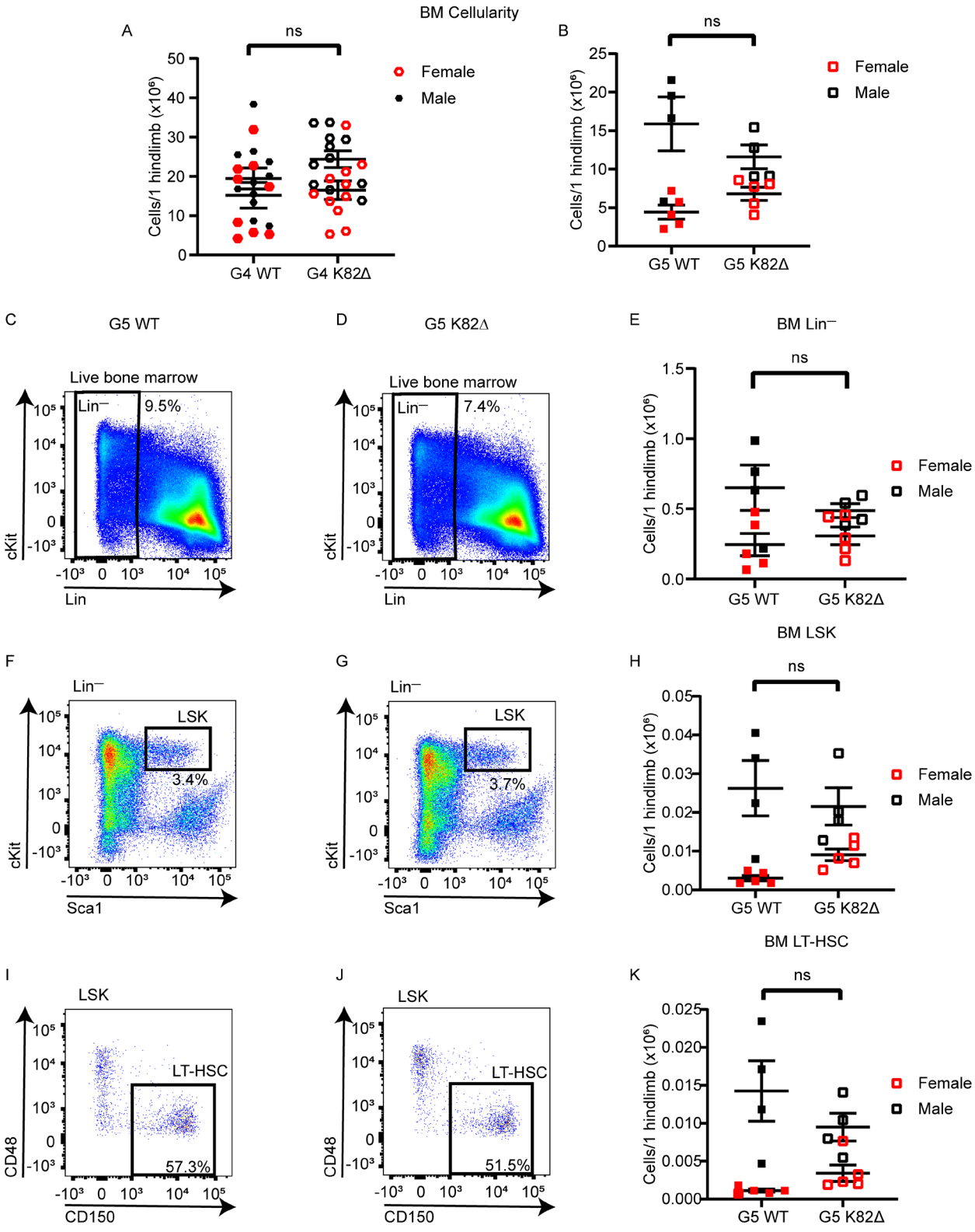

Figure 2.5 K82Δ mutant mice do not develop bone marrow failure.

(A-B) BM cellularity for 1 hindlimb per mouse for WT and K82Δ mice in **(A)** G4 and **(B)** G5. **(C-K)** Representative **(C-D)** lineage negative (Lin^{-}), **(F-G)** $Lin^{-}Sca\text{-}1^{+}cKit$ (LSK), and **(I-J)** $CD150^{+}$ $CD48^{-}$ LSK cells (LT-HSCs) flow cytometry plots of G5 WT **(C, F, I)**, G5 K82Δ mice **(D, G, J)** with quantitation **(E, H, K)** showing equal frequencies in K82Δ mice compared to WT. Red indicates female mice, black indicates male mice, filled symbols indicate WT, and open symbols indicate K82Δ mice. $n \geq 4$; mean with 95% confidence interval.

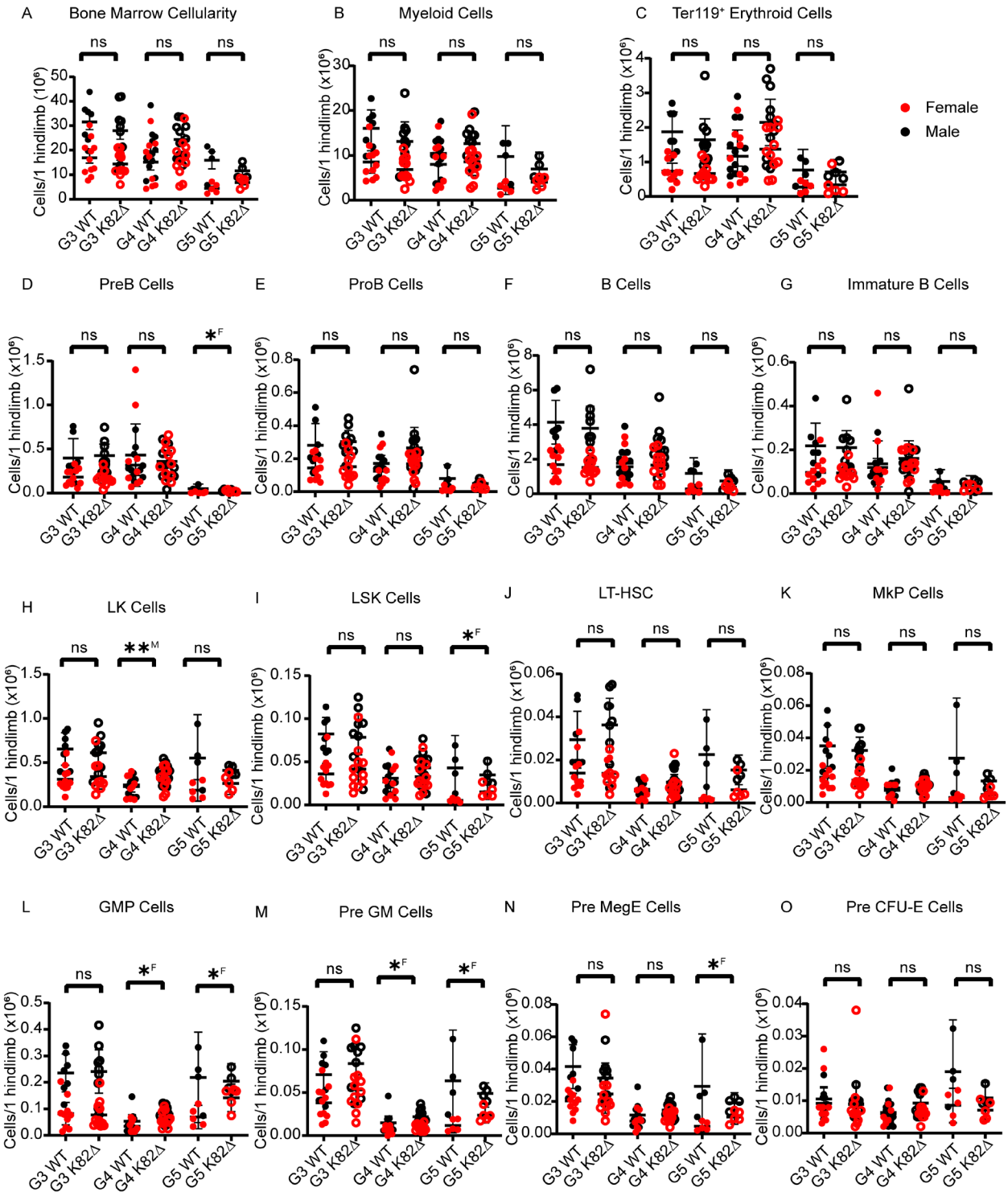

Figure 2.6 Analysis of mature and progenitor bone marrow cells in K82Δ mice does not reveal defects in hematopoiesis.

(A-O) Quantitation across G3-G5 mice; red filled circles indicate female WT mice, red open circles indicate female K82Δ mice, black filled circles indicate male WT mice, and black open

circles indicate male K82Δ mice. Specific parameters studied include **(A)** cellularity, **(B)** $CD11b^{+}$ $GR\text{-}1^{+}$ myeloid cells, **(C)** $Ter119^{+}$ erythroid cells, **(D)** $B220^{+}$ $CD43^{-}$ $sIgM^{-}$ $CD93^{+}$ Pre B cells, **(E)** $B220^{+}$ $CD43^{+}$ $CD19^{+}$ $CD93^{+}$ Pro B cells, **(F)** $CD19^{+}$ $B220^{+}$ B cells **(G)** $B220^{+}$ $CD43^{-}$ $sIgM^{+}$ $CD93^{+}$ immature B cells, **(H)** Lin^{-} $Sca\text{-}1^{-}$ $cKIT^{+}$LK cells, **(I)** Lin^{-} $Sca\text{-}1^{+}$ $cKIT^{+}$ LSK cells, **(J)** $CD150^{+}$ $CD48^{-}$ LSK cells (LT-HSCs), **(K)** Lin^{-} $Sca\text{-}1^{-}$ $cKIT^{+}$ $CD150^{+}$ $CD41^{+}$ MkP cells, **(L)** Lin^{-} $Sca\text{-}1^{-}$ $cKIT^{+}$ $CD41^{-}$ $CD16\text{-}32^{+}$ $CD150^{-}$ GMP cells, **(M)** Lin^{-} $Sca\text{-}1^{-}$ $cKIT^{+}$ $CD41^{-}$ $CD16\text{-}32^{-}$ $CD150^{-}$ $CD105^{-}$ Pre GM cells, **(N)** Lin^{-} $Sca\text{-}1^{-}$ $cKIT^{+}$ $CD41^{-}$ $CD16\text{-}32^{-}$ $CD150^{+}$ $CD105^{-}$ Pre MegE cells, **(O)** Lin^{-} $Sca\text{-}1^{-}$ $cKIT^{+}$ $CD41^{-}$ $CD16\text{-}32^{-}$ $CD150^{+}$ $CD105^{+}$ Pre CFU-E cells. G3 WT: n = 18 (7 males and 11 females); K82Δ: n = 20 (9 males and 11 females). Mean with 95% confidence interval. * <0.05, ** <0.01; ^{M} or ^{F} indicates significance for male (M) or female (F). See methods for more information about antibodies (manufacturer, clone names).

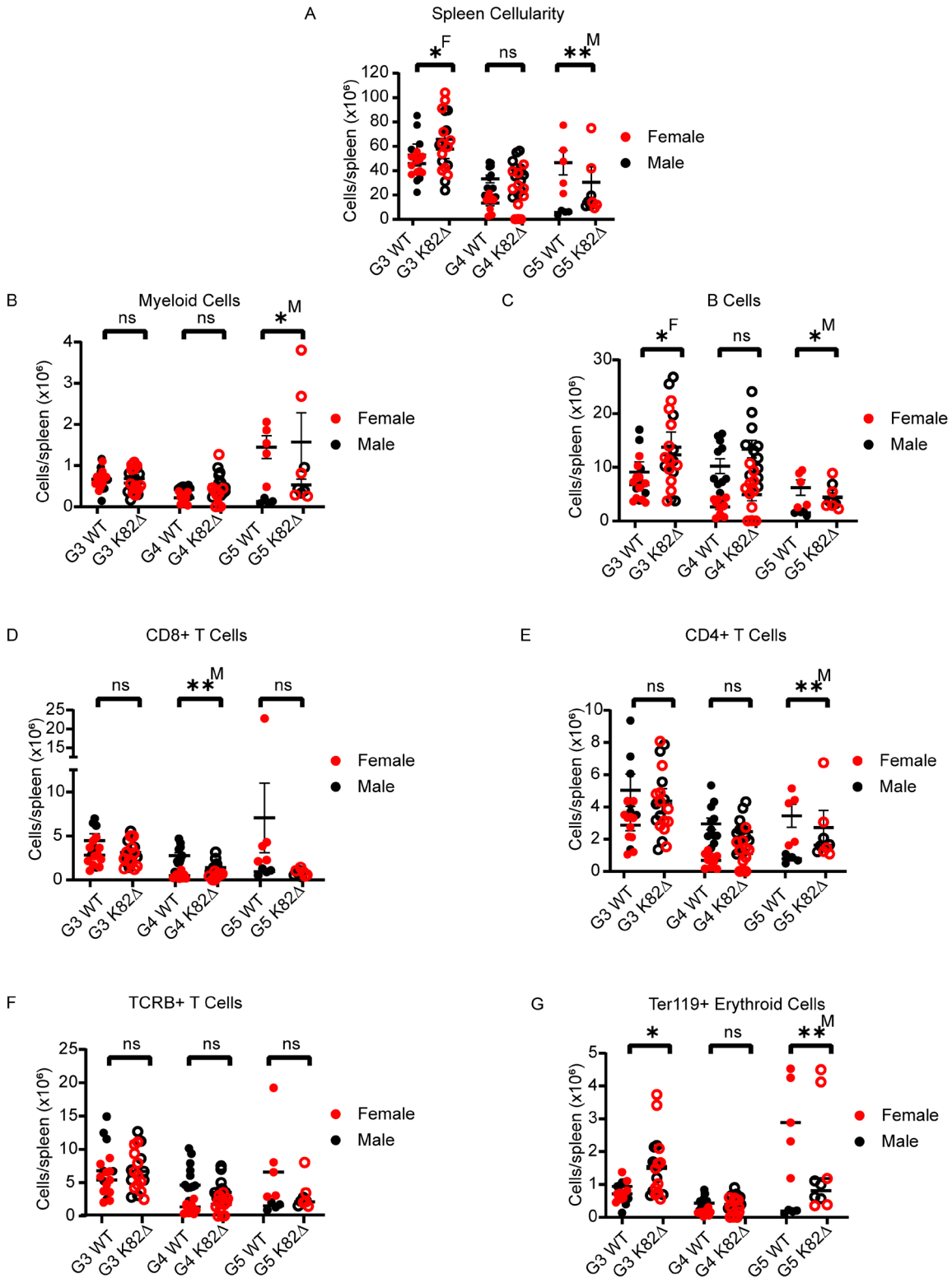

Figure 2.7 Analysis of splenocytes in K82Δ mice does not reveal defects in spleen-resident populations.

(A-G) Quantitation across G3-G5 mice; red filled circles indicate female WT mice, red open circles indicate female K82Δ mice, black filled circles indicate male WT mice, black open circles indicate male K82Δ mice. Specific parameters studied include **(A)** cellularity, **(B)** $CD11b^+$ $GR\text{-}1^+$ myeloid cells, **(C)** $CD19^+$ $B220^+$ B cells, **(D)** $CD8^+$ T-cells, **(E)** $CD4^+$ T-cells, **(F)** $TCRB^+$ T-cells and **(G)** $Ter119^+$ erythroid cells. G4 WT: n = 20 (11 males and 9 females); K82Δ: n = 22 (11 males and 11 females). Mean with 95% confidence interval. * <0.05, ** <0.01; ^{M} or ^{F} indicates significance for male (M) or female (F). See Methods for more details on antibodies used.

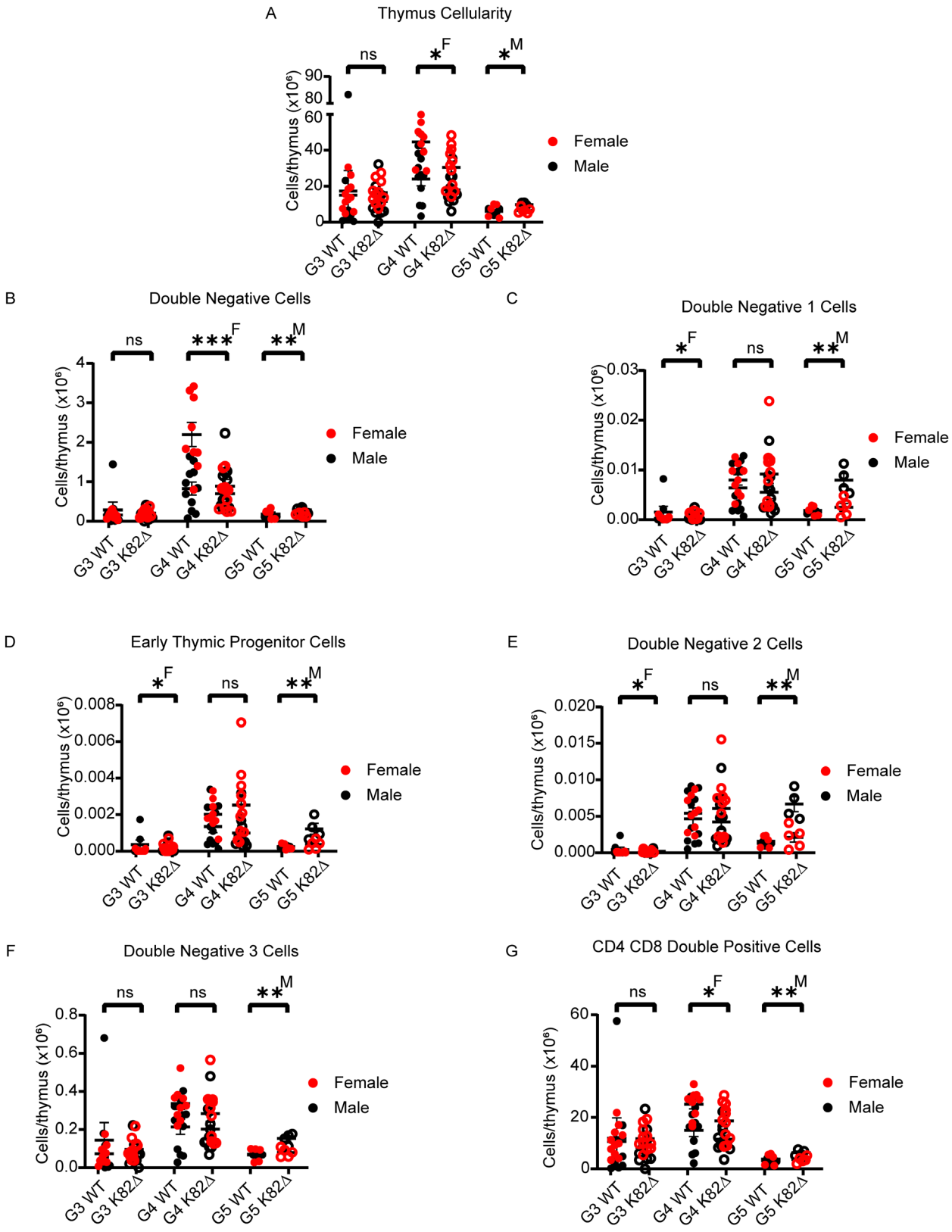

Figure 2.8 Analysis of thymocytes in K82Δ mice does not reveal defects in T lineage development

(A-G) Quantitation across G3-G5 mice; red filled circles indicate female WT mice, red open circles indicate female K82Δ mice, black filled circles indicate male WT mice, and black open circles indicate male K82Δ mice. Specific parameters studied include **(A)** cellularity, **(B)** Lin^{-} $CD8^{-}$ double-negative cells, **(C)** $CD44^{+}$ $c\text{-}KIT^{+}$ Lin^{-} $CD8^{-}$ double-negative 1 cells, **(D)** $CD25^{-}$ $CD44^{+}$ $c\text{-}KIT^{+}$ Lin^{-} $CD8^{-}$ early thymic progenitor cells, **(E)** $CD25^{+}$ $CD44^{+}$ $c\text{-}KIT^{+}$ Lin^{-} $CD8^{-}$ double-negative 2 cells, **(F)** $c\text{-}KIT^{low}$ $CD25^{+}$ Lin^{-} $CD8^{-}$ double-negative 3 cells and **(G)** $CD8^{+}$ $CD4^{+}$ double-positive cells. G5 WT: n = 9 (4 males and 5 females); K82Δ: n = 9 (4 males and 5 females). Mean with 95% confidence interval. * <0.05, ** <0.01, *** <0.001; ^{M} or ^{F} indicates significance for male (M) or Female (F). See Methods for more details on antibodies used.

Chapter 3 : Role of TPP1 K82Δ in the Germline

Portions of this chapter have been adapted from the following publication:

Graniel JV, Bisht K, Friedman A, White J, Perkey E, Vanderbeck A, Moroz A, Carrington LJ, Brandstadter JD, Allen F, Shami AN, Thomas P, Crayton A, Manzor M, Mychalowych A, Chase J, Hammoud SS, Keegan CE, Maillard I, Nandakumar J. (2021). Differential impact of a dyskeratosis congenita mutation in TPP1 on mouse hematopoiesis and germline. Life Sci Alliance 5(1):e202101208.

AUTHOR CONTRIBUTIONS: J.V.G., K.B., J.N., I.M., and C.E.K. conceived the study. K.B. performed the CRISPR-editing experiments in conjunction with the Transgenic Animal Core of the University of Michigan. J.V.G. was involved in the design, execution, and analysis of all remaining experiments with assistance from others as indicated below. A. Moroz, P.T., A.C., M.M., A. Mychalowych, J.W., and J.V.G., performed mouse maintenance, including feeding, setting up breeding cages, genotyping, terminal harvests, and organ preservation/embedding. J. V.G. performed all experiments involving the reproductive system with assistance from A.N.S. and under the supervision of S.S.H. All authors contributed to data analysis. J.V.G., I.M., and J.N. developed the first draft of the manuscript, followed by contributions from C.E.K, and S.S.H., and input from all authors

3.1 Introduction

As stated in chapter 1, telomere maintenance by telomerase is important in somatic stem cell and germ stem cells. It could be argued that telomere maintenance is even more important in the germline as these stem cells are responsible for the formation of gametes and the next generation. There is evidence that as telomeres shorten with age in the soma, the germline maintains telomere length (de Lange et al., 1990). Telomerase has been shown to play a role in telomere maintenance in the germline since loss of TR in mice causes infertility in late generation mutant male and female mice but much of what we know about telomerase's role in this phenotype is in the context of the male germline, where it caused telomere dysfunction-induced apoptosis in the testis (Hemann et al., 2001). In addition, telomerase levels have been found to be much more elevated in undifferentiated spermatogonia, the earliest germline stem cells in the cascade of spermatogenesis, and telomerase is downregulated as spermatogonia differentiate. Moreover, higher telomerase activity was found in the testis compared to somatic stem/progenitor cells in the small intestine and BM based on TRAP activity assays, corresponding to a 10-fold increase in telomerase in the testes compared to BM (Pech et al., 2015).

While the argument for how loss of telomerase can result in infertility in males is more obvious, how loss of telomerase causes infertility in females is less clear. In contrast to the male germline, telomerase is not expressed in adult oocytes, nor do they contain germ stem cells akin to undifferentiated spermatogonia (Kalmbach et al., 2013). Therefore, there is a loss of fertility in females that occurs normally with age. While telomerase is not expressed in oocytes, it has been shown that telomerase is active in the preantral and antral follicles (Kosebent & Ozturk, 2021). There are a few correlative studies that have shown a tenuous link between human infertility and

telomere shortening. Looking at women who underwent IVF, those who were not able to conceive had shorter telomeres compared to those who could (Vasilopoulos et al., 2019). Another study found that women with an increased risk of miscarriages also had shorter telomeres (Giri et al., 2021). When looking at women with telomere biology disorders (TBDs), there have been a few studies correlating reduced levels of Anti-Mullerian Hormone (AMH) (marker for ovarian reserve) with DC (also in Fanconi anemia, an inherited BM disorder but not a telomeropathy) (Giri et al., 2017) and incidence of infertility in patients with other telomeropathies such as idiopathic pulmonary fibrosis (IPF) (Alder et al., 2015). Barring these isolated case studies, there really is no evidence that adults with TBDs suffer from infertility, especially not to the same degree as somatic failure (e.g., BM failure).

Although telomere shortening and degeneration in reproductive tissues occurs during normal aging in humans (Keefe, 2016), the primary vulnerability in humans caused by telomere shortening seems to lie in the BM and other somatic tissues. Thus, the tissue-specific phenotypes in telomerase-deficient mice is reversed in DC patients. While the BM failure is overt, resulting in patients with degrees of cytopenias and often cancers of the blood and/or BM failure, the connection with fertility is tenuous. Despite the divergent manifestation of telomerase-dependent telomere length maintenance defects in *mTR*$^{-/-}$ mice and human patients suffering from telomeropathies, a detailed investigation of the developmental programs of gametogenesis, including in-depth analysis of stem, progenitor, and differentiating cell populations, has not been performed using equivalent genetic perturbations. Here, in contrast to chapter 2, I describe how this mutation compromises mouse spermatogenesis.

3.2 Materials/Methods

Mice: A CRISPR-Cas9 mouse line carrying a specific mutation in the *TPP1* gene (K82Δ; equivalent to human mutation K170Δ) in a C57BL/6 (B6) background was generated at the Transgenic Animal Model Core at the University of Michigan under the supervision of Dr. Thomas Saunders. Purified DNA/RNA was microinjected into fertilized eggs obtained by mating (C57BL/6 X SJL)F1 or C57BL/6 female mice with (C57BL/6 X SJL)F1 male mice and pronuclear microinjection was performed as described (Pease et al., 2011). A heterozygous founder was obtained using this approach and was genotyped using Sanger sequencing for the existence of the K82Δ mutation and the absence of any other unwanted changes in the flanking regions on the *Acd* locus. The founder mouse was crossed with WT B6 mouse to generate the line and backcrossed for 4 generations, thereby eliminating any off-target effects of genome editing. Once backcrossed, heterozygous mice were intercrossed to produce homozygous mice starting with generation 1 (G1). Homozygous mice were crossed together to breed successive generations (G2, G3, and so on). +/+ (WT) mice were also bred in parallel. All animals were housed in environmentally controlled conditions with 14 h light and 10 h dark cycles with food and water provided *ad libitum*. Mice were harvested at the indicated times for the generations tested in this study: G1: 23-25 months, G3: 16-16.5 months, G4: 14-21 months, and G5: 15.5-17 months. All protocols were approved by the Institutional Animal Care & Use Committee (IACUC) at the University of Michigan and the University of Pennsylvania and comply with policies, standards, and guidelines set by the States of Michigan and Pennsylvania and the United States Government.

Histology: Mice were euthanized by isoflurane then cervical dislocation. Testes were removed and fixed overnight in Bouin's solution or 4% paraformaldehyde. Samples were dehydrated through a graded series of ethanol, embedded in paraffin, and sectioned at 7 μm thickness with a Spencer Microtome (American Optical). Sections were stained with hematoxylin and eosin (H&E) following standard protocols. After staining, the slides were mounted with coverslips and Permount mounting media (Fisher SP15-500) and allowed to dry overnight in a fume hood. Digital images were captured using a Leica upright DM5000B microscope and Leica DFC310 FX Digital camera.

Immunofluorescence (IF): This was performed as described previously (Vlangos et al., 2009). Briefly, deparaffinized sections were boiled in 0.1 M Sodium Citrate for 10 minutes for antigen retrieval and sections were blocked in suppressor serum (5% goat serum (Jackson ImmunoResearch #005-000-1210), 95% blocking solution (3% BSA and 0.5% Tween in PBS)) for 20 min at RT in a humidifying chamber. Sections were incubated with primary antibodies diluted in suppressor serum overnight at 4C in a humidifying chamber. At least 1 section for each slide was incubated in the absence of primary antibody to serve as a negative control. After a series of PBS washes, secondary antibodies diluted in suppressor serum were added to all sections in the dark and incubated in a humidifying chamber at RT for 1 h. Sections were washed again with PBS and counterstained with DAPI and PNA-lectin for 1 h at RT in a humidifying box. After the final three PBS wash steps, mounting media (Permount, Fisher SP15-500) was added and the coverslips and slides were left to dry overnight before imaging and stored at 4°C. Digital images were captured with the Olympus BX53F microscope, Olympus DP80 digital camera, and CellSens Standard software. Antibodies and stains used are as follows: mouse anti-

SCP3 (1:200; abcam, ab97672), rabbit anti-PLZF (1:200; Santa Cruz Biotechnology, sc-22839), rabbit-anti-Sox9 (1:666; Millipore/Sigma Aldrich, AB5535), goat anti-rabbit IgG, Alexa Fluor 488 (1:200; Invitrogen/ThermoFisher, A11008), goat anti-rabbit IgG, Alexa Fluor 568 (1:200;Invitrogen/ThermoFisher, A11011), goat anti-mouse IgG, Alexa Fluor 568 (1:200; Invitrogen/ThermoFisher, A11004), goat anti-mouse IgG, Alexa Fluor 488 (1:200; Invitrogen/ThermoFisher, A11001), Rat anti-BrdU (1:200; Oxford Biotechnology, OBT0030CX), rabbit anti-cleaved caspase-3 (1:400; Cell Signaling Technology, 9661S), Lectin PNA, Alexa Fluor 488 conjugate (1:1000; Invitrogen/Fisher Scientific; L21409), DAPI (1:1000; Kirkegaard & Perry Laboratories, 71-03-00).

Fertility measurement: Data was extracted from breeding cage cards to determine the litter sizes and the number of pups that survived past weaning for each mating pair of WT and K82Δ mice generations G1 through G5.

Testes weight measurement: Mice were individually weighed before euthanasia, following which testes were dissected, weighed, and photographed. Quantitation of testes weight was made using testes weight per mouse total weight for each mouse.

Sperm count and morphology: Sperm was collected by dissecting out vas deferens and epididymis, mincing into a single suspension with PBS, and incubation for 1 h at 37°C. Sperm were diluted and spotted on slides and allowed to dry. Six slides per mouse were analyzed (n = 4 G5 WT and n = 4 G5 K82Δ). Sperm were counted using a Makler chamber, with a minimum of four rows. Slides were then fixed in methanol for 15 min and stained with H&E as described

above. Sperm morphology was quantified blinded and in triplicate. Sperm were designated as normal if they had an intact comma-shaped head, midpiece, and tail. Abnormal indicated a deviation from normal with the major difference being in head morphology.

Staging of seminiferous tubules and evaluation of ordered/disordered tubules: Cell quantitation was performed to attain the absolute numbers of each cell type in this study. In each testis from G1 WT, G1 K82Δ, G5 WT, G5 K82Δ mice, and *acd/acd*, three 7 µm-thick sections, separated by a distance of more than 100 µm, were cut and analyzed. In all seminiferous tubules, the stages of spermatogenesis were determined by the shape of acrosomes stained by PNA-lectin. Staging was performed blinded. Number and mice and tubules analyzed: G1 WT: 2 mice, 532 tubules; G1 K82Δ: 2 mice, 501 tubules; G5 WT: 2 mice, 330 tubules; G5 K82Δ: 2 mice, 729 tubules; *acd/acd* hypomorph: 1 mouse, 175 tubules.

Quantitation of germline and Sertoli cell number per tubule: Cell number counting was performed to attain the absolute numbers of each cell type. In each testis from G1 WT, G1 K82Δ, G5 WT, G5 K82Δ mice, or *acd/acd* hypomorph, at least two 7 µm-thick sections, separated by a distance of more than 100 µm, were cut and analyzed. Undifferentiated spermatogonia were identified using PLZF, spermatocytes were identified using SCP3, and Sertoli cells were marked with SOX9. Each cell positive for each marker was counted per seminiferous tubule for all tubules using ImageJ software (NIH; Bethesda, MD; http://imagej.nih.gov/ij/). Different sections from the same mouse were co-immunostained for the following pairs of markers: PLZF and BrdU, Cleaved Caspase-3 and SCP3, and BrdU and SOX9. Following the addition of secondary Alexa fluor-conjugated antibodies, all sections were stained with PNA-lectin and DAPI and

imaged at 200x total magnification using a 20X objective lens. In all sections, long (i.e., non-circular) tubules were excluded as they likely represent longitudinal rather than radial sections. Number and mice and tubules analyzed for each marker: PLZF/BrdU: G1 WT: 2 mice, 182 tubules; G1 K82Δ: 2 mice, 185 tubules; G5 WT: 2 mice, 116 tubules; G5 K82Δ: 2 mice, 264 tubules; *acd/acd* hypomorph: 1 mouse, 49 tubules. Caspase-3/SCP3: G1 WT: 2 mice, 161 tubules; G1 K82Δ: 2 mice, 158 tubules; G5 WT: 2 mice, 91 tubules; G5 K82Δ: 2 mice, 205 tubules; *acd/acd* hypomorph: 1 mouse, 41 tubules. BrdU/SOX9: G1 WT: 2 mice, 189 tubules; G1 K82Δ: 2 mice, 158 tubules; G5 WT: 2 mice, 123 tubules; G5 K82Δ: 2 mice, 260 tubules; *acd/acd* hypomorph: 1 mouse, 85 tubules.

BrdU staining and quantitation: To detect cell proliferation, mice were injected intraperitoneally with BrdU at 100 mg/g body weight for 24 hours before organ removal. BrdU staining was performed as described in IF protocol above. BrdU positive tubules were designated positive if they had two or more positive foci. Images were scored blind to genotype. Quantitation of BrdU positive tubules in tubules that were stageable was performed and subjected to a Student's t-test to evaluate significant differences between WT and K82Δ in each generation. Number of mice and tubules analyzed: G1 WT: 2 mice, 371 tubules; G1 K82Δ: 2 mice, 343 tubules; G5 WT: 2 mice, 239 tubules; G5 K82Δ: 2 mice, 524 tubules.

Cleaved Caspase-3 staining and quantitation: Cleaved Caspase-3 (CC3) IF was performed as described above. CC3 tubules were designated positive if tubules had at least one positive focus. Images were scored blind to genotype and the number of positive tubules was counted irrespective of the stage of spermiogenesis. A Student's t-test was calculated to determine

significant differences between WT and K82Δ in each generation. Number of mice and tubules analyzed: G1 WT: 2 mice, 161 tubules analyzed: G1 K82Δ: 2 mice, 158 tubules; G5 WT: 2 mice, 91 tubules; G5 K82Δ: 2 mice, 205 tubules; *acd/acd* hypomorph: 1 mouse, 41 tubules.

Statistical analysis

Statistical tests were performed using Prism software (GraphPad version 8). Experiments were analyzed between WT and mutant mice only. Analysis between generations was not included as they were not conducted at the identical age or cohort size. Student's t-tests were used between WT and mutant mice for each experiment. Graphs were generated in Prism software and represented as mean with 95% confidence interval for hematopoietic data and mean with SEM for germline data. Adjusted *p* values for comparisons were reported as $*p < 0.05$, $**p < 0.01$, and $***p < 0.001$. M or F symbols were superscripted to denote significance in either males (M) or females (F). It should be noted that due to the many outcomes studied, there are some stochastic statistically significant results that are not consistent across genotype, generation, or sex. Independent confirmatory experiments would need to be conducted in a larger scale to follow up any of these isolated findings, especially those approaching $p = 0.05$.

Study Approval

Approved protocols by the University of Pennsylvania's Office of Regulatory Affairs or the University of Michigan's Committee on Use and Care of Animals were strictly adhered to while performing all mouse experiments in this work.

3.3 Results

3.3.1 K82Δ results in reproductive defects and progressive loss of fertility

Using the same mice generated in Chapter 2, we turned our attention to fertility as a readout for germ cell function, as complete KO of telomerase is known to cause infertility in late-generation mice. We observed a striking decrease in fertility in G4 K82Δ mice, as evidenced by a reduced number of litters per breeding pair, a trend that persisted in G5 K82Δ mice (Fig. 3.1A). Remarkably, only one out of 13 G4 K82Δ breeding pairs produced litters. Among four breeding pairs set up for G5 K82Δ mice, only one female G6 K82Δ was born, thereby terminating the breeding of the K82Δ line. Furthermore, of the mice born, litter size and the total number of pups that survived past weaning was significantly lower in G4 and G5 K82Δ breeding pairs, suggesting that impaired germline proliferation and/or maturation caused by shortened telomeres resulted in prenatal and perinatal lethality of K82Δ mice (Fig. 3.1B). Both sexes were affected as breeding of G5 K82Δ male and female mice to WT females and males, respectively, did not result in progeny (data not shown). The reproductive defects observed for TPP1 K82Δ are reminiscent of sterility observed in *acd/acd* hypomorphic mice (Keegan et al., 2005) and late-generation $mTR^{-/-}$ mice (Hemann et al., 2001; Lee et al., 1998). It is striking that a decrease in telomerase function caused by this single amino acid deletion in the TPP1 TEL patch region is sufficient to cause mouse infertility to a similar degree as mouse models with larger scale deletions in telomerase or TPP1. This data demonstrates that disruption of telomerase-dependent telomere length maintenance causes mouse infertility in late generations under conditions where no spontaneous BM defects are evident.

3.3.2 K82Δ mutation in mice reduces testis/body weight ratio and sperm counts

To further understand the basis for reduced fertility in K82Δ mice, we examined testicular size and observed a significant reduction in testis weight/body weight in G3-G5 male mutant mice (Fig. 3.1C-D). Cross-sections of G5 K82Δ testes revealed no changes in the diameter of seminiferous tubules (Fig. 3.1E), but a reduction in the number of tubules was observed compared to WT (Fig. 3.1E-F). Testosterone levels remained unchanged (data not shown). Furthermore, G5 K82Δ male mice had lower sperm counts (Fig. 3.1G) and a significantly increased proportion of sperm with abnormal morphology (Fig. 3.1H-I). Specifically, the mutant sperm lacked the hook-like structure involved in sperm progression and attachment to the female reproductive tract (Varea-Sánchez et al., 2016). Together, these data indicate that TPP1 K82Δ mice have profound reproductive defects that could arise from underlying defects in the germline and/or somatic compartments of the testis.

3.3.3 K82Δ results in an increased incidence of disordered and empty seminiferous tubules

We next analyzed seminiferous tubule cellularity to gain deeper insights into the reproductive defects observed in K82Δ mice. To monitor acrosome dynamics and determine the rough stage of the seminiferous tubule cycle, we used PNA lectin immunofluorescence (Fig. 3.2A) (Nakata et al., 2015). We collapsed the 12 stages of the seminiferous tubule into four bins (stages I-III; stages IV-VI; stages VII-VIII; stages IX-XII) and quantified the frequency of tubule stages in WT and mutant mice. For these studies, we used the hypomorphic *acd/acd* mouse model as a positive control for a severe germline defect as it is known to exhibit degenerated tubules (Keegan et al., 2005). No differences in spermatogenesis were observed for mutant versus WT G1 mice (Fig. 3.2B, D, and F). However, the G5 K82Δ mice had a significant increase in the number of tubules that were not stageable (e.g., due to absence or paucity of spermatids) (Fig.

3.2C, and F). Of the G5 K82Δ tubules that could be staged, there was a significant decrease in early-stage I-III tubules and an increase in stage IV-XII tubules (Fig. 3.2E). Strikingly, we observed two distinct phenotypes in G5 K82Δ mice: a loss of the ordered organization of tubules and an elevation in the frequency of empty tubules (Fig. 3.2G-I). While these results highlight the deleterious effects of the K82Δ mutation in the mouse male reproductive system, they raise the question of whether the TPP1 mutation leads to loss of germ cells, somatic cells, or both cell types in the testis.

3.3.4 K82Δ mutation results in a reduction of germline stem cells but not somatic cells

To better understand if K82Δ elicits its effects directly through the germline compartment rather than through a broader impact on reproductive tissue development, we quantified the number of spermatogonia, spermatocytes, and Sertoli cells in WT and K82Δ G1 and G5 mice. PLZF was used as a spermatogonial marker (Buaas et al., 2004; Costoya et al., 2004; Lovelace et al., 2016) to examine the effects of K82Δ on this germline compartment (Fig. 3.3A). The total PLZF+ foci were counted per tubule in all tubules for each genotype in G1 and G5 mice. G1 WT and G1 K82Δ mice contained an average of 5.2 and 5.1 spermatogonia per tubule, respectively. Similarly, G5 WT tubules contained an average of 4.7 spermatogonia per tubule. However, G5 K82Δ mice exhibited a marked reduction in the number of spermatogonia, averaging 2.8 spermatogonia per tubule (Fig. 3.3B). This decrease cannot be attributed to an altered tubule size as G5 K82Δ testes displayed normal tubule diameter (Fig. 3.1E). Meiotic prophase I spermatocytes were identified using SCP3 (Synaptonemal Complex Protein 3) (Fig. 3.3C) (Yuan et al., 2000). G1 WT, G5 WT, and G1 K82Δ testes displayed a similar number of spermatocytes per tubule (averages of 65.0, 63.9, and 63.8, respectively). G5 K82Δ mice exhibited a significant

reduction in the number of spermatocytes per tubule (average of 27.2) (Fig. 3.3D). The decrease in both spermatogonia and spermatocytes is consistent with the apoptosis-mediated surveillance of the male mouse germline described in *mTR*$^{-/-}$ models (Hemann et al., 2001; Lee et al., 1998), although in older (15-17-month) G5 K82Δ mice that have already undergone substantial germline degeneration, we did not observe apoptotic markers likely due to prior clearance of dead cells (Fig. 3.4B, and D). Sertoli cells were identified using SOX9 as a marker (Fig. 3.3E) (Barrionuevo et al., 2006; Chaboissier et al., 2004). In stark contrast to the observations in the germline, G5 K82Δ mice did not show a decrease in the number of Sertoli cells per tubule compared to G1 WT, G5 WT, or G1 K82Δ mice. Instead, a mild, but statistically significant, increase in the number of Sertoli cells per tubule was observed in G5 K82Δ compared to G5 WT control mice (Fig. 3.3F). However, no changes in BrdU activity seemed to contribute to this increase (Fig. 3.4A and C). A decrease in both spermatogonia and spermatocytes but an increase in the number of Sertoli cells was also seen in *acd/acd* hypomorphic mice, suggesting an inverse correlation between the phenotypes observed in the germline versus the somatic components of the mutant seminiferous tubules. Spermatogonial stem cells are highly proliferative and thus depend on telomerase to overcome the end replication problem (Pech et al., 2015). These data suggest that the reduction in telomere length maintenance due to reduced telomerase recruitment to telomeres by TPP1 K82Δ limits spermatogonia replicative lifespan, resulting in eventual germline stem cell exhaustion. As Sertoli cells of mature testes are largely non-proliferative, a lack of a severe phenotype in this compartment is not surprising. A modest increase in the number of Sertoli cells is consistent with activation of a compensatory mechanism in the face of germline failure, as Sertoli cells nourish developing sperm (França et al., 2016; Larose et al.,

2019). Together, our data demonstrate that the TPP1 K82Δ mutation reduces mouse germline stem cell count and culminates in diminished gamete production that causes infertility in males.

3.4 Discussion

Infertility has been reported in *mTR*$^{-/-}$ mice (Lee et al., 1998) but reproducing this phenotype with a mutation in TPP1 that solely disrupts recruitment of, but not the expression or composition of, telomerase confirms beyond reasonable doubt that telomerase-dependent telomere shortening is sufficient to cause mouse infertility in the absence of concomitant spontaneous HSC failure. K82Δ mice started developing fertility defects at G4 that culminated in only one viable G6 (female) K82Δ mouse. Reduction in testes size, seminiferous tubule number, and sperm count were visible as early as G3 in K82Δ male mice. Furthermore, K82Δ sperm have a globozoospermia-like phenotype (round-shaped sperm head), which has been previously linked with male infertility (Yan, 2009). To our knowledge, we are the first to observe a split phenotype from telomere shortening as some K82Δ seminiferous tubules showed loss of germ cells while others exhibited severe disorganization. It is unclear whether tubule disorganization and depletion of germ cells occur sequentially or if the two phenotypes are alternative outcomes of telomere shortening in the spermatogonial stem cells. Our in-depth quantitation of cell types in the testis confirmed that the TPP1 mutation decreases cell numbers for spermatogonia and differentiating cell types (spermatocytes and spermatids). Somatic cells in the testes like Sertoli cells were completely spared by the K82Δ mutation, consistent with a germline-specific mechanism for the downstream infertility defect. In fact, K82Δ slightly increased the number of nursing Sertoli cells, perhaps to compensate for reduced germline function.

It will be interesting to determine if germ cell loss results solely from stem cells succumbing to the end replication problem or if premature differentiation of spermatogonia as a result of telomere dysfunction also contributes to this phenotype. Although our study was restricted to the effect of TPP1 K82Δ on the mouse male germline (as early stages of mouse female germline development occur *in utero* and are therefore difficult to study), both male and female mice with the mutation were unable to produce offspring with wild-type mating partners. It should be noted that previous work in telomerase-deficient mouse models as well as this study show variance in the onset of phenotypes (G1 vs G3 vs G5) which could be due to differences in baseline telomere length at the very start of breeding. However, the sequence of defects is distinctly reproducible with the germline being affected first in steady-state conditions across mouse models. Together with previous studies, our data suggest that telomere lengthening afforded by telomerase is critical to the maintenance of the mouse germline. Although telomere attrition in reproductive tissues has been proposed to contribute to the natural process of reproductive aging in humans (Keefe, 2016), the above defects we see in K82Δ mice have not been noted in telomeropathies. Thus, the mouse germline seems to be more vulnerable towards telomere shortening than the human germline.

3.5 Figures

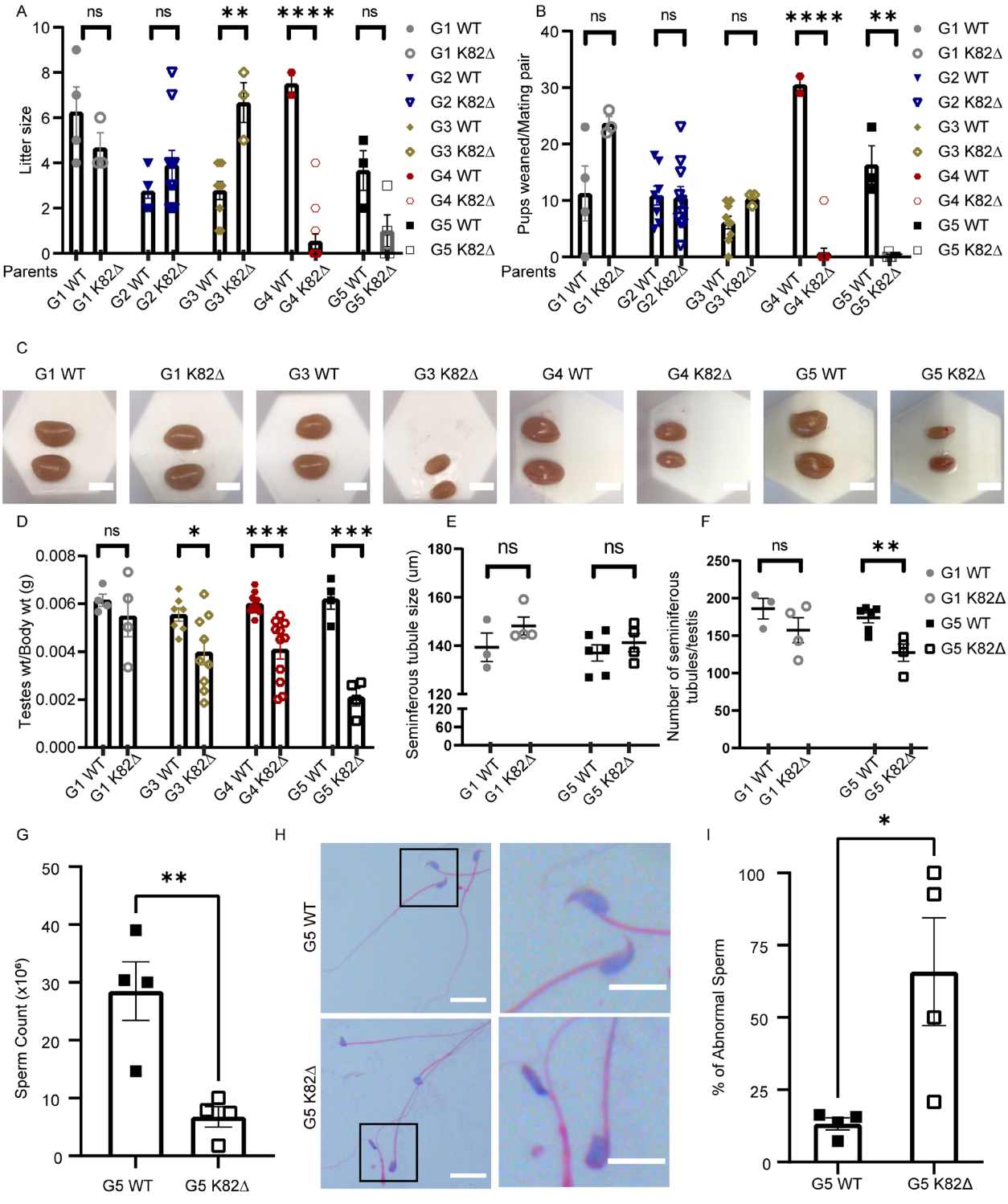

Figure 3.1 TPP1 K82Δ mutation leads to reproductive defects in later generations.

(A-B) x-axis indicates genotype of the parents. **(A)** Quantitation of the number of offspring per litter for the indicated generation number and genotype analyzed in this study. **(B)** Quantitation of the total number of pups that survived past weaning per mating pair for the indicated generation number of WT and K82Δ mice. Number of mating pairs used for data in panels **(A)** and **(B)**: G1 WT: n = 4; G1 K82Δ: n = 3; G2 WT: n = 8; G2 K82Δ: n = 10; G3 WT: n = 9; G3 K82Δ: n = 3; G4 WT: n = 2; G4: K82Δ n = 13; G5 WT: n = 3; G5 K82Δ: n = 4. **(C)** Representative gross morphology images of testes for the indicated generation number and genotype of mice studied. **(D)** Quantitation of testes/body weight of WT and K82Δ mice. n = 4 – 11. **(E-F)** Whole testis sections were stained with H&E and imaged and analyzed for seminiferous tubule **(E)** diameter and **(F)** number in G1 and G5, WT and K82Δ, mice. At least two mice were evaluated per generation and genotype. Slides separated by at least 100 μm were used as technical replicates **(G)** Number of sperm collected from vas deferens and epididymis from G5 WT and G5 K82Δ mice. n = 4. p = 0.0067. **(H)** Representative sperm morphology from G5 WT and G5 K82Δ mice by H&E staining. Magnified views of boxed areas are shown on the right. Scale bar: 20 μm. **(I)** Quantitation of the percentage of abnormal sperm. n = 4.

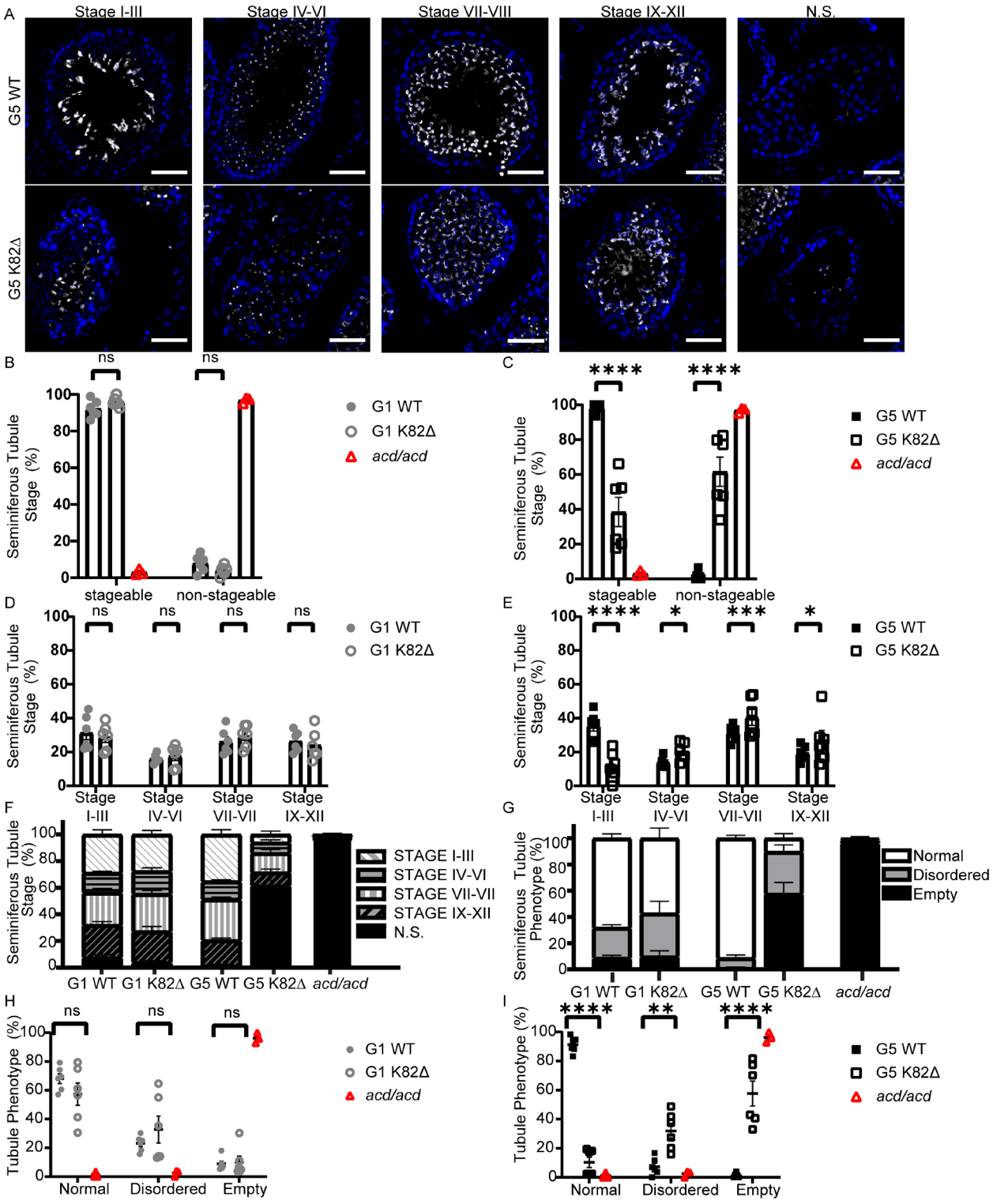

Figure 3.2 Late-generation K82Δ mice testes are comprised primarily of disordered or empty tubules.

(A) Immunofluorescence (IF) for PNA-lectin (spermatid acrosomes; grey) and DAPI (nuclei; blue) in cross-sections of testes from G5 WT and G5 K82Δ mice in each stage including those

that were not-stageable (N.S.) because they were devoid of spermatids, which are necessary for accurately staging tubules. Scale bar: 50 μm. **(B-C)** Quantitation of total tubules that are stageable or not-stageable in **(B)** G1 WT, G1 K82Δ mice, and *acd/acd* or **(C)** G5 WT, G5 K82Δ, and *acd/acd* mice. **(D-E)** Quantitation of the percentage of stageable seminiferous tubules in a given stage of spermatogenesis in **(D)** G1 WT and G1 K82Δ mice and **(E)** G5 WT and G5 K82Δ mice. **(F)** Quantitation of the breakdown of each stage within G1 WT, G1 K82Δ, G5 WT, G5 K82Δ, and *acd/acd* mice. White diagonal lines indicate % of tubules in stages I-III, black horizontal lines are stages IV-VI, grey vertical lines are stages VII-VIII, black diagonal lines are stages IX-XII, and black filled bars are not-stageable. **(G)** Quantitation of tubule phenotype denoted as either normal organization (white bar), disordered organization (grey bar), or empty tubules (black bar) in G1 WT, G1 K82Δ, G5 WT, G5 K82Δ, and *acd/acd* mice. **(H-I)** Quantitation of the percentage of seminiferous tubules with either normal, disordered, or empty tubule phenotype in **(H)** G1 WT, G1 K82Δ, and *acd/acd* mice and **(I)** G5 WT, G5 K82Δ, and *acd/acd* mice. *acd/acd* was used as a positive control of gonadal defect. In panels **(B, D, H)**: G1 WT (grey filled circles), G1 K82Δ (grey open circles). In panels **(C, E, I)**: G5 WT (black filled squares), G5 K82Δ (black open squares). In panels **(B, C, H, I)**: *acd/acd* (red open triangle).

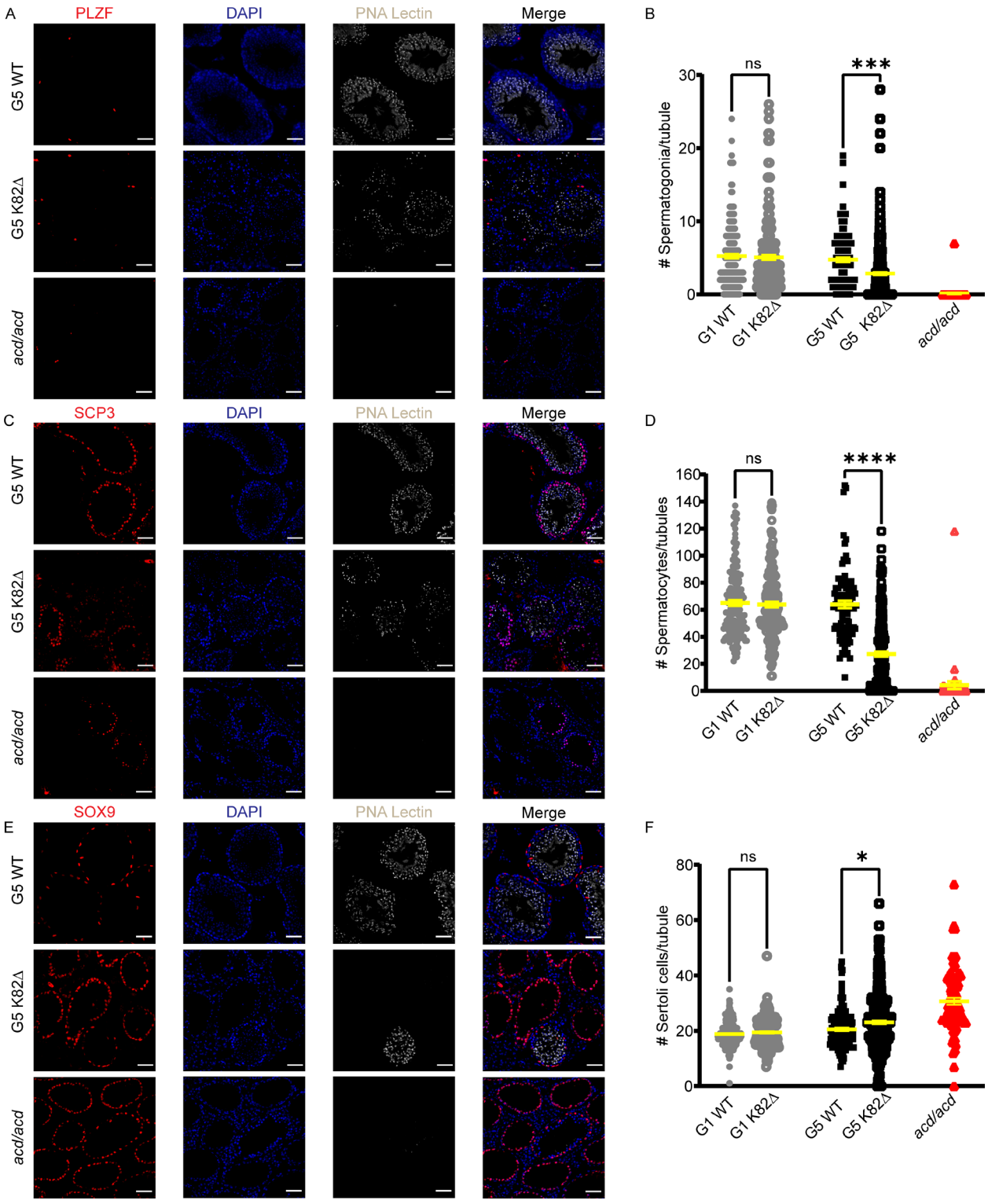

Figure 3.3 K82Δ mutation results in a reduction of germ cells but an increase in somatic Sertoli cells.

(A, C, E) Immunofluorescence for **(A)** PLZF (undifferentiated spermatogonia; red) **(C)** SCP3 (spermatocytes; red), **(E)** SOX9 (Sertoli cells; red), DAPI (nuclei; blue), and PNA Lectin (spermatid acrosomes; grey) in cross-sections of testes from G5 WT, G5 K82Δ mice, and *acd/acd* mice. Scale bar: 50 μm. **(B, D, F)** Quantitation of the number of **(B)** spermatogonia, **(D)** spermatocytes, and **(F)** Sertoli cells per tubule in G1 WT, G1 K82Δ G5 WT, G5 K82Δ, and *acd/acd* mice. See methods for total number of mice and tubules analyzed.

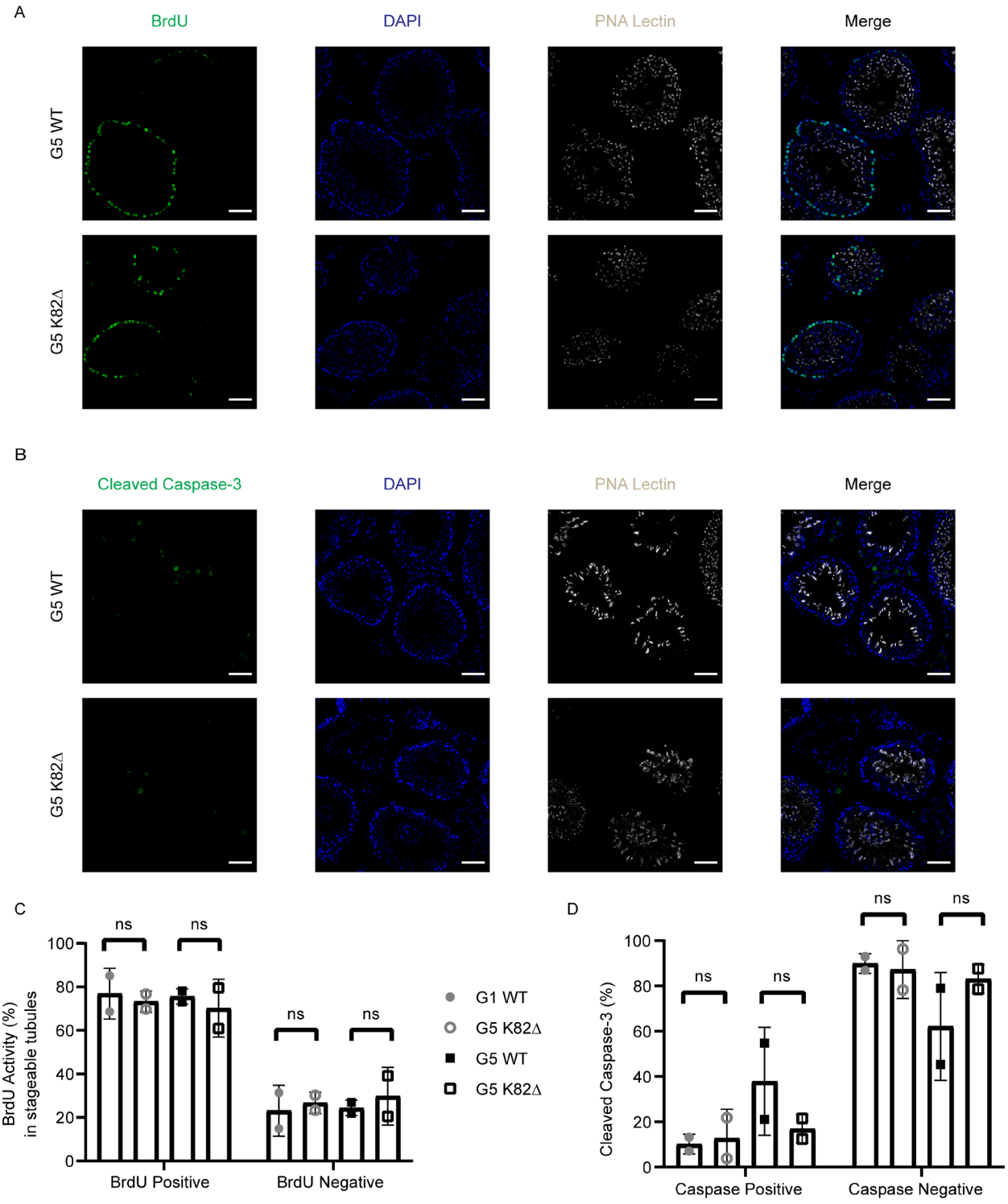

Figure 3.4 K82Δ mutant testes do not show changes in proliferation or apoptosis compared to WT mice.

(A-B) Immunofluorescence for **(A)** BrdU (proliferation; green) or **(B)** cleaved Caspase-3 (apoptosis; green); DAPI (nuclei; blue), and PNA Lectin (spermatid acrosomes; grey) in cross-

sections of testes from G5 WT and G5 K82Δ mice. Scale bar: 50 μm. **(C-D)** Quantitation of the percentage of **(C)** BrdU-positive and **(D)** cleaved Caspase-3-positive cells per tubule in G1 WT, G1 K82Δ, G5 WT, and G5 K82Δ mice.

Chapter 4 : Discussion and Future Outlook

4.1 Overview

In this dissertation, I first highlighted key findings over the years that have shed light on how the various telomere biology proteins and complexes work together to protect our chromosome ends and allow for the extension of telomeres by telomerase in the context of germ stem cells and somatic stem cells. I also described what transpires when telomere length maintenance is disrupted, resulting in disease (Chapter 1). I then presented work that addressed a gap in our understanding of the *in vivo* consequence of a separation-of-function mutation in TPP1, drawing from the extensive *in vitro* work elucidating the mechanism of action of TPP1 K170Δ mutation, a mutation causative of DC in humans. We generated a mouse model in which the equivalent mutation TPP1 K82Δ was knocked in and followed homozygous wild-type and mutant mice for multiple generations to study the effect this mutation has on telomere length and stem cell maintenance. We discovered this mutation was sufficient to shorten telomeres in mutant mice as early as generation 1 and continued to shorten in successive generations akin to telomerase KO mice. We looked extensively in multiple lymphoid organs and found no evidence of a hematopoietic defect, concluding that K82Δ mice do not undergo spontaneous hematopoietic failure (Chapter 2). However, this mutation resulted in a striking reproductive phenotype consisting of low brood size, decreased testes size, disordered or empty seminiferous tubules and a decrease in germ stem cells, eventually resulting in sterility in both male and female mutant mice in generation 5 (Chapter 3).

Collectively, this work provides insight into the molecular interplay between TPP1's role in end replication and stem cell maintenance. Notably, our work combined with the extensive literature on telomerase KO mice suggests an increased vulnerability of the mouse germline over the soma, which is reversed in human patients with this disease (that succumb to BM failure). Theoretically, this mutation should impact all stem cell compartments uniformly, however, in practice, different organ systems present different vulnerabilities to telomere shortening in mice and humans. Perhaps, if the sterility phenotype in mice could be overcome, they would eventually develop BM failure. Similarly, if human patients with DC lived long enough without succumbing to BM failure, it is possible that they could develop reproductive defects more rapidly than unaffected individuals in the population. However, our work suggests that the trigger underlying the manifestation of disease is context-dependent and may weigh heavily on replicative burden. Thus, my thesis has major implications for how we model telomere biology disorders in animals in the future.

4.2 Differential impact of telomere shortening on hematopoiesis in mice versus humans

My work has resulted in the first mouse model for telomerase-dependent telomere shortening caused by a telomeropathy mutation that leaves end protection and the structure and composition of telomerase intact. Generation of mice homozygous for TPP1 K82Δ resulted in telomere shortening at every generation which was measured by adapting Flow-FISH, allowing us to determine absolute telomere length in mice. We next undertook an extensive and thorough analysis of stem, progenitor, and mature cells within the four hematopoietic organs: BM, spleen,

thymus and blood. Despite our rigorous analysis, K82Δ mice did not reveal consistent or overt changes across time points in any of the hematopoietic compartments tested compared to WT. Unlike in patients, but like mice knocked out for telomerase, K82Δ mice do not develop spontaneous BM failure. All our experiments were performed in steady state conditions. Based on other mouse models of telomerase deficiency, we would predict that K82Δ hematopoiesis could become defective if exposed to severe stress caused by serial transplantations, or other types of hematopoietic stress. However, at least in steady state, these mice do not succumb to gross hematopoietic failure.

4.3 Differential impact of telomere shortening on germline development in mice versus humans.

Despite not seeing a phenotype in any hematopoietic compartment, a phenotype did indeed emerge in mice homozygous for TPP1 K82Δ in later generations. At G3, male mutant mice had statistically smaller testes/body weight compared to WT. This phenotype persisted into later generations. Furthermore, K82Δ mice started developing fertility defects at G4 that culminated in termination of the mutant line as only one viable G6 female K82Δ mouse was born. A reduction in seminiferous tubule number, and sperm count were observed in G5 K82Δ male mice. Also observed was as an increase in abnormal sperm morphology with K82Δ sperm displaying a globozoospermia-like phenotype (round-shaped sperm head), which has been previously linked with male infertility (Yan, 2009). Telomerase KO mice were shown to have apoptotic seminiferous tubules and loss of germ cells, however our study observed a secondary phenotype not addressed previously. While some K82Δ seminiferous tubules showed loss of germ cells resulting in what looks like empty tubules, others maintained germ cell populations but exhibited

severe disorganization extremely disruptive to the regulated radial manner in which seminiferous tubules are organized. Our study did not address if both phenotypes occur in parallel or if disorganization of the tubule occurs prior to germ cell loss. Our in-depth quantitation of cell types in testes revealed that the K82Δ mutation decreases cell numbers for spermatogonia and spermatocytes. Somatic cells in the testes like Sertoli cells were completely spared by the mutation, consistent with a germline-specific mechanism for the downstream infertility defect. In fact, K82Δ slightly increased the number of nursing Sertoli cells, perhaps to compensate for reduced germline function.

Our studies reproduce this infertility phenotype seen in mice deficient for telomerase. However, our model results from a single amino acid deletion in TPP1 that disrupts the recruitment of telomerase while keeping telomerase holoenzyme intact and maintaining TPP1's role in end-protection. Our data confirms that the mouse infertility phenotype is caused by telomerase-dependent telomere shortening.

It would be interesting to follow these phenotypes more closely and determine if the cause of these phenotypes is indeed due to specific telomere shortening in undifferentiated spermatogonia. Undifferentiated spermatogonia are a subset of spermatogonia that retain self-renewal capacity and can differentiate into more limited spermatogonia and eventually spermatocytes and spermatids (Griswold, 2018). Mice deficient in PLZF (a marker of undifferentiated spermatogonia) show reduction in testes size and tubule degeneration similar to our model (Buaas et al., 2004; Costoya et al., 2004). Since only undifferentiated spermatogonia express PLZF, it is reasonable to postulate that tubules with a reduction in spermatogonia, and therefore a reduction in PLZF, trigger an initial burst of proliferation followed by exhaustion of

the proliferative spermatogonial compartment. This increased proliferative activity has been associated with increased tubule degeneration and cell death at later stages. Critically short telomeres in undifferentiated spermatogonia could explain the reduction in germ cells we observe in our model and mirror what is seen in *Plzf*$^{-/-}$ mice. In addition, this expansion in proliferation could result in an acceleration in telomere shortening, worsening the phenotype in successive generations. This could also explain why Sertoli cell numbers are not affected as they do not derive from spermatogonia.

Further work needs to be performed to better understand how K82Δ affects reproduction in female mice. While we know that both sexes were affected and became infertile by generation 5, telomerase activity and telomere length are regulated differently in males and females. Isolated studies have shown that women with DC may have a reduction in ovarian reserve and so if ovarian reserve is reduced and continues to diminish in successive generations, it could contribute to the infertility seen in K82Δ female mice.

Collectively, our work shows that mice homozygous for the K82Δ mutation do not exhibit hematopoietic defects like in human patients with the equivalent mutation but rather succumb to sterility that is not seen in patients with DC. Accordingly, the mouse germline seems to be more vulnerable towards telomere shortening than the human germline.

4.4 Basis for species-specific impact of telomere shortening on hematopoiesis

Using a targeted mutation in TPP1, our results confirm the differential impact of telomere shortening in mice and humans. It is noteworthy that laboratory-derived inbred CAST/Ei mice,

which are known for their abnormally short (i.e., similar to human) telomere length, or mice stressed using serial transplantation, show BM defects in a telomerase negative background. These observations confirm that the longer telomeres of wild-type laboratory mice offer protection against hematopoietic failure in telomerase null (Lee et al., 1998; Rudolph et al., 1999) or deficient (Erdmann et al., 2004) background at steady-state. What is the evolutionary basis for the reduced dependence of mouse hematopoietic homeostasis on telomere length maintenance? A comparative analysis of telomere length in several animals revealed that smaller and short-lived mammals have longer telomeres than humans and other large animals (Gomes et al., 2011). As smaller and short-lived animals are expected to undergo fewer total somatic cell divisions in life, it is hypothesized that they do not rely on a telomere length threshold to check against unregulated cell division or accumulation of oncogenic mutations with age (Gomes et al., 2011). The lack of such a threshold could allow species like mice to harbor very long telomeres in their soma that would not be sensitive to telomere shortening caused by a telomeropathy mutation (in one lifetime). Given the total number of cell divisions in humans, especially in high-turnover organs such as skin and blood, enhanced somatic stem cell sensitivity to telomere shortening serves an important anti-tumorigenic role. Thus, the human somatic tissues would be expected to be especially vulnerable to accelerated telomere shortening caused by telomeropathy mutations. Our results support this model and suggest that hematopoiesis in laboratory mice is resilient to subtle or gross perturbations to the telomerase machinery.

4.5 Evolutionary model for differential vulnerabilities of human and mouse tissues towards telomere shortening

It is intriguing that no somatic phenotypes are observed in mice upon telomere shortening for five-six generations under steady state. It could be argued that the long telomeres of laboratory mice provide a telomere reserve that protects against the earlier appearance of such phenotypes. However, these reserves are still unable to prevent the decrease in fertility in G4-G5 animals, suggesting an inherent vulnerability of the mouse germline towards telomere shortening that is mirrored in the human BM and other somatic tissues. Our study falls into the crux of two theories, the "disposable soma theory" and the "life history theory" and we speculate that these distinct species-specific tissue sensitivities evolved to optimize species fitness.

The "disposable soma theory" attempts to explain that aging is caused by a trade-off between reproduction and survival (Kirkwood, 1977). The "life history theory" explains how organisms optimize the distribution of energy to either survival or reproduction to maximize the fitness of the species (Kavanagh & Kahl, 2016). While both theories are related, they are not the same and species-specific demands could influence what priorities are evolved in a given species.

While reproduction is essential to the production of offspring, survival to the age of sexual maturity is essential to the ability to reproduce. The weightage of survival to reproductive investment is influenced by the growth environment of the species. Harsh conditions such as the threat of predation, or competition from the same sex (e.g., polyandrous behavior), have resulted in smaller animals called "r-selected" species such as mice exhibiting shorter lifespans, accelerated time to sexual maturity, and an increase in the number of offspring. This is achieved

by tilting the balance of resources towards reproductive traits over somatic development. In contrast, less-threatened, larger animals called “K-selected” species including humans invest in somatic growth to produce and nurture healthy offspring, albeit at the expense of long gestation periods and fewer offspring. We envision that telomerase-mediated telomere length maintenance helps tilt the balance of energy allocation towards somatic and germline investment in larger and smaller animals, respectively. As mice have shorter lifespans, their resources are devoted towards producing more offspring while humans, who have longer lifespans, tend to devote their resources towards living longer to produce and nurture healthy offspring.

In humans, telomere length maintenance is likely more critical in somatic stem and progenitor cells, such as those in the hematopoietic system, to meet the replicative demand for these cells to ensure healthy progression to the age of sexual maturity. This function may be secondary in mice given their smaller size and much shorter lifespan. In contrast, telomere length maintenance in mice is likely more critical to uphold the elevated demand for germline proliferation to ensure accelerated sexual development and an increase in both the number of offspring per litter and total litters in life. The notion of a differential dependence of human and mouse germ cells on telomere length maintenance is supported by a stark difference in germline development in the two species. The mouse testis is comprised predominantly of sperm and other differentiated germ cells, with spermatogonia representing only 0.3% of all cells in this organ (Larose et al., 2019). In contrast, spermatogonial stem cells are 22% of cells in the human testis (Larose et al., 2019). The severely lowered ratio of stem cells to mature sperm in the mouse testes highlights the extraordinary replicative burden on a small number of mouse germline stem cells for generating the entire sperm pool of the animal throughout its reproductive lifespan.

4.6 Implications for mammalian models of telomeropathies

Combined with previous findings in telomerase KO mice, our data mandate a change in the use of existing models to understand the importance of telomerase-mediated telomere lengthening in human health and disease. The resilience of mice to the somatic absence of telomerase-mediated telomere lengthening is well known. It has been hypothesized that the abnormally long telomere length in laboratory mice is primarily responsible for this species-specificity although it is also likely that these distinct vulnerabilities are, at least in part, manifestations of the different evolutionary strategies of mice and humans. Hematopoietic defects are observed in $mTR^{-/-}$ mice in a CAST/EiJ background that harbors short telomeres, qualifying them as a potential system to model telomeropathies (Armanios et al., 2009). However, it is unlikely that resetting telomeres to a shorter length is sufficient to reverse the long-optimized evolutionary strategy of any strain of mice. In this regard, it is likely that mouse strains with shorter telomeres also suffer from reduced reproductive capacity compared to the wild-type strain. Instead of "humanizing" mice, it seems more appropriate, although more challenging, to investigate the biomedical relevance of telomerase and telomere length maintenance in mammals that more closely mimic humans in their vulnerability to telomere shortening.

4.7 Future studies

My dissertation has shown that deletion of TPP1 K82Δ in the whole organism does not result in spontaneous BM failure in up to five generations. It is possible that the telomeres in these mice are not yet at a critically short telomere length to result in hematopoietic defects. The answer to

why a reproductive defect arises first in these mutant mice may derive from the much higher replicative burden in the mouse germline compared to humans. Since the mutation affects TPP1's ability to properly recruit telomerase to chromosome ends, it would be understandable that telomeres would be shorter in these mice compared to WT. However, the need for this much smaller pool of cells to continuously replicate may provide the basis for the sensitivity we see in the mouse germline. Furthermore, this species-specific difference in stem cell pools does not exist in the BM as HSCs have been found to comparable between mice and humans (Abkowitz et al., 2002). If true, we hypothesize that the telomeres in the germline shorten at a rate faster than those in the soma of the mutant mouse. To answer this, we could modify the BM flow-FISH assay I optimized and describe in Chapter 2, to measure telomere length of both the BM and the germline of the same mouse. For this, we would dissect hindlimbs and testes from the same mouse and generate individual single cell suspensions from WT and K82Δ mice in G1 versus G5 and perform telomere length analysis. In G1 K82Δ mice, we would expect to see shorter telomeres in both BM and testes cells compared to G1 WT, but the extent of shortening would be greater in the testes. Since the reproductive phenotype does not emerge until ~G4, telomere length measurement in the testes of G5 K82Δ mice would provide the most sensitive setup for discerning BM versus testes differences in the mutant mouse. In this case, we would expect age-matched G5 WT and G1 WT to look identical in both BM and testes compartments. In G5 K82Δ mice, we would expect to see a stark reduction in telomere length in BM and testes compared to WT, but within G5 K82Δ mice, we would expect to see a reduction in testes telomere length to values that are representative of critically short telomeres.

Even though my work suggests a change in the modeling of telomeropathies, it does raise interesting questions in stem cell biology about differential vulnerabilities of organ systems in mice. For example, it would be interesting to investigate in greater detail how specific stem cell compartments respond to telomere shortening caused by the TPP1 mutation. Specifically, it would be interesting to ask if spontaneous BM failure could emerge in K82Δ mice if TPP1 WT expression was restored in the germline. To test this, we could generate a mouse with a successfully integrated loxP-flanked stop sequence prior to TPP1 WT. Using a knock-in approach utilizing the well-characterized ROSA26 locus (Soriano, 1999) which is ubiquitously expressed and allows for targeted and conditional overexpression in Cre-expressing lines by placing a *loxP*-STOP-*loxP* floxed STOP element upstream of our gene of interest (Carofino et al., 2013) I would suggest designing ROSA26 floxed-stop *Acd* construct injected into our mutant heterozygous mice (e.g. female K82Δ/+ mice) and then crossing those mice to Vasa-cre^{ERT2} (John et al., 2008) mice we would generate mice that under homozygous conditions express K82Δ/K82Δ everywhere that TPP1 is present however, in the presence of tamoxifen Acd will be overexpressed only in germ cells. This will allow us to breed mice starting at G0 that are deficient in TPP1 until we provide tamoxifen. This allows us control in analyzing rescue of TPP1 in the germline in early, mid or late generations. I would hypothesize that mice that are WT for TPP1 in the germline would be fertile in later generations. Therefore, we would be able to analyze what other stem cell compartments are sensitive to this mutation without inference from the sterility phenotype.

To delve even deeper on understanding how telomere erosion affects the germline versus the hematopoietic compartments, we could challenge each system to study the impact on stem cell

maintenance through either BM or germline transplants. Our hypothesis is that the replicative burden of germline stem cells is greater than the replicative burden of BM stem cells. It has previously been shown that spermatogonial stem cells can be consecutively passaged at three month intervals for more than three years (Ryu et al., 2006), contrasting strikingly with HSCs that after four-five transplants can no longer replicate (Ogden & Mickliem, 1976; Siminovitch et al., 1964). To test our hypothesis, we could use a different genetic system, one that employs the ROSA26 LacZ or eGFP system to cross to *Acd K82*$\Delta^{+/-}$ G0 mice. We would breed successive generations and generate testes single cell suspensions for G1 and G5 WT and mutant male mice. We would then enrich for spermatogonial stem cells from three-month-old mice and transplant them into ablated WT mice to compare how mutant germline stem cells engraft compared to WT. Using the ROSA26 LacZ or eGFP system will allow us to visualize colonies grown from donor-derived spermatogenesis. We would expect G5 mutants to engraft much more poorly than G5 WT. If there is no change in stem cell activity, we could then examine the stem cell niche as a contributing factor to infertility. For this, we will perform the reverse transplantation – we would enrich for spermatogonial stem cells from three-month-old WT mice and transplant them into ablated mutant mice to ask how WT germline stem cells engraft in the mutant niche.

In conclusion, my Ph.D. dissertation work provides new insights into the importance of telomerase-based telomere lengthening in the mouse hematopoietic versus germline tissues and reveals species-specific differences in the importance of this biological process in mouse versus humans. My studies inspire new hypotheses in stem cell biology with respect to the differential burden on somatic versus germline regeneration for defining species fitness. My studies have important implications for telomeropathies, strongly encouraging a change in the animal

modeling of these diseases in the future to better understand disease mechanism and develop potential therapeutic interventions.

Bibliography

Abkowitz, J. L., Catlin, S. N., McCallie, M. T., & Guttorp, P. (2002, Oct 01). Evidence that the number of hematopoietic stem cells per animal is conserved in mammals. *Blood, 100*(7), 2665-2667. https://doi.org/10.1182/blood-2002-03-0822

Abreu, E., Aritonovska, E., Reichenbach, P., Cristofari, G., Culp, B., Terns, R. M., Lingner, J., & Terns, M. P. (2010, Jun). TIN2-tethered TPP1 recruits human telomerase to telomeres in vivo. *Mol Cell Biol, 30*(12), 2971-2982. https://doi.org/10.1128/mcb.00240-10

Akincilar, S. C., Chan, C. H. T., Ng, Q. F., Fidan, K., & Tergaonkar, V. (2021, May). Non-canonical roles of canonical telomere binding proteins in cancers. *Cell Mol Life Sci, 78*(9), 4235-4257. https://doi.org/10.1007/s00018-021-03783-0

Alder, J. K., Stanley, S. E., Wagner, C. L., Hamilton, M., Hanumanthu, V. S., & Armanios, M. (2015, May). Exome sequencing identifies mutant TINF2 in a family with pulmonary fibrosis. *Chest, 147*(5), 1361-1368. https://doi.org/10.1378/chest.14-1947

Allsopp, R. C., Morin, G. B., DePinho, R., Harley, C. B., & Weissman, I. L. (2003, Jul 15). Telomerase is required to slow telomere shortening and extend replicative lifespan of HSCs during serial transplantation. *Blood, 102*(2), 517-520. https://doi.org/10.1182/blood-2002-07-2334

Armanios, M. (2012, Feb 01). Telomerase and idiopathic pulmonary fibrosis. *Mutat Res, 730*(1-2), 52-58. https://doi.org/10.1016/j.mrfmmm.2011.10.013

Armanios, M., Alder, J. K., Parry, E. M., Karim, B., Strong, M. A., & Greider, C. W. (2009, Dec). Short telomeres are sufficient to cause the degenerative defects associated with aging. *Am J Hum Genet, 85*(6), 823-832. https://doi.org/10.1016/j.ajhg.2009.10.028

Armanios, M., & Blackburn, E. H. (2012, Oct). The telomere syndromes. *Nat Rev Genet, 13*(10), 693-704. https://doi.org/10.1038/nrg3246

Armbruster, B. N., Etheridge, K. T., Broccoli, D., & Counter, C. M. (2003, May). Putative telomere-recruiting domain in the catalytic subunit of human telomerase. *Mol Cell Biol, 23*(9), 3237-3246. https://doi.org/10.1128/mcb.23.9.3237-3246.2003

Armbruster, B. N., Linardic, C. M., Veldman, T., Bansal, N. P., Downie, D. L., & Counter, C. M. (2004, Apr). Rescue of an hTERT mutant defective in telomere elongation by fusion

with hPot1. *Mol Cell Biol, 24*(8), 3552-3561. https://doi.org/10.1128/MCB.24.8.3552-3561.2004

Baerlocher, G. M., Vulto, I., de Jong, G., & Lansdorp, P. M. (2006). Flow cytometry and FISH to measure the average length of telomeres (flow FISH). *Nat Protoc, 1*(5), 2365-2376. https://doi.org/10.1038/nprot.2006.263

Ballew, B. J., & Savage, S. A. (2013, Jun). Updates on the biology and management of dyskeratosis congenita and related telomere biology disorders. *Expert Rev Hematol, 6*(3), 327-337. https://doi.org/10.1586/ehm.13.23

Barrionuevo, F., Bagheri-Fam, S., Klattig, J., Kist, R., Taketo, M. M., Englert, C., & Scherer, G. (2006, Jan). Homozygous inactivation of Sox9 causes complete XY sex reversal in mice. *Biol Reprod, 74*(1), 195-201. https://doi.org/10.1095/biolreprod.105.045930

Baumann, P., & Cech, T. R. (2001, May 11). Pot1, the putative telomere end-binding protein in fission yeast and humans. *Science, 292*(5519), 1171-1175. http://www.ncbi.nlm.nih.gov/entrez/query.fcgi?cmd=Retrieve&db=PubMed&dopt=Citation&list_uids=11349150

Baumann, P., Podell, E., & Cech, T. R. (2002, Nov). Human Pot1 (protection of telomeres) protein: cytolocalization, gene structure, and alternative splicing. *Mol Cell Biol, 22*(22), 8079-8087. https://doi.org/10.1128/mcb.22.22.8079-8087.2002

Bianchi, A., Smith, S., Chong, L., Elias, P., & de Lange, T. (1997, Apr 01). TRF1 is a dimer and bends telomeric DNA. *EMBO J, 16*(7), 1785-1794. https://doi.org/10.1093/emboj/16.7.1785

Bilaud, T., Brun, C., Ancelin, K., Koering, C. E., Laroche, T., & Gilson, E. (1997, Oct). Telomeric localization of TRF2, a novel human telobox protein. *Nat Genet, 17*(2), 236-239. https://doi.org/10.1038/ng1097-236

Bisht, K., Smith, E. M., Tesmer, V. M., & Nandakumar, J. (2016, 11). Structural and functional consequences of a disease mutation in the telomere protein TPP1. *Proc Natl Acad Sci U S A, 113*(46), 13021-13026. https://doi.org/10.1073/pnas.1605685113

Blasco, M. A., Lee, H. W., Hande, M. P., Samper, E., Lansdorp, P. M., DePinho, R. A., & Greider, C. W. (1997, Oct). Telomere shortening and tumor formation by mouse cells lacking telomerase RNA. *Cell, 91*(1), 25-34. https://doi.org/10.1016/s0092-8674(01)80006-4

Boyer, L. A., Latek, R. R., & Peterson, C. L. (2004, Feb). The SANT domain: a unique histone-tail-binding module? *Nat Rev Mol Cell Biol, 5*(2), 158-163. https://doi.org/10.1038/nrm1314

Broccoli, D., Chong, L., Oelmann, S., Fernald, A. A., Marziliano, N., van Steensel, B., Kipling, D., Le Beau, M. M., & de Lange, T. (1997, Jan). Comparison of the human and mouse genes encoding the telomeric protein, TRF1: chromosomal localization, expression and conserved protein domains. *Hum Mol Genet, 6*(1), 69-76. https://doi.org/10.1093/hmg/6.1.69

Broccoli, D., Smogorzewska, A., Chong, L., & de Lange, T. (1997, Oct). Human telomeres contain two distinct Myb-related proteins, TRF1 and TRF2. *Nat Genet, 17*(2), 231-235. https://doi.org/10.1038/ng1097-231

Bryan, T. M., Goodrich, K. J., & Cech, T. R. (2000a, Aug 04). A mutant of Tetrahymena telomerase reverse transcriptase with increased processivity. *J Biol Chem, 275*(31), 24199-24207. https://doi.org/10.1074/jbc.M003246200

Bryan, T. M., Goodrich, K. J., & Cech, T. R. (2000b, Aug). Telomerase RNA bound by protein motifs specific to telomerase reverse transcriptase. *Mol Cell, 6*(2), 493-499. https://doi.org/10.1016/s1097-2765(00)00048-4

Buaas, F. W., Kirsh, A. L., Sharma, M., McLean, D. J., Morris, J. L., Griswold, M. D., de Rooij, D. G., & Braun, R. E. (2004, Jun). Plzf is required in adult male germ cells for stem cell self-renewal. *Nat Genet, 36*(6), 647-652. https://doi.org/10.1038/ng1366

Canudas, S., Houghtaling, B. R., Bhanot, M., Sasa, G., Savage, S. A., Bertuch, A. A., & Smith, S. (2011, Sep 01). A role for heterochromatin protein 1γ at human telomeres. *Genes Dev, 25*(17), 1807-1819. https://doi.org/10.1101/gad.17325211

Carofino, B. L., Ayanga, B., & Justice, M. J. (2013, Nov). A mouse model for inducible overexpression of Prdm14 results in rapid-onset and highly penetrant T-cell acute lymphoblastic leukemia (T-ALL). *Dis Model Mech, 6*(6), 1494-1506. https://doi.org/10.1242/dmm.012575

Celli, G. B., & de Lange, T. (2005, Jul). DNA processing is not required for ATM-mediated telomere damage response after TRF2 deletion. *Nat Cell Biol, 7*(7), 712-718. https://doi.org/10.1038/ncb1275

Chaboissier, M. C., Kobayashi, A., Vidal, V. I., Lützkendorf, S., van de Kant, H. J., Wegner, M., de Rooij, D. G., Behringer, R. R., & Schedl, A. (2004, May). Functional analysis of Sox8 and Sox9 during sex determination in the mouse. *Development, 131*(9), 1891-1901. https://doi.org/10.1242/dev.01087

Chen, Y., Yang, Y., van Overbeek, M., Donigian, J. R., Baciu, P., de Lange, T., & Lei, M. (2008, Feb 22). A shared docking motif in TRF1 and TRF2 used for differential recruitment of telomeric proteins. *Science, 319*(5866), 1092-1096. https://doi.org/10.1126/science.1151804

Chiang, Y. J., Kim, S. H., Tessarollo, L., Campisi, J., & Hodes, R. J. (2004, Aug). Telomere-associated protein TIN2 is essential for early embryonic development through a telomerase-independent pathway. *Mol Cell Biol, 24*(15), 6631-6634. https://doi.org/10.1128/mcb.24.15.6631-6634.2004

Chong, L., van Steensel, B., Broccoli, D., Erdjument-Bromage, H., Hanish, J., Tempst, P., & de Lange, T. (1995, Dec 08). A human telomeric protein. *Science, 270*(5242), 1663-1667. https://doi.org/10.1126/science.270.5242.1663

Choudhury, A. R., Ju, Z., Djojosubroto, M. W., Schienke, A., Lechel, A., Schaetzlein, S., Jiang, H., Stepczynska, A., Wang, C., Buer, J., Lee, H. W., von Zglinicki, T., Ganser, A., Schirmacher, P., Nakauchi, H., & Rudolph, K. L. (2007, Jan). Cdkn1a deletion improves stem cell function and lifespan of mice with dysfunctional telomeres without accelerating cancer formation. *Nat Genet, 39*(1), 99-105. https://doi.org/10.1038/ng1937

Chu, T. W., D'Souza, Y., & Autexier, C. (2016, Jan 01). The Insertion in Fingers Domain in Human Telomerase Can Mediate Enzyme Processivity and Telomerase Recruitment to Telomeres in a TPP1-Dependent Manner. *Mol Cell Biol, 36*(1), 210-222. https://doi.org/10.1128/mcb.00746-15

Chu, T. W., MacNeil, D. E., & Autexier, C. (2016, Apr 15). Multiple Mechanisms Contribute to the Cell Growth Defects Imparted by Human Telomerase Insertion in Fingers Domain Mutations Associated with Premature Aging Diseases. *J Biol Chem, 291*(16), 8374-8386. https://doi.org/10.1074/jbc.M116.714782

Collins, K. (2008, 2008 Jan-Feb). Physiological assembly and activity of human telomerase complexes. *Mech Ageing Dev, 129*(1-2), 91-98. https://doi.org/10.1016/j.mad.2007.10.008

Coppin, E., Florentin, J., Vasamsetti, S. B., Arunkumar, A., Sembrat, J., Rojas, M., & Dutta, P. (2018, Mar 11). Splenic hematopoietic stem cells display a pre-activated phenotype. *Immunol Cell Biol*. https://doi.org/10.1111/imcb.12035

Costoya, J. A., Hobbs, R. M., Barna, M., Cattoretti, G., Manova, K., Sukhwani, M., Orwig, K. E., Wolgemuth, D. J., & Pandolfi, P. P. (2004, Jun). Essential role of Plzf in maintenance of spermatogonial stem cells. *Nat Genet, 36*(6), 653-659. https://doi.org/10.1038/ng1367

D'Amours, D., & Jackson, S. P. (2002, May). The Mre11 complex: at the crossroads of dna repair and checkpoint signalling. *Nat Rev Mol Cell Biol, 3*(5), 317-327. https://doi.org/10.1038/nrm805

de Lange, T., Shiue, L., Myers, R. M., Cox, D. R., Naylor, S. L., Killery, A. M., & Varmus, H. E. (1990, Feb). Structure and variability of human chromosome ends. *Mol Cell Biol, 10*(2), 518-527. https://doi.org/10.1128/mcb.10.2.518-527.1990

Dokal, I. (2011). Dyskeratosis congenita. *Hematology Am Soc Hematol Educ Program, 2011*, 480-486. https://doi.org/10.1182/asheducation-2011.1.480

Doksani, Y., Wu, J. Y., de Lange, T., & Zhuang, X. (2013, Oct 10). Super-resolution fluorescence imaging of telomeres reveals TRF2-dependent T-loop formation. *Cell, 155*(2), 345-356. https://doi.org/10.1016/j.cell.2013.09.048

Doulatov, S., Notta, F., Laurenti, E., & Dick, J. E. (2012, Feb 03). Hematopoiesis: a human perspective. *Cell Stem Cell, 10*(2), 120-136. https://doi.org/10.1016/j.stem.2012.01.006

Egan, E. D., & Collins, K. (2010, Jun). Specificity and stoichiometry of subunit interactions in the human telomerase holoenzyme assembled in vivo. *Mol Cell Biol, 30*(11), 2775-2786. https://doi.org/10.1128/mcb.00151-10

Erdmann, N., Liu, Y., & Harrington, L. (2004, Apr 20). Distinct dosage requirements for the maintenance of long and short telomeres in mTert heterozygous mice. *Proc Natl Acad Sci U S A, 101*(16), 6080-6085. https://doi.org/10.1073/pnas.0401580101

Famili, F., Wiekmeijer, A. S., & Staal, F. J. (2017, Aug). The development of T cells from stem cells in mice and humans. *Future Sci OA, 3*(3), FSO186. https://doi.org/10.4155/fsoa-2016-0095

Forsyth, N. R., Wright, W. E., & Shay, J. W. (2002, Jan). Telomerase and differentiation in multicellular organisms: turn it off, turn it on, and turn it off again. *Differentiation, 69*(4-5), 188-197. https://doi.org/10.1046/j.1432-0436.2002.690412.x

França, L. R., Hess, R. A., Dufour, J. M., Hofmann, M. C., & Griswold, M. D. (2016, Mar). The Sertoli cell: one hundred fifty years of beauty and plasticity. *Andrology, 4*(2), 189-212. https://doi.org/10.1111/andr.12165

Frank, A. K., Tran, D. C., Qu, R. W., Stohr, B. A., Segal, D. J., & Xu, L. (2015, Jul). The Shelterin TIN2 Subunit Mediates Recruitment of Telomerase to Telomeres. *PLoS Genet, 11*(7), e1005410. https://doi.org/10.1371/journal.pgen.1005410

Frescas, D., & de Lange, T. (2014, Jan 15). A TIN2 dyskeratosis congenita mutation causes telomerase-independent telomere shortening in mice. *Genes Dev, 28*(2), 153-166. https://doi.org/10.1101/gad.233395.113

Friedman, K. L. (2011, Jun). Telomerase reverse transcriptase and Wnt signaling. *Mol Cell Biol, 31*(12), 2366-2368. https://doi.org/10.1128/mcb.05462-11

Ghanim, G. E., Fountain, A. J., van Roon, A. M., Rangan, R., Das, R., Collins, K., & Nguyen, T. H. D. (2021, 05). Structure of human telomerase holoenzyme with bound telomeric DNA. *Nature, 593*(7859), 449-453. https://doi.org/10.1038/s41586-021-03415-4

Ghosh, A., Saginc, G., Leow, S. C., Khattar, E., Shin, E. M., Yan, T. D., Wong, M., Zhang, Z., Li, G., Sung, W. K., Zhou, J., Chng, W. J., Li, S., Liu, E., & Tergaonkar, V. (2012, Dec). Telomerase directly regulates NF-κB-dependent transcription. *Nat Cell Biol, 14*(12), 1270-1281. https://doi.org/10.1038/ncb2621

Giri, N., Alter, B. P., Savage, S. A., & Stratton, P. (2021, 06). Gynaecological and reproductive health of women with telomere biology disorders. *Br J Haematol, 193*(6), 1238-1246. https://doi.org/10.1111/bjh.17545

Giri, N., Stratton, P., Savage, S. A., & Alter, B. P. (2017, 10 05). Pregnancies in patients with inherited bone marrow failure syndromes in the NCI cohort. *Blood, 130*(14), 1674-1676. https://doi.org/10.1182/blood-2017-08-802991

Gomes, N. M., Ryder, O. A., Houck, M. L., Charter, S. J., Walker, W., Forsyth, N. R., Austad, S. N., Venditti, C., Pagel, M., Shay, J. W., & Wright, W. E. (2011, Oct). Comparative biology of mammalian telomeres: hypotheses on ancestral states and the roles of telomeres in longevity determination. *Aging Cell, 10*(5), 761-768. https://doi.org/10.1111/j.1474-9726.2011.00718.x

Greider, C. W., & Blackburn, E. H. (1985, Dec). Identification of a specific telomere terminal transferase activity in Tetrahymena extracts. *Cell, 43*(2 Pt 1), 405-413. https://doi.org/10.1016/0092-8674(85)90170-9

Greider, C. W., & Blackburn, E. H. (1989, Jan 26). A telomeric sequence in the RNA of Tetrahymena telomerase required for telomere repeat synthesis. *Nature, 337*(6205), 331-337. https://doi.org/10.1038/337331a0

Grill, S., Bisht, K., Tesmer, V. M., Shami, A. N., Hammoud, S. S., & Nandakumar, J. (2019, Jun 18). Two Separation-of-Function Isoforms of Human TPP1 Dictate Telomerase Regulation in Somatic and Germ Cells. *Cell Rep, 27*(12), 3511-3521 e3517. https://doi.org/10.1016/j.celrep.2019.05.073

Grill, S., & Nandakumar, J. (2020, Nov). Molecular mechanisms of telomere biology disorders. *J Biol Chem, 296*, 100064. https://doi.org/10.1074/jbc.REV120.014017

Grill, S., Padmanaban, S., Friedman, A., Perkey, E., Allen, F., Tesmer, V. M., Chase, J., Khoriaty, R., Keegan, C. E., Maillard, I., & Nandakumar, J. (2021, 05 10). TPP1 mutagenesis screens unravel shelterin interfaces and functions in hematopoiesis. *JCI Insight, 6*(9). https://doi.org/10.1172/jci.insight.138059

Grill, S., Tesmer, V. M., & Nandakumar, J. (2018, 01). The N Terminus of the OB Domain of Telomere Protein TPP1 Is Critical for Telomerase Action. *Cell Rep, 22*(5), 1132-1140. https://doi.org/10.1016/j.celrep.2018.01.012

Griswold, M. D. (2018, 07 01). 50 years of spermatogenesis: Sertoli cells and their interactions with germ cells. *Biol Reprod, 99*(1), 87-100. https://doi.org/10.1093/biolre/ioy027

Gu, P., Jia, S., Takasugi, T., Tesmer, V. M., Nandakumar, J., Chen, Y., & Chang, S. (2021, 09 17). Distinct functions of POT1 proteins contribute to the regulation of telomerase recruitment to telomeres. *Nat Commun, 12*(1), 5514. https://doi.org/10.1038/s41467-021-25799-7

Guo, Y., Kartawinata, M., Li, J., Pickett, H. A., Teo, J., Kilo, T., Barbaro, P. M., Keating, B., Chen, Y., Tian, L., Al-Odaib, A., Reddel, R. R., Christodoulou, J., Xu, X., Hakonarson, H., & Bryan, T. M. (2014, Oct 30). Inherited bone marrow failure associated with germline mutation of ACD, the gene encoding telomere protein TPP1. *Blood, 124*(18), 2767-2774. https://doi.org/10.1182/blood-2014-08-596445

He, H., Multani, A. S., Cosme-Blanco, W., Tahara, H., Ma, J., Pathak, S., Deng, Y., & Chang, S. (2006, Nov 01). POT1b protects telomeres from end-to-end chromosomal fusions and aberrant homologous recombination. *EMBO J, 25*(21), 5180-5190. https://doi.org/10.1038/sj.emboj.7601294

He, H., Wang, Y., Guo, X., Ramchandani, S., Ma, J., Shen, M. F., Garcia, D. A., Deng, Y., Multani, A. S., You, M. J., & Chang, S. (2009, Jan). Pot1b deletion and telomerase haploinsufficiency in mice initiate an ATR-dependent DNA damage response and elicit phenotypes resembling dyskeratosis congenita. *Mol Cell Biol, 29*(1), 229-240. https://doi.org/10.1128/MCB.01400-08

He, Y., Wang, Y., Liu, B., Helmling, C., Sušac, L., Cheng, R., Zhou, Z. H., & Feigon, J. (2021, 05). Structures of telomerase at several steps of telomere repeat synthesis. *Nature, 593*(7859), 454-459. https://doi.org/10.1038/s41586-021-03529-9

Hemann, M. T., Rudolph, K. L., Strong, M. A., DePinho, R. A., Chin, L., & Greider, C. W. (2001, Jul). Telomere dysfunction triggers developmentally regulated germ cell apoptosis. *Mol Biol Cell, 12*(7), 2023-2030. https://doi.org/10.1091/mbc.12.7.2023

Herrera, E., Martínez-A, C., & Blasco, M. A. (2000, Feb 01). Impaired germinal center reaction in mice with short telomeres. *EMBO J, 19*(3), 472-481. https://doi.org/10.1093/emboj/19.3.472

Herrera, E., Samper, E., Martín-Caballero, J., Flores, J. M., Lee, H. W., & Blasco, M. A. (1999, Jun 01). Disease states associated with telomerase deficiency appear earlier in mice with short telomeres. *EMBO J, 18*(11), 2950-2960. https://doi.org/10.1093/emboj/18.11.2950

Hockemeyer, D., Daniels, J. P., Takai, H., & de Lange, T. (2006, Jul 14). Recent expansion of the telomeric complex in rodents: Two distinct POT1 proteins protect mouse telomeres. *Cell, 126*(1), 63-77. https://doi.org/10.1016/j.cell.2006.04.044

Hockemeyer, D., Palm, W., Else, T., Daniels, J. P., Takai, K. K., Ye, J. Z., Keegan, C. E., de Lange, T., & Hammer, G. D. (2007, Aug). Telomere protection by mammalian Pot1

requires interaction with Tpp1. *Nat Struct Mol Biol, 14*(8), 754-761. https://doi.org/10.1038/nsmb1270

Hockemeyer, D., Palm, W., Wang, R. C., Couto, S. S., & de Lange, T. (2008, Jul 1). Engineered telomere degradation models dyskeratosis congenita. *Genes Dev, 22*(13), 1773-1785. https://doi.org/10.1101/gad.1679208

Hockemeyer, D., Sfeir, A. J., Shay, J. W., Wright, W. E., & de Lange, T. (2005, Jul 20). POT1 protects telomeres from a transient DNA damage response and determines how human chromosomes end. *EMBO J, 24*(14), 2667-2678. https://doi.org/10.1038/sj.emboj.7600733

Hosokawa, K., & Arai, F. (2018, Jun). The role of telomere binding molecules for normal and abnormal hematopoiesis. *Int J Hematol, 107*(6), 646-655. https://doi.org/10.1007/s12185-018-2432-4

Houghtaling, B. R., Cuttonaro, L., Chang, W., & Smith, S. (2004, Sep 21). A dynamic molecular link between the telomere length regulator TRF1 and the chromosome end protector TRF2. *Curr Biol, 14*(18), 1621-1631. https://doi.org/10.1016/j.cub.2004.08.052

Jacobs, S. A., Podell, E. R., & Cech, T. R. (2006, Mar). Crystal structure of the essential N-terminal domain of telomerase reverse transcriptase. *Nat Struct Mol Biol, 13*(3), 218-225. https://doi.org/10.1038/nsmb1054

Jiang, J., Wang, Y., Sušac, L., Chan, H., Basu, R., Zhou, Z. H., & Feigon, J. (2018, 05 17). Structure of Telomerase with Telomeric DNA. *Cell, 173*(5), 1179-1190.e1113. https://doi.org/10.1016/j.cell.2018.04.038

John, G. B., Gallardo, T. D., Shirley, L. J., & Castrillon, D. H. (2008, Sep 1). Foxo3 is a PI3K-dependent molecular switch controlling the initiation of oocyte growth. *Dev Biol, 321*(1), 197-204. https://doi.org/10.1016/j.ydbio.2008.06.017

Jones, M., Bisht, K., Savage, S. A., Nandakumar, J., Keegan, C. E., & Maillard, I. (2016, 05). The shelterin complex and hematopoiesis. *J Clin Invest, 126*(5), 1621-1629. https://doi.org/10.1172/jci84547

Jones, M., Osawa, G., Regal, J. A., Weinberg, D. N., Taggart, J., Kocak, H., Friedman, A., Ferguson, D. O., Keegan, C. E., & Maillard, I. (2014, Jan). Hematopoietic stem cells are acutely sensitive to Acd shelterin gene inactivation. *J Clin Invest, 124*(1), 353-366. https://doi.org/10.1172/JCI67871

Kalmbach, K. H., Fontes Antunes, D. M., Dracxler, R. C., Knier, T. W., Seth-Smith, M. L., Wang, F., Liu, L., & Keefe, D. L. (2013, Jan). Telomeres and human reproduction. *Fertil Steril, 99*(1), 23-29. https://doi.org/10.1016/j.fertnstert.2012.11.039

Karlseder, J., Broccoli, D., Dai, Y., Hardy, S., & de Lange, T. (1999, Feb 26). p53- and ATM-dependent apoptosis induced by telomeres lacking TRF2. *Science, 283*(5406), 1321-1325. https://doi.org/10.1126/science.283.5406.1321

Karlseder, J., Hoke, K., Mirzoeva, O. K., Bakkenist, C., Kastan, M. B., Petrini, J. H., & de Lange, T. (2004, Aug). The telomeric protein TRF2 binds the ATM kinase and can inhibit the ATM-dependent DNA damage response. *PLoS Biol, 2*(8), E240. https://doi.org/10.1371/journal.pbio.0020240

Karlseder, J., Kachatrian, L., Takai, H., Mercer, K., Hingorani, S., Jacks, T., & de Lange, T. (2003, Sep). Targeted deletion reveals an essential function for the telomere length regulator Trf1. *Mol Cell Biol, 23*(18), 6533-6541. https://doi.org/10.1128/mcb.23.18.6533-6541.2003

Kavanagh, P. S., & Kahl, B. L. (2016). Life History Theory. In V. Weekes-Shackelford, T. K. Shackelford, & V. A. Weekes-Shackelford (Eds.), *Encyclopedia of Evolutionary Psychological Science* (pp. 1-12). Springer International Publishing. https://doi.org/10.1007/978-3-319-16999-6_1914-1

Keefe, D. L. (2016, 12). Telomeres, Reproductive Aging, and Genomic Instability During Early Development. *Reprod Sci, 23*(12), 1612-1615. https://doi.org/10.1177/1933719116676397

Keegan, C. E., Hutz, J. E., Else, T., Adamska, M., Shah, S. P., Kent, A. E., Howes, J. M., Beamer, W. G., & Hammer, G. D. (2005, Jan 1). Urogenital and caudal dysgenesis in adrenocortical dysplasia (acd) mice is caused by a splicing mutation in a novel telomeric regulator. *Hum Mol Genet, 14*(1), 113-123. https://doi.org/10.1093/hmg/ddi011

Kim, H., Lee, O. H., Xin, H., Chen, L. Y., Qin, J., Chae, H. K., Lin, S. Y., Safari, A., Liu, D., & Songyang, Z. (2009, Apr). TRF2 functions as a protein hub and regulates telomere maintenance by recognizing specific peptide motifs. *Nat Struct Mol Biol, 16*(4), 372-379. https://doi.org/10.1038/nsmb.1575

Kim, S. H., Kaminker, P., & Campisi, J. (1999, Dec). TIN2, a new regulator of telomere length in human cells. *Nat Genet, 23*(4), 405-412. https://doi.org/10.1038/70508

Kipling, D., & Cooke, H. J. (1990, Sep 27). Hypervariable ultra-long telomeres in mice. *Nature, 347*(6291), 400-402. https://doi.org/10.1038/347400a0

Kirkwood, T. B. (1977, Nov 24). Evolution of ageing. *Nature, 270*(5635), 301-304. https://doi.org/10.1038/270301a0

Kocak, H., Ballew, B. J., Bisht, K., Eggebeen, R., Hicks, B. D., Suman, S., O'Neil, A., Giri, N., Maillard, I., Alter, B. P., Keegan, C. E., Nandakumar, J., Savage, S. A., Laboratory, N. D. C. G. R., & Group, N. D. C. S. W. (2014, Oct). Hoyeraal-Hreidarsson syndrome caused

by a germline mutation in the TEL patch of the telomere protein TPP1. *Genes Dev, 28*(19), 2090-2102. https://doi.org/10.1101/gad.248567.114

Kosebent, E. G., & Ozturk, S. (2021, 07 30). Telomere associated gene expression as well as TERT protein level and telomerase activity are altered in the ovarian follicles of aged mice. *Sci Rep, 11*(1), 15569. https://doi.org/10.1038/s41598-021-95239-5

Larose, H., Shami, A. N., Abbott, H., Manske, G., Lei, L., & Hammoud, S. S. (2019). Gametogenesis: A journey from inception to conception. *Curr Top Dev Biol, 132*, 257-310. https://doi.org/10.1016/bs.ctdb.2018.12.006

Latrick, C. M., & Cech, T. R. (2010, Mar 03). POT1-TPP1 enhances telomerase processivity by slowing primer dissociation and aiding translocation. *EMBO J, 29*(5), 924-933. https://doi.org/10.1038/emboj.2009.409

Lee, H. W., Blasco, M. A., Gottlieb, G. J., Horner, J. W., Greider, C. W., & DePinho, R. A. (1998, Apr). Essential role of mouse telomerase in highly proliferative organs. *Nature, 392*(6676), 569-574. https://doi.org/10.1038/33345

Lei, M., Podell, E. R., & Cech, T. R. (2004, Dec). Structure of human POT1 bound to telomeric single-stranded DNA provides a model for chromosome end-protection. *Nat Struct Mol Biol, 11*(12), 1223-1229. https://doi.org/10.1038/nsmb867

Li, B., Oestreich, S., & de Lange, T. (2000, May 26). Identification of human Rap1: implications for telomere evolution. *Cell, 101*(5), 471-483. https://doi.org/10.1016/s0092-8674(00)80858-2

Lingner, J., Hughes, T. R., Shevchenko, A., Mann, M., Lundblad, V., & Cech, T. R. (1997, Apr 25). Reverse transcriptase motifs in the catalytic subunit of telomerase. *Science, 276*(5312), 561-567. https://doi.org/10.1126/science.276.5312.561

Listerman, I., Gazzaniga, F. S., & Blackburn, E. H. (2014, Jan). An investigation of the effects of the core protein telomerase reverse transcriptase on Wnt signaling in breast cancer cells. *Mol Cell Biol, 34*(2), 280-289. https://doi.org/10.1128/mcb.00844-13

Liu, D., Safari, A., O'Connor, M. S., Chan, D. W., Laegeler, A., Qin, J., & Songyang, Z. (2004, Jul). PTOP interacts with POT1 and regulates its localization to telomeres. *Nat Cell Biol, 6*(7), 673-680. https://doi.org/10.1038/ncb1142
ncb1142 [pii]

Loayza, D., & De Lange, T. (2003, Jun 26). POT1 as a terminal transducer of TRF1 telomere length control. *Nature, 423*(6943), 1013-1018. https://doi.org/10.1038/nature01688
nature01688 [pii]

Loayza, D., Parsons, H., Donigian, J., Hoke, K., & de Lange, T. (2004, Mar 26). DNA binding features of human POT1: a nonamer 5'-TAGGGTTAG-3' minimal binding site, sequence

specificity, and internal binding to multimeric sites. *J Biol Chem, 279*(13), 13241-13248. https://doi.org/10.1074/jbc.M312309200

Lovelace, D. L., Gao, Z., Mutoji, K., Song, Y. C., Ruan, J., & Hermann, B. P. (2016, 06 01). The regulatory repertoire of PLZF and SALL4 in undifferentiated spermatogonia. *Development, 143*(11), 1893-1906. https://doi.org/10.1242/dev.132761

Lue, N. F., Lin, Y. C., & Mian, I. S. (2003, Dec). A conserved telomerase motif within the catalytic domain of telomerase reverse transcriptase is specifically required for repeat addition processivity. *Mol Cell Biol, 23*(23), 8440-8449. https://doi.org/10.1128/mcb.23.23.8440-8449.2003

Maida, Y., Yasukawa, M., Furuuchi, M., Lassmann, T., Possemato, R., Okamoto, N., Kasim, V., Hayashizaki, Y., Hahn, W. C., & Masutomi, K. (2009, Sep 10). An RNA-dependent RNA polymerase formed by TERT and the RMRP RNA. *Nature, 461*(7261), 230-235. https://doi.org/10.1038/nature08283

Martínez, P., & Blasco, M. A. (2011, Mar). Telomeric and extra-telomeric roles for telomerase and the telomere-binding proteins. *Nat Rev Cancer, 11*(3), 161-176. https://doi.org/10.1038/nrc3025

Martinez, P., Thanasoula, M., Carlos, A. R., Gomez-Lopez, G., Tejera, A. M., Schoeftner, S., Dominguez, O., Pisano, D. G., Tarsounas, M., & Blasco, M. A. (2010, Aug). Mammalian Rap1 controls telomere function and gene expression through binding to telomeric and extratelomeric sites. *Nat Cell Biol, 12*(8), 768-780. https://doi.org/10.1038/ncb2081

Mason, P. J., & Bessler, M. (2011, Dec). The genetics of dyskeratosis congenita. *Cancer Genet, 204*(12), 635-645. https://doi.org/10.1016/j.cancergen.2011.11.002

McClintock, B. (1941, Mar). The Stability of Broken Ends of Chromosomes in Zea Mays. *Genetics, 26*(2), 234-282. https://doi.org/10.1093/genetics/26.2.234

Meyerson, M., Counter, C. M., Eaton, E. N., Ellisen, L. W., Steiner, P., Caddle, S. D., Ziaugra, L., Beijersbergen, R. L., Davidoff, M. J., Liu, Q., Bacchetti, S., Haber, D. A., & Weinberg, R. A. (1997, Aug 22). hEST2, the putative human telomerase catalytic subunit gene, is up-regulated in tumor cells and during immortalization. *Cell, 90*(4), 785-795. https://doi.org/10.1016/s0092-8674(00)80538-3

Muller, H. J. (1938). The remaking of chromosomes. . *13*, 182–198.

Nakata, H., Wakayama, T., Takai, Y., & Iseki, S. (2015, 02). Quantitative analysis of the cellular composition in seminiferous tubules in normal and genetically modified infertile mice. *J Histochem Cytochem, 63*(2), 99-113. https://doi.org/10.1369/0022155414562045

Nandakumar, J., Bell, C. F., Weidenfeld, I., Zaug, A. J., Leinwand, L. A., & Cech, T. R. (2012, Dec). The TEL patch of telomere protein TPP1 mediates telomerase recruitment and processivity. *Nature, 492*(7428), 285-289. https://doi.org/10.1038/nature11648

Nguyen, T. H. D., Tam, J., Wu, R. A., Greber, B. J., Toso, D., Nogales, E., & Collins, K. (2018, 05). Cryo-EM structure of substrate-bound human telomerase holoenzyme. *Nature, 557*(7704), 190-195. https://doi.org/10.1038/s41586-018-0062-x

Niewisch, M. R., & Savage, S. A. (2019, 12). An update on the biology and management of dyskeratosis congenita and related telomere biology disorders. *Expert Rev Hematol, 12*(12), 1037-1052. https://doi.org/10.1080/17474086.2019.1662720

Ogden, D. A., & Mickliem, H. S. (1976, Sep). The fate of serially transplanted bone marrow cell populations from young and old donors. *Transplantation, 22*(3), 287-293. https://doi.org/10.1097/00007890-197609000-00010

Palm, W., & de Lange, T. (2008). How shelterin protects mammalian telomeres. *Annu Rev Genet, 42*, 301-334. https://doi.org/10.1146/annurev.genet.41.110306.130350

Palm, W., Hockemeyer, D., Kibe, T., & de Lange, T. (2009, Jan). Functional dissection of human and mouse POT1 proteins. *Mol Cell Biol, 29*(2), 471-482. https://doi.org/MCB.01352-08 [pii]
10.1128/MCB.01352-08

Park, J. I., Venteicher, A. S., Hong, J. Y., Choi, J., Jun, S., Shkreli, M., Chang, W., Meng, Z., Cheung, P., Ji, H., McLaughlin, M., Veenstra, T. D., Nusse, R., McCrea, P. D., & Artandi, S. E. (2009, Jul 02). Telomerase modulates Wnt signalling by association with target gene chromatin. *Nature, 460*(7251), 66-72. https://doi.org/10.1038/nature08137

Parry, E. M., Alder, J. K., Qi, X., Chen, J. J., & Armanios, M. (2011, May 26). Syndrome complex of bone marrow failure and pulmonary fibrosis predicts germline defects in telomerase. *Blood, 117*(21), 5607-5611. https://doi.org/10.1182/blood-2010-11-322149

Pease, S., Saunders, T. L., & International Society for Transgenic Technologies. (2011). *Advanced protocols for animal transgenesis : an ISTT manual*. Springer. http://www.springerprotocols.com/BookToc/doi/10.1007/978-3-642-20792-1 Springer Protocols

Pech, M. F., Garbuzov, A., Hasegawa, K., Sukhwani, M., Zhang, R. J., Benayoun, B. A., Brockman, S. A., Lin, S., Brunet, A., Orwig, K. E., & Artandi, S. E. (2015, Dec 01). High telomerase is a hallmark of undifferentiated spermatogonia and is required for maintenance of male germline stem cells. *Genes Dev, 29*(23), 2420-2434. https://doi.org/10.1101/gad.271783.115

Pendlebury, D. F., Fujiwara, Y., Tesmer, V. M., Smith, E. M., Shibuya, H., Watanabe, Y., & Nandakumar, J. (2017, Dec). Dissecting the telomere-inner nuclear membrane interface

formed in meiosis. *Nat Struct Mol Biol, 24*(12), 1064-1072. https://doi.org/10.1038/nsmb.3493

Petrova, O. A., Mantsyzov, A. B., Rodina, E. V., Efimov, S. V., Hackenberg, C., Hakanpää, J., Klochkov, V. V., Lebedev, A. A., Chugunova, A. A., Malyavko, A. N., Zatsepin, T. S., Mishin, A. V., Zvereva, M. I., Lamzin, V. S., Dontsova, O. A., & Polshakov, V. I. (2018, 02 16). Structure and function of the N-terminal domain of the yeast telomerase reverse transcriptase. *Nucleic Acids Res, 46*(3), 1525-1540. https://doi.org/10.1093/nar/gkx1275

Podlevsky, J. D., & Chen, J. J. (2012, Feb 01). It all comes together at the ends: telomerase structure, function, and biogenesis. *Mutat Res, 730*(1-2), 3-11. https://doi.org/10.1016/j.mrfmmm.2011.11.002

Rossi, D. J., Bryder, D., Seita, J., Nussenzweig, A., Hoeijmakers, J., & Weissman, I. L. (2007, Jun 7). Deficiencies in DNA damage repair limit the function of haematopoietic stem cells with age. *Nature, 447*(7145), 725-729. https://doi.org/10.1038/nature05862

Rudolph, K. L., Chang, S., Lee, H. W., Blasco, M., Gottlieb, G. J., Greider, C., & DePinho, R. A. (1999, Mar). Longevity, stress response, and cancer in aging telomerase-deficient mice. *Cell, 96*(5), 701-712. https://doi.org/10.1016/s0092-8674(00)80580-2

Ryu, B. Y., Orwig, K. E., Oatley, J. M., Avarbock, M. R., & Brinster, R. L. (2006, Jun). Effects of aging and niche microenvironment on spermatogonial stem cell self-renewal. *Stem Cells, 24*(6), 1505-1511. https://doi.org/10.1634/stemcells.2005-0580

Samper, E., Fernández, P., Eguía, R., Martín-Rivera, L., Bernad, A., Blasco, M. A., & Aracil, M. (2002, Apr 15). Long-term repopulating ability of telomerase-deficient murine hematopoietic stem cells. *Blood, 99*(8), 2767-2775. https://doi.org/10.1182/blood.v99.8.2767

Savage, S. A. (2014). Human telomeres and telomere biology disorders. *Prog Mol Biol Transl Sci, 125*, 41-66. https://doi.org/10.1016/b978-0-12-397898-1.00002-5

Savage, S. A., & Alter, B. P. (2009, Apr). Dyskeratosis congenita. *Hematol Oncol Clin North Am, 23*(2), 215-231. https://doi.org/10.1016/j.hoc.2009.01.003

Savage, S. A., & Bertuch, A. A. (2010, Dec). The genetics and clinical manifestations of telomere biology disorders. *Genet Med, 12*(12), 753-764. https://doi.org/10.1097/GIM.0b013e3181f415b5

Savage, S. A., Giri, N., Baerlocher, G. M., Orr, N., Lansdorp, P. M., & Alter, B. P. (2008, Feb). TINF2, a component of the shelterin telomere protection complex, is mutated in dyskeratosis congenita. *Am J Hum Genet, 82*(2), 501-509. https://doi.org/10.1016/j.ajhg.2007.10.004

Sbodio, J. I., & Chi, N. W. (2002, Aug 30). Identification of a tankyrase-binding motif shared by IRAP, TAB182, and human TRF1 but not mouse TRF1. NuMA contains this RXXPDG motif and is a novel tankyrase partner. *J Biol Chem, 277*(35), 31887-31892. https://doi.org/10.1074/jbc.M203916200

Sbodio, J. I., Lodish, H. F., & Chi, N. W. (2002, Feb 01). Tankyrase-2 oligomerizes with tankyrase-1 and binds to both TRF1 (telomere-repeat-binding factor 1) and IRAP (insulin-responsive aminopeptidase). *Biochem J, 361*(Pt 3), 451-459. https://doi.org/10.1042/0264-6021:3610451

Schmidt, J. C., Dalby, A. B., & Cech, T. R. (2014, Oct 01). Identification of human TERT elements necessary for telomerase recruitment to telomeres. *Elife, 3*. https://doi.org/10.7554/eLife.03563

Sekulovic, S., Gylfadottir, V., Vulto, I., Gasparetto, M., Even, Y., Brookes, C., Smith, C., Eaves, C. J., Lansdorp, P. M., Rossi, F. M., & Humphries, R. K. (2011, Aug). Prolonged self-renewal activity unmasks telomerase control of telomere homeostasis and function of mouse hematopoietic stem cells. *Blood, 118*(7), 1766-1773. https://doi.org/10.1182/blood-2010-11-319632

Sen, D., & Gilbert, W. (1988, Jul 28). Formation of parallel four-stranded complexes by guanine-rich motifs in DNA and its implications for meiosis. *Nature, 334*(6180), 364-366. https://doi.org/10.1038/334364a0

Sexton, A. N., Youmans, D. T., & Collins, K. (2012, Oct 05). Specificity requirements for human telomere protein interaction with telomerase holoenzyme. *J Biol Chem, 287*(41), 34455-34464. https://doi.org/10.1074/jbc.M112.394767

Sfeir, A., Kosiyatrakul, S. T., Hockemeyer, D., MacRae, S. L., Karlseder, J., Schildkraut, C. L., & de Lange, T. (2009, Jul 10). Mammalian telomeres resemble fragile sites and require TRF1 for efficient replication. *Cell, 138*(1), 90-103. https://doi.org/10.1016/j.cell.2009.06.021

Shay, J. W., & Wright, W. E. (2010, Sep 10). Telomeres and telomerase in normal and cancer stem cells. *FEBS Lett, 584*(17), 3819-3825. https://doi.org/10.1016/j.febslet.2010.05.026

Siminovitch, l., Till, j. E., & Mcculloch, e. A. (1964, Aug). Decline in colony-forming ability of marrow cells subjected to serial transplantation into irradiated mice. *J Cell Comp Physiol, 64*, 23-31. https://doi.org/10.1002/jcp.1030640104

Smith, E. M., Pendlebury, D. F., & Nandakumar, J. (2020, Jan). Structural biology of telomeres and telomerase. *Cell Mol Life Sci, 77*(1), 61-79. https://doi.org/10.1007/s00018-019-03369-x

Smith, S., Giriat, I., Schmitt, A., & de Lange, T. (1998, Nov 20). Tankyrase, a poly(ADP-ribose) polymerase at human telomeres. *Science, 282*(5393), 1484-1487. https://doi.org/10.1126/science.282.5393.1484

Smogorzewska, A., van Steensel, B., Bianchi, A., Oelmann, S., Schaefer, M. R., Schnapp, G., & de Lange, T. (2000, Mar). Control of human telomere length by TRF1 and TRF2. *Mol Cell Biol, 20*(5), 1659-1668. https://doi.org/10.1128/MCB.20.5.1659-1668.2000

Soriano, P. (1999, Jan). Generalized lacZ expression with the ROSA26 Cre reporter strain. *Nat Genet, 21*(1), 70-71. https://doi.org/10.1038/5007

Stansel, R. M., de Lange, T., & Griffith, J. D. (2001, Oct 01). T-loop assembly in vitro involves binding of TRF2 near the 3' telomeric overhang. *EMBO J, 20*(19), 5532-5540. https://doi.org/10.1093/emboj/20.19.5532

Strong, M. A., Vidal-Cardenas, S. L., Karim, B., Yu, H., Guo, N., & Greider, C. W. (2011, Jun). Phenotypes in mTERT$^{+/-}$ and mTERT$^{-/-}$ mice are due to short telomeres, not telomere-independent functions of telomerase reverse transcriptase. *Mol Cell Biol, 31*(12), 2369-2379. https://doi.org/10.1128/mcb.05312-11

Takai, H., Smogorzewska, A., & de Lange, T. (2003, Sep 02). DNA damage foci at dysfunctional telomeres. *Curr Biol, 13*(17), 1549-1556. https://doi.org/10.1016/s0960-9822(03)00542-6

Takai, K. K., Hooper, S., Blackwood, S., Gandhi, R., & de Lange, T. (2010, Jan 08). In vivo stoichiometry of shelterin components. *J Biol Chem, 285*(2), 1457-1467. https://doi.org/10.1074/jbc.M109.038026

Takai, K. K., Kibe, T., Donigian, J. R., Frescas, D., & de Lange, T. (2011, Nov 18). Telomere protection by TPP1/POT1 requires tethering to TIN2. *Mol Cell, 44*(4), 647-659. https://doi.org/10.1016/j.molcel.2011.08.043

Tesmer, V. M., Smith, E. M., Danciu, O., Padmanaban, S., & Nandakumar, J. (2019, Dec 10). Combining conservation and species-specific differences to determine how human telomerase binds telomeres. *Proc Natl Acad Sci U S A*. https://doi.org/10.1073/pnas.1911912116

Tummala, H., Collopy, L. C., Walne, A. J., Ellison, A., Cardoso, S., Aksu, T., Yarali, N., Aslan, D., Fikret Akata, R., Teo, J., Songyang, Z., Pontikos, N., Fitzgibbon, J., Tomita, K., Vulliamy, T., & Dokal, I. (2018, 09 20). Homozygous OB-fold variants in telomere protein TPP1 are associated with dyskeratosis congenita-like phenotypes. *Blood, 132*(12), 1349-1353. https://doi.org/10.1182/blood-2018-03-837799

van Steensel, B., & de Lange, T. (1997, Feb 20). Control of telomere length by the human telomeric protein TRF1. *Nature, 385*(6618), 740-743. https://doi.org/10.1038/385740a0

van Steensel, B., Smogorzewska, A., & de Lange, T. (1998, Feb 06). TRF2 protects human telomeres from end-to-end fusions. *Cell, 92*(3), 401-413. https://doi.org/10.1016/s0092-8674(00)80932-0

Varea-Sánchez, M., Tourmente, M., Bastir, M., & Roldan, E. R. (2016, 07). Unraveling the Sperm Bauplan: Relationships Between Sperm Head Morphology and Sperm Function in Rodents. *Biol Reprod, 95*(1), 25. https://doi.org/10.1095/biolreprod.115.138008

Vasilopoulos, E., Fragkiadaki, P., Kalliora, C., Fragou, D., Docea, A. O., Vakonaki, E., Tsoukalas, D., Calina, D., Buga, A. M., Georgiadis, G., Mamoulakis, C., Makrigiannakis, A., Spandidos, D. A., & Tsatsakis, A. (2019, Aug). The association of female and male infertility with telomere length (Review). *Int J Mol Med, 44*(2), 375-389. https://doi.org/10.3892/ijmm.2019.4225

Vlangos, C. N., O'Connor, B. C., Morley, M. J., Krause, A. S., Osawa, G. A., & Keegan, C. E. (2009, Oct 15). Caudal regression in adrenocortical dysplasia (acd) mice is caused by telomere dysfunction with subsequent p53-dependent apoptosis. *Dev Biol, 334*(2), 418-428. https://doi.org/10.1016/j.ydbio.2009.07.038

Walne, A. J., Vulliamy, T., Beswick, R., Kirwan, M., & Dokal, I. (2008, Nov 01). TINF2 mutations result in very short telomeres: analysis of a large cohort of patients with dyskeratosis congenita and related bone marrow failure syndromes. *Blood, 112*(9), 3594-3600. https://doi.org/10.1182/blood-2008-05-153445

Wang, F., Podell, E. R., Zaug, A. J., Yang, Y., Baciu, P., Cech, T. R., & Lei, M. (2007, Feb 1). The POT1-TPP1 telomere complex is a telomerase processivity factor. *Nature, 445*(7127), 506-510. http://www.ncbi.nlm.nih.gov/entrez/query.fcgi?cmd=Retrieve&db=PubMed&dopt=Citation&list_uids=17237768

Wu, L., Multani, A. S., He, H., Cosme-Blanco, W., Deng, Y., Deng, J. M., Bachilo, O., Pathak, S., Tahara, H., Bailey, S. M., Behringer, R. R., & Chang, S. (2006, Jul 14). Pot1 deficiency initiates DNA damage checkpoint activation and aberrant homologous recombination at telomeres. *Cell, 126*(1), 49-62. https://doi.org/10.1016/j.cell.2006.05.037

Xie, M., Podlevsky, J. D., Qi, X., Bley, C. J., & Chen, J. J. (2010, Apr). A novel motif in telomerase reverse transcriptase regulates telomere repeat addition rate and processivity. *Nucleic Acids Res, 38*(6), 1982-1996. https://doi.org/10.1093/nar/gkp1198

Xin, H., Liu, D., Wan, M., Safari, A., Kim, H., Sun, W., O'Connor, M. S., & Songyang, Z. (2007, Feb 1). TPP1 is a homologue of ciliate TEBP-beta and interacts with POT1 to recruit telomerase. *Nature, 445*(7127), 559-562. https://doi.org/nature05469 [pii]
10.1038/nature05469

Yan, W. (2009, Jul 10). Male infertility caused by spermiogenic defects: lessons from gene knockouts. *Mol Cell Endocrinol, 306*(1-2), 24-32. https://doi.org/10.1016/j.mce.2009.03.003

Yang, D., He, Q., Kim, H., Ma, W., & Songyang, Z. (2011, Jul 1). TIN2 protein dyskeratosis congenita missense mutants are defective in association with telomerase. *J Biol Chem, 286*(26), 23022-23030. https://doi.org/M111.225870 [pii]
10.1074/jbc.M111.225870

Ye, J. Z., Hockemeyer, D., Krutchinsky, A. N., Loayza, D., Hooper, S. M., Chait, B. T., & de Lange, T. (2004, Jul 15). POT1-interacting protein PIP1: a telomere length regulator that recruits POT1 to the TIN2/TRF1 complex. *Genes Dev, 18*(14), 1649-1654. https://doi.org/10.1101/gad.1215404
1215404 [pii]

Yuan, L., Liu, J. G., Zhao, J., Brundell, E., Daneholt, B., & Höög, C. (2000, Jan). The murine SCP3 gene is required for synaptonemal complex assembly, chromosome synapsis, and male fertility. *Mol Cell, 5*(1), 73-83. https://doi.org/10.1016/s1097-2765(00)80404-9

Zaug, A. J., Podell, E. R., Nandakumar, J., & Cech, T. R. (2010, Mar). Functional interaction between telomere protein TPP1 and telomerase. *Genes Dev, 24*(6), 613-622. https://doi.org/10.1101/gad.1881810

Zhong, F. L., Batista, L. F., Freund, A., Pech, M. F., Venteicher, A. S., & Artandi, S. E. (2012, Aug). TPP1 OB-fold domain controls telomere maintenance by recruiting telomerase to chromosome ends. *Cell, 150*(3), 481-494. https://doi.org/10.1016/j.cell.2012.07.012

Zhong, Z., Shiue, L., Kaplan, S., & de Lange, T. (1992, Nov). A mammalian factor that binds telomeric TTAGGG repeats in vitro. *Mol Cell Biol, 12*(11), 4834-4843. https://doi.org/10.1128/mcb.12.11.4834-4843.1992